Structure of the Cape Fold Belt in the Ceres Syntaxis

by

C. H. DE BEER

THESIS PRESENTED IN PARTIAL FULFILMENT OF THE REQUIREMENTS

FOR THE DEGREE OF **MASTER OF SCIENCE**

AT THE UNIVERSITY OF STELLENBOSCH

STUDY LEADER: Prof. I.W. Hälbich September 1989

Stellenbosch University http://scholar.sun.ac.za

DEDICATED TO MY PARENTS

Stellenbosch University http://scholar.sun.ac.za

Declaration

I the undersigned hereby declare that the work contained in this thesis is my own original work and has not previously in its entirety or in part been submitted at any university for a degree.

Signature Date: 8 Jan 1990

Stellenbosch University http://scholar.sun.ac.za

ABSTRACT

The Ceres Syntaxis comprises that part of the Cape Fold Belt Syntaxis that lies north of the Worcester Fault. Most of the area consists of folded Cape Supergroup (primarily Witteberg Group) rocks. Fold styles of all fold trends are essentially the same. However, different multilayer rheologies led to the development of either sinusoidal or kink-like fold geometries in different parts of the cover sequence. The character of Witteberg sediments led to the development of large megakink folds and peculiar fold zones in this part of the sequence. Fold trends in the Ceres Syntaxis vary between NW-SE, NE-SW and E-W. The southern part of the area is dominated by the NE-SW trend, with the NW-SE trend being only important in the west. Interference between these two trends only exists in the Witteberg Group, where it occurs as crossing linear fold zones and conjugate, intersecting kink folds . Cross-folding relationships in the north-eastern part of the Ceres Syntaxis indicate that the area had been affected by two contemporaneous, orthogonally opposed compressions that worked simultaneously in different parts of the multilayer. Differences in the magnitude of strain, or in the local timing of fold initiation, produced local refolding or transecting relationships. The microfabric of Witteberg sandstones suggests deformation under conditions of low temperature and pressure, as well as low strain rates. Some microfabrics also indicate that substantial buckle shortening occurred while the Middle and Upper Witteberg beds were still unlithified. Isotopic dating of Cedarberg shale from both main trends did not yield unequivocal results, mainly due to the low deformational intensity. The positioning of the Cape Fold Belt Syntaxis was strongly influenced by basement tectonic grain and basin floor relief. The NW and NE fold trends formed on a heterogeneous basement that resolved the external stress configuration into components which acted simultaneously towards the north-west and north-east. Ecca and Beaufort Group sedimentation patterns in the western Karoo corroborate the above findings.

Stellenbosch University http://scholar.sun.ac.za

OPSOMMING

Die Ceres-sintaks beslaan daardie deel van die sintaks van die Kaapse Plooigordel wat noord van die Worcesterverskuiwing lê. Die gebied bestaan grotendeels uit geplooide gesteentes van die Supergroep Kaap (hoofsaaklik Groep Witteberg). Alle plooirigtings openbaar dieselfde plooistyl. Reologiese verskille in die multilae het egter gelei tot die ontwikkeling van òf sinusoidale òf knikvormige plooie in verskillende dele van die dekgesteentes. Die Wittebergsedimente se aard het veroorsaak dat megaknikke en eienaardige plooisones in hierdie deel van die opeenvolging ontstaan het. Plooirigtings in die Ceres-sintaks wissel tussen NW-SO, NO-SW en O-W. Die NO-SW plooirigting oorheers in die suidelike deel van die gebied, terwyl die NW-SO plooirigting eintlik net in die weste belangrik is. Interferensie van hierdie twee hoofrigtings kom slegs voor in die Groep Witteberg, waar dit as dwarssnydende lineêre plooisones en snydende, konjugerende knikke aanwesig is. Onderlinge verhoudings tussen kruisplooie in die noordoostelike Ceres-sintaks, toon dat die gebied beinvloed is deur twee gelyktydige drukspannings wat reghoekig op mekaar ingewerk het, somtyds in effens verskillende dele van die multilaag. Verskille in die spanningsbedrag en tydsberekening het lokale herplooiing of dwarssnydende strukture veroorsaak. Die mikromaaksel van die Wittebergsandsteen toon dat die vervorming onder lae temperatuur- en druktoestande, tesame met 'n lae vervormingstempo, plaasgevind het. Die maaksel toon ook aan dat heelwat buigplooiing plaasgevind het terwyl die Middel- en Bo-Witteberglae nog ongekonsolideer was. Isotopiese datering van Sederbergskalie afkomstig van die twee hoof-plooirigtings, het weens die lae vervormingsintensiteit swak resultate gelewer. Die posisie van die sintaks van die Kaapse Plooigordel, insluitende die van die Ceres-sintaks, is sterk beïnvloed deur die tektoniese grein en reliëf van die vloergesteentes. Die heterogene vloer waarop die NW en NO plooie gevorm het, het daartoe gelei dat die eksterne spanningsopset verdeel is in komponente wat gelyktydig na die noordweste en noordooste gewerk het. Sedimentasiepatrone in die Groepe Ecca en Beaufort ondersteun bostaande afleidings.

Stellenbosch University http://scholar.sun.ac.za

INDEX

		Page
1.	**INTRODUCTION**	1
1.1	GENERAL GEOLOGICAL SETTING	1
1.2	REVIEW OF PREVIOUS WORK	3
1.3	PURPOSE OF THE INVESTIGATION	6
2.	**STRATIGRAPHY**	8
3.	**STRUCTURAL ELEMENTS**	11
3.1	PLANAR STRUCTURES	11
3.1.1	Cross-lamination	11
3.1.2	Bedding	11
3.1.3	Vein arrays	12
3.1.4	Cleavage	13
3.1.5	Faults	14
3.2	LINEAR STRUCTURES	15
3.2.1	Lineations	15
4.	**FOLDS AND FOLD STYLE**	19
4.1	TABLE MOUNTAIN GROUP	19
4.2	BOKKEVELD GROUP	22
4.3	WITTEBERG GROUP	23
5.	**REGIONAL ORIENTATION ANALYSIS**	35
5.1	BEDDING	35
5.2	CLEAVAGE	42

Stellenbosch University http://scholar.sun.ac.za

Page

5.3 FOLD AXES 44

6. **THE FOLD ZONES OF SUBAREA 11** 50

7. **CROSS-FOLDING RELATIONSHIPS** 57

7.1 GENERAL 57

7.2 N'WARDOUW TO SKITTERYKLOOF 60

7.2.1 N'wardouwskloof Subdomain 61

7.2.2 Hartnekskloof Subdomain 70

7.2.3 Skitterykloof Subdomain 72

7.3 Seekoegat 74

7.4 EVIDENCE FROM THE PLATKLIP AREA 78

7.5 SUMMARY OF CROSS-FOLDING RELATIONSHIPS 78

8. **ORIENTATION OF PRINCIPAL STRESSES**..... 80

9. **MICROFABRIC** 83

9.1 INTRODUCTION 83

9.2 MICROSTRUCTURE 85

9.3 CRYSTALLOGRAPHIC PREFERRED ORIENTATION 88

9.4 RESULTS 90

9.4.1 Sample CFB 56 90

9.4.2 Sample CFB 64 93

9.4.3 Sample CFB 60 95

9.4.4 Sample CFB 62 96

9.4.5 Sample CFB 68 98

9.4.6 Sample CFB 72 101

Stellenbosch University http://scholar.sun.ac.za

page

9.4.7 Sample CFB 73 104

9.4.8 Sample CFB 74 105

9.5 CONCLUSIONS FROM THE MICROFABRIC ANALYSIS 108

10. **DATING THE DEFORMATION**..... 111

10.1 INTRODUCTION 111

10.2 SAMPLE DESCRIPTION AND AGE SPECTRA 112

11. **SYNTHESIS** 115

ACKNOWLEDGEMENTS

REFERENCES

MAP 1

Stellenbosch University http://scholar.sun.ac.za

1. INTRODUCTION

1.1 GENERAL GEOLOGICAL SETTING

The Cape Fold Belt Syntaxis is situated at the intersection of the NNW-SSE striking so-called Cedarberg Folds and the E-W striking southern Cape Folds. This north-east trending syntaxial terrain covers an area of nearly 20 000 km² in the south-western Cape Province, between Ceres in the north and Cape Hangklip in the south (Figure 1.1). The area exhibits a complex arrangement of arcuate and linear features.

Both the NNW and E trends form arcs with their convex sides facing east and north-west respectively. Where these arcs merge between Worcester and Cape Hangklip, a broad zone of linear, north-east striking structures are displayed. The terrain south of the Worcester Fault is characterized by many north-east trending faults of both compressional and tensional origin. Deformation in this area around Villiersdorp is also more intense than in the syntaxis north of the Worcester Fault.

The part of the syntaxis lying north of the Worcester Fault, here termed the "Ceres Syntaxis", differs in various respects from the area described above. It exhibits a gradual change in fold trend from N-S to NE-SW to E-W. The deformation in this part of the Cape Fold Belt Syntaxis was much lower than in the southern Villiersdorp area, because no cleavage or NE-trending faults occur. The latter fault trend is replaced by WNW-ESE

Stellenbosch University http://scholar.sun.ac.za

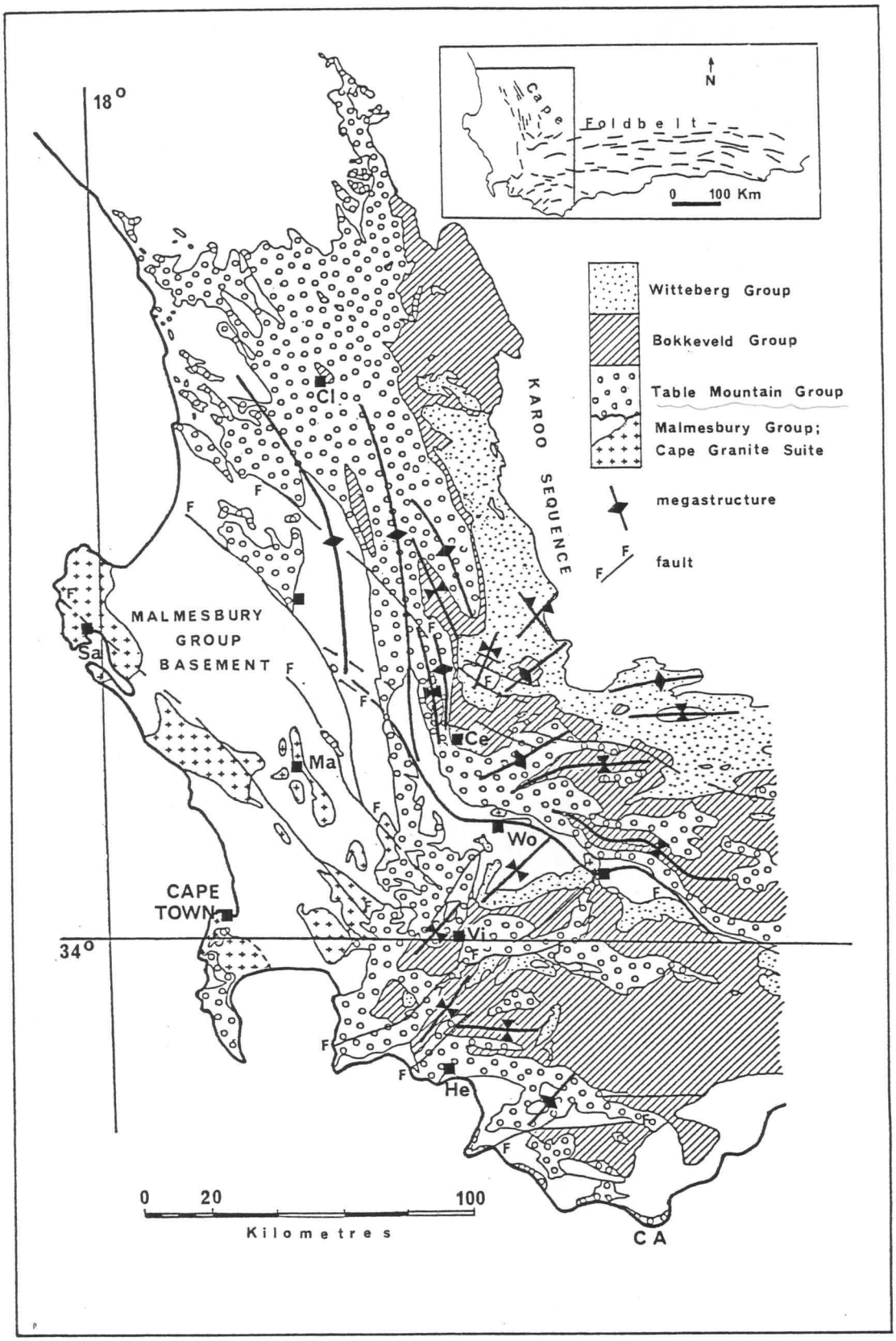

Figure 1.1
General geological setting of the Cape Fold Belt Syntaxis in the south-western Cape Province. Sa =Saldanha; Cl = Clanwilliam; Ce = Ceres; Wo = Worcester; Vi =Villiersdorp; He = Hermanus; CA = Cape Agulhas ; CH = Cape Hangklip.

Stellenbosch University http://scholar.sun.ac.za

trending tensional faults that are partly related to the break-up of Gondwanaland. North-east trending folds, related to the main Hex River Mountains mega-anticline, are the dominant structures over most of the area of the central Ceres Syntaxis. These are replaced to the west and north by N-S as well as NNW-SSE structures of the Cedarberg trend, while to the east, the north-east trends diverge and ultimately join the southern Cape Fold Belt.

The Ceres Syntaxis (Figure 1.2) was chosen as study area, because it was thought that fold interference effects would be best displayed in the Witteberg Group rocks, which build most of the area. The absence of cleavage and the low deformation intensity precluded the use of conventional methods for unravelling interference patterns. Consequently, the investigations had to rely mostly on fold trend interrelationships.

The area was investigated by using 1:50 000 geological base maps of the Geological Survey. Additional structural mapping was subsequently done on standard aerial photographs (scale 1:50000), as well as 1:16000 photographs of selected areas where detailed work was required. As no previous structural investigation was ever undertaken in this area, the study was initially a regional one, stretching from the Hex River Valley northwards to Op-die-Berg in the Cold Bokkeveld, thus covering an area of almost 2500 km².

Stellenbosch University http://scholar.sun.ac.za

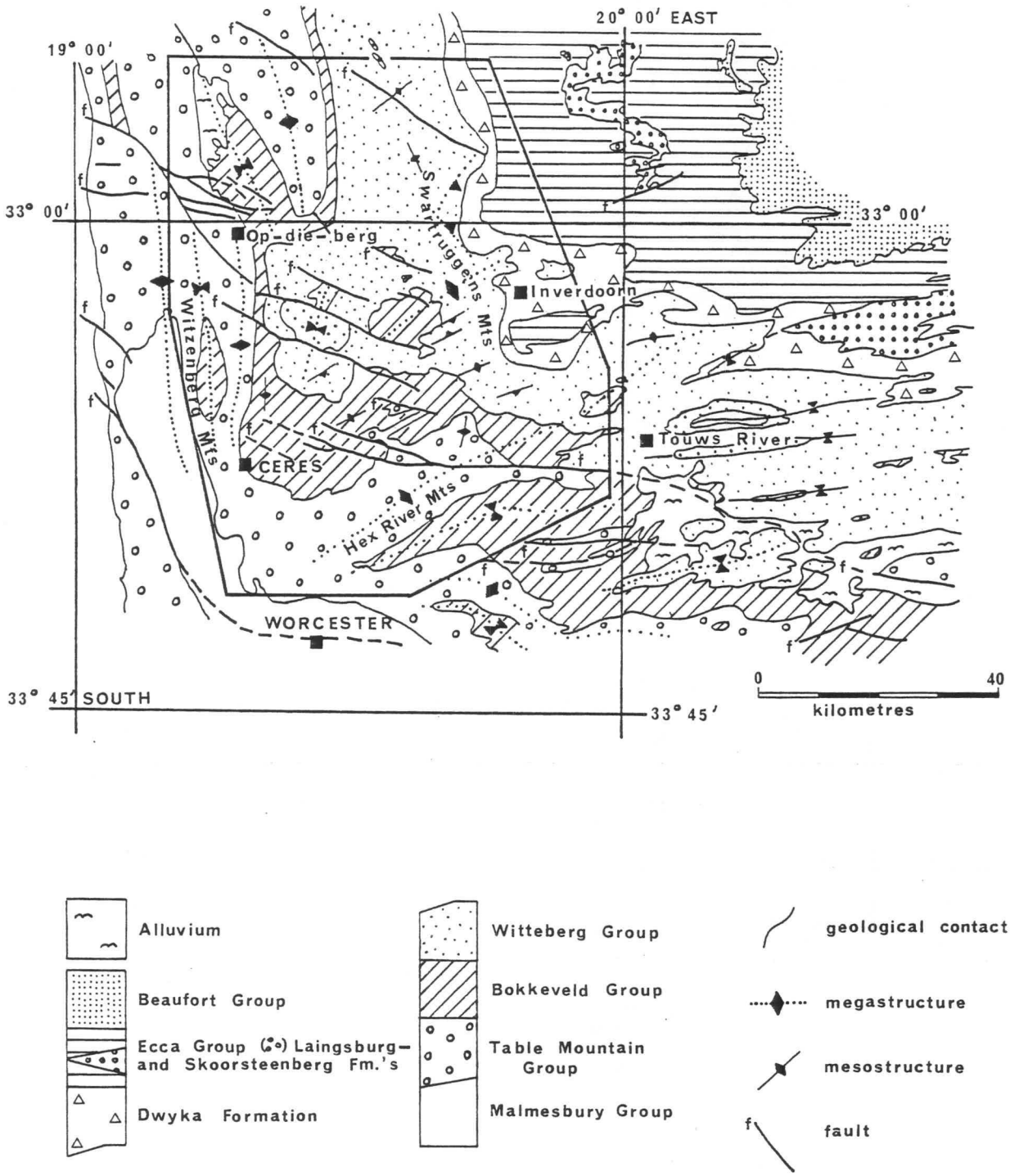

Figure 1.2
The Ceres Syntaxis with study area outlined.

Stellenbosch University http://scholar.sun.ac.za

As most of the area is mountainous, exposures are excellent and folds can be viewed in profile in most of the area covered by Witteberg Group rocks. The Bokkeveld Group, however, has poor outcrops in the Ceres intermontane valley, except for the eastern part near Theronsberg and Swaarmoed (Map 1).

Field work was undertaken during 1986, whereas microfabric investigation and interpretation of the data were accomplished during 1987-1988.

1.2 REVIEW OF PREVIOUS WORK

Any discussion of the Cape Fold Belt Syntaxis must invariably consider previous research in both the western and southern fold belts.

The review of the Cape Orogeny by De Villiers (1944) gave an excellent account of the main features of both fold belts. Personal communications to A.L. du Toit and A.W. Rogers, in which these authors expressed their views on the structure and probable origin of the Cape Fold Belt, were also included in this very important paper by De Villiers. These workers more or less agreed on fold style, fold vergence and also on probably the most important aspect of all concerning the syntaxis, namely that the western fold belt came into existence slightly earlier than the southern fold belt.

A review by De Villiers (1956) demonstrated the general parallelism of pre- and post-Cape structural trends in the

Stellenbosch University http://scholar.sun.ac.za

syntaxis as a whole. A dynamic model for the folding, which involved a shear couple brought about by tangential shortening from the south and simultaneous flow of material outwards from under the Karoo geosynclinal hinge-line, was postulated to explain northward fold vergence in the southern Cape Fold Belt.

The research of Rust (1967) and Theron (1972) brought about a better understanding of the stratigraphy and sedimentary tectonics of the Table Mountain and Bokkeveld Groups, which comprise the Cape Supergroup.

The pioneering work by Newton (1973), although it relied heavily on photo-interpretation, gave a good account of the regional structure in the south-western Cape, while simultaneously some of the peculiarities of the folding were pointed out. In a paper published after completion of his doctoral dissertation (1975), Newton further advocated the idea that gravity tectonics played an important role in the southern Cape Fold Belt, and agreed with De Villiers (1956) that there were no fold interference effects in the syntaxis. They differed, however, on the amount of basement control on the fold trends in the south-western Cape.

De Swardt et al. (1974) drew attention to a pervasive south-dipping cleavage in the southern Cape Fold Belt, which was believed to represent the regional plane of transport of a shear fold episode. De Swardt and Rowsell (1974) made a contribution regarding the diagenesis of cover sediments in the Cape Fold Belt.

Stellenbosch University http://scholar.sun.ac.za

A plate tectonic model for the Cape Orogeny was postulated by Rhodes (1974), later modified by Lock (1980) and then denied by Newton (1980), who drew attention to the intra-plate nature of the orogeny.

Basement involvement in the folding was debated in various papers. The work done by Gresse (1976), Krynauw (1977) and Le Roux (1977) did much to further understanding of basement behaviour during deformation in the southern Cape. In the south-western Cape, however, much remains to be done. The studies by Hartnady (1969) and Toogood (1976) in the Worcester area were the first modern structural analyses, and unfortunately, still the only recent work done in the syntaxis as far as basement is concerned. Both authors were uncertain as to what extent structures could be related to either pre- or post-Cape deformation.

Major contributions regarding the sedimentology and transport directions of the Karoo Supergroup, which was deposited during the Cape folding, were made by Theron (1967), Ryan (1967), Wickens (1984) and Visser (1979, 1982, 1986).

Summaries of the state of knowledge regarding the Cape Fold Belt were presented by Tankard et al. (1982) and more extensively by Söhnge and Hälbich (1983), as well as Hälbich (1983) who reported on important, and in many ways, pioneering work done during the National Geodynamics Project since 1973. However, little attention was given to structures in the syntaxis region apart from speculation on possible

Stellenbosch University http://scholar.sun.ac.za

interference folding in the Ceres area, descriptions of the regional arcuate structures and a commitment by Newton (in Tankard et al., 1982) that there is not enough evidence for making the western (Cedarberg) branch older than the southern Cape Folds.

1.3 PURPOSE OF THE INVESTIGATION

The area has never been subjected to modern structural analysis and previous work on the Cape Fold Belt as a whole, was never intended to go into much detail as far as the syntaxis is concerned. A number of questions, of which the results are applicable to the Ceres syntaxis, were addressed during this investigation, while many more regarding the southern Villiersdorp syntaxis still remain unanswered.

It was hoped that an age relationship between the western Cedarberg and the southern Cape Fold Belts could be established. The viewpoint of earlier workers, namely that the first folding occurred in the western branch, has recently been strongly questioned (Tankard et al., 1982). Söhnge (1983) suggested that outcrop patterns of the Bokkeveld and Witteberg rocks in the Ceres area indicate mild cross-folding, while until now, various authors (De Villiers, 1956 and Newton, 1975) have ruled it out.

As the mega- and meso-scale fold style of the NW-SE, NE-SW and E-W trends could have an important bearing on different fold ages, a clearer understanding of this aspect for the above

Stellenbosch University http://scholar.sun.ac.za

trends was imperative. An investigation of fold geometry, intensity and vergence over the area was needed to decide on the relationship between the NE-SW and E-W folds. This would also show if there were fundamental geometrical differences between these trends that might imply vertical tectonics for the western folds (Söhnge, 1983). One of the main problems of this investigation of the syntaxis is the fact that the western fold belt has received but very scant attention in past years and little is actually known about it.

The main objectives of the investigation were to ascertain if the area was affected by two orogenies separated in time, or by one orogeny which resulted in three fold trends (NW-SE, NE-SW and E-W) by a mechanism of complex stress distribution, influenced by pre-Cape structural grain and cover basin control.

Stellenbosch University http://scholar.sun.ac.za

2. STRATIGRAPHY

The Cape Orogeny affected a Paleozoic to Early Mesozoic sedimentary cover sequence laid down on basement rocks of Late Precambrian age. Outcrops in the Tulbagh valley suggest that the basement probably consists of Malmesbury Group metapelites and quartzites. Nearly 5000 metres of deformed Cape and Karoo sediments are exposed in the study area (Table 2.1).

Thick-bedded quartz-arenites, belonging to the Peninsula Formation and Nardouw Subgroup, dominate the lower 2000 metres of the succession. The Cedarberg Shale Formation (maximum thickness 120 metres) forms the only major discontinuity in this monotonous sequence of Ordovician to Silurian age. A penecontemporaneous soft-sediment deformational episode which affected the uppermost Peninsula Formation (Blignault, 1970), resulting in the so-called "Fold Zone", exists everywhere below the Pakhuis Tillite (Rust, 1967) from the Witzenberge to the Hex River Mountains. These high mountain ranges that border the Ceres syntaxis on the western and southern sides, are built by Peninsula and Nardouw quartzitic sandstones.

The Bokkeveld Group, which rests conformably on Rietvlei arenites, is dominated by pro-delta shales of Devonian age (Theron, 1972). Out of a total thickness of around 1165 metres, approximately 385 metres consist of delta-front sands, which are now quartzitic sandstones (De Swardt and Rowsell, 1974). This sequence contains five well-defined sandstone units and six incompetent shale or mudrock units. Outcrops in

Stellenbosch University http://scholar.sun.ac.za

GROUP	SUBGROUP	FORMATION	LITHOLOGY	(m)
		Dwyka	tillite	700
WITTEBERG	Lake Mentz	Waaipoort	shale	80
		Floriskraal	sandstone	60
		Kweekvlei	shale	100
		Witpoort	sandstone	310
		Swartruggens	sandstone	
			siltstone	280
		Blinkberg	sandstone	140
		Wagen Drift	sandstone	
			shale	140
BOKKEVELD	Bidouw	Karoopoort	shale	50
		Osberg	sandstone	50
		Klipbokkop	shale	170
		Wuppertal	sandstone	65
		Waboomberg	shale	200
	Ceres	Boplaas	sandstone	30
		Tra-Tra	shale	85
		Hex River	sandstone	100
		Voorstehoek	shale	115
		Gamka	sandstone	135
		Gydo	shale	160
TABLE MOUNTAIN	Nardouw	Rietvlei	sandstone	120
		Skurweberg	sandstone	120
		Goudini	sandstone	160
		Cedarberg	shale	120
		Pakhuis	tillite	40
		Peninsula	sandstone	1150
		Graafwater	sandstone	
			siltstone	50?
		Piekeniers-kloof	sandstone conglomerate	50?

Table 2.1
Lithostratigraphy of the Ceres Syntaxis.

Stellenbosch University http://scholar.sun.ac.za

the Gydo and Theronsberg Passes show that the mudrock is essentially structureless, while the sandstones and silty beds display cross-bedding and channels. The latter structures provided the beds with additional slip discontinuities that could partake in the folding. Bokkeveld beds are fossiliferous in parts, as for example in Gydo Pass.

Dominantly quartzitic, well- and thin-bedded sediments of the Devonian Witteberg Group, overlie the Bokkeveld beds conformably. The total thickness of sediment belonging to this group in the Ceres Syntaxis, is around 1110 metres, very similar to the thickness of the underlying Bokkeveld Group. Witteberg lithology differs markedly from that of the Bokkeveld in many respects, but mostly in that it is a "mixed" succession. This means that from a structural point of view, it displays no clear subdivisions of different competency in the lower 910 metres or so. The percentage of siltstone in the succession gave rise to a natural subdivision of the lower part into the Wagendrift, Blinkberg and Swartruggens Formations. However, a unit like the Blinkberg Formation, which by definition consists of resistant white quartzite (SACS, 1980), still contains many thin silty beds. This is especially true of the Witpoort sandstone (310 metres approximately), which shows numerous silty interbeds within the quartzites. Only towards the top of the Witteberg Group in the Carboniferous Kweekvlei, Floriskraal and Waaipoort Formations, does a clear separation of lithological units appear. Figure 2.1 shows the lower part of the Witteberg Group in the Ceres area (Basson, 1984). Unfortunately, the Witpoort Formation was not

UNIVERSITEITSBIBLIOTEEK

Stellenbosch University http://scholar.sun.ac.za

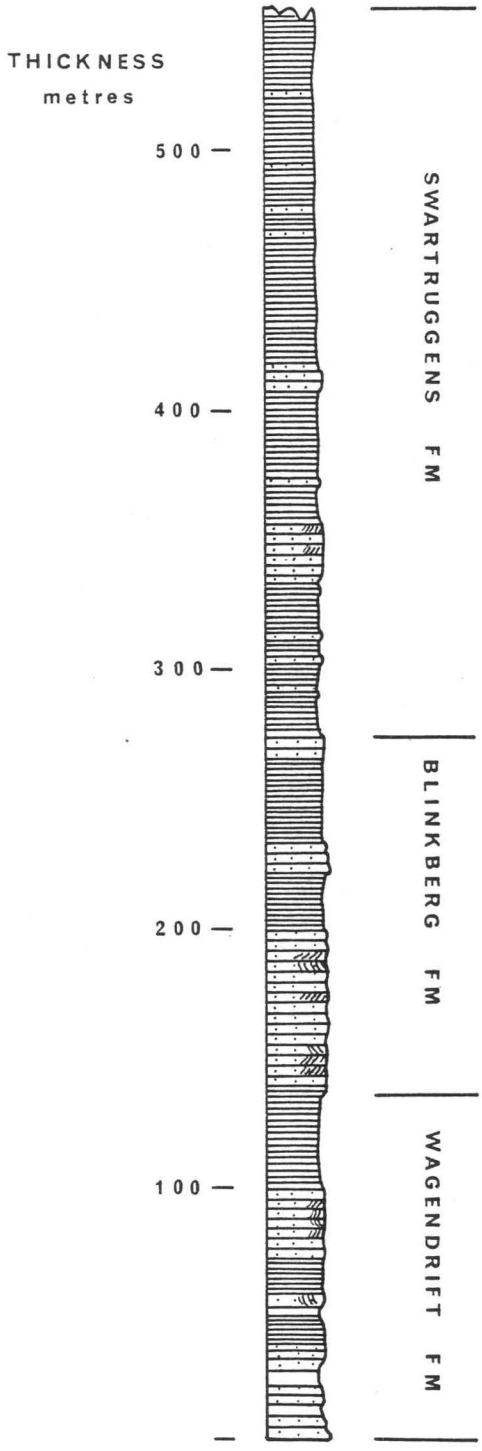

Figure 2.1
Section showing the lower three formations of the Witteberg Group to indicate the well-developed layering and mixed lithological character of the sediments.

Stellenbosch University http://scholar.sun.ac.za

measured. The upper boundary of the Witteberg Group in the south-western Cape is a "paraconformity" (Loock, 1967). North of the farm De Vallei, in the Ceres-Karoo, the Dwyka Formation rests progressively on lower units of the Witteberg until just north of Skitterykloof, the whole of the Lake Mentz Subgroup is absent and basal tillites rest directly on Witpoort quartzites. In the Droehoek area north-east of Gydo Pass, only the Waaipoort shales are absent.

The Dwyka Formation attains thicknesses of between 400 and 650 metres in the south-western Karoo (obtained from Soekor drill-holes OL1/69, KL1/65 and SA1/66Z). Tillite of this formation is commonly structureless or shows a faint bedding in areas of low fold intensity. The unit was deposited during Late Carboniferous-Permian times as a result of continental glaciation. Ice-flow directions during maximum glaciation were dominantly from east to west and to a lesser extent from south to north in the area now occupied by the Ceres Syntaxis (Visser, 1987).

Stellenbosch University http://scholar.sun.ac.za

3. STRUCTURAL ELEMENTS

3.1 PLANAR STRUCTURES

3.1.1 Cross-lamination

Although deformation of cross-lamination was not used as a structural tool during the investigation, it nevertheless deserves attention. Planar, trough, festoon and rare hummocky cross-stratification are ubiquitous in all arenitic sediments of the area. It is very difficult to distinguish between soft sediment or penecontemporaneous structures and tectonic folds (Hobbs et al., 1976; Maltman, 1984). In the Ceres Syntaxis, and especially in Witteberg rocks, the general parallelism of "soft sediment folds" and definite tectonic structures further complicates the matter. For these reasons, cross-lamination was not analysed as a planar element during the investigations.

3.1.2 Bedding

All cover rocks in the area possess well-developed layering, except for certain mudrock units in the Bokkeveld Group and the Dwyka tillite, where bedding is only rarely visible. Bedding thickness is at a maximum in the Peninsula and Skurweberg Formations. It is less in the Goudini and Rietvlei Formations as well as in the average Bokkeveld sandstone, but highly variable in the Witteberg Group. The Witteberg sandstones are dominantly well-layered, with parallel or near-parallel layers, from a fraction of a millimetre to several centimetres thick.

Stellenbosch University http://scholar.sun.ac.za

In the purer quartzitic units such as the Blinkberg Formation, thin siltstone partings exist between the thicker layers, but interbedded siltstone-sandstone units such as the Swartruggens Formation commonly display an average layer thickness of the order of 10-30 centimetres. Extensive slip occurred on bedding planes. This slip did not always occur exclusively on sandstone-siltstone interfaces, but also on intrabed laminae of 1-2 centimetre thickness, as demonstrated by slip-related lineations.

3.1.3 Vein Arrays

Extensional and shear-vein arrays are common features of many folds in the area. One to three differently oriented sets of principal veins (those continuing for a few metres) may be seen at many localities, often forming prominent networks. Frequently, the veins of different sets do not cross-cut at vein intersections, but coalesce to form a continuous network. In other instances, cross-cutting relationships show that one set opened up before the other. Many minor, well-healed fractures, fractions of a millimetre thick and several centimetres long, occur in very pure quartzitic sandstone of the Witteberg Group.

The quartz infilling of the cracks is commonly of the fibrous and not the drusy variety. It is probable that most veins never evolved as open, fluid-filled cavities (Beach, 1977), but that infilling kept pace with opening-up of the cracks. The aspect-ratio of some veins shows that they developed quite

Stellenbosch University http://scholar.sun.ac.za

early during folding, while the sediment was still soft. Other long and thin veins evidently formed later than these short, thick veins.

In some strongly deformed Witteberg beds, a penetrative B-lineation in impure sandstones is often accompanied by intense quartz veining in the clean arenites. Small-scale faults that form various intersection lineations with bedding, are also commonly quartz-veined. Where fold interference occurs, many planar veins that are tautozonal about the local fold axis and which cross-cut bedding at low angles, show slip and aligned quartz fibres (slickenfibres).

3.1.4 Cleavage

A faint regional cleavage is present in Bokkeveld shales south of the Hex River Mountains, but no regional cleavage developed to the north in the Ceres Syntaxis. This cleavage is displayed in beds just north of the Hex River Pass, where it intersects bedding at low angles. Cleavage intensity increases rapidly towards the south. In road cuttings on the Matroosberg Station - Montagu road, the cleavage appears to be axial planar to the folds. Cedarberg shales in the Hex River anticline display quite intense cleavage on the southern limb of the structure, but on the northern limb, cleavage is barely discernible, partly because it lies close to bedding. In the Skurweberg anticline and the Witzenberge to the west of Ceres, Cedarberg shales developed a near-vertical cleavage in the lowermost 5 metres. In all the above cases, the cleavage is of the regular

Stellenbosch University http://scholar.sun.ac.za

or irregular, usually discontinuous, discrete solution type, but always displays dark to opaque colouring along the foliation planes (Figure 3.1.). The cleavage is thus approximately similar to that described by Hälbich and Cornell (1983, p.136) for areas of very low deformational intensity. Conspicuous is the absence of cleavage in Witteberg beds. This is a common phenomenon right through the Cape Fold Belt, even where deformational intensities are much higher on a regional scale, as in the Southern Cape Fold Belt (Hälbich, pers. comm.,1988).

3.1.5 Faults

Minor faults with small, mesoscopically indeterminable offsets, are common in all folds. The infill material of faults is either quartz or minor breccia. Determinable offsets are observed in certain sandstone beds which have undergone considerable layer-parallel compression. These faults are typically reverse faults, the fault-planes lie at a high angle to bedding and displacement occurs on a centimetre-scale. Disharmonic folding in thin-bedded, incompetent sediments of the Witteberg Group is commonly followed by small-scale reverse faulting in an overlying competent unit. The lengths of these inclined faults are usually less than a few tens of centimetres (the thickness of the competent bed) and the displacement is small.

No major thrust or reverse faulting occurred in the Ceres Syntaxis. Deformation never reached the intensity of the

Stellenbosch University http://scholar.sun.ac.za

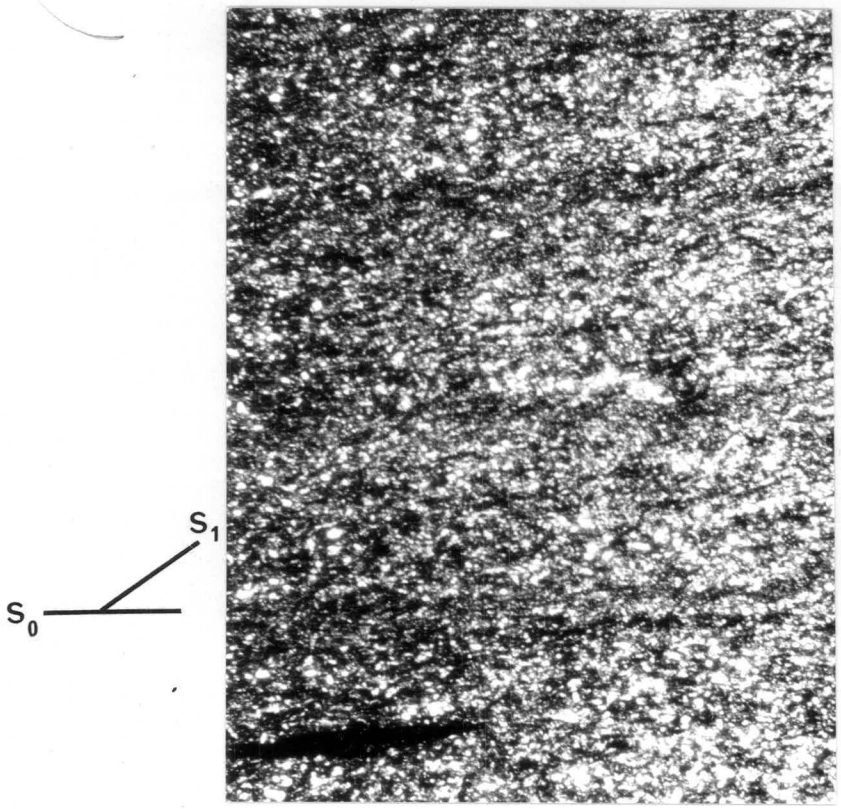

Figure 3.1
Cleavage developed in Cedarberg shale of the Hex River anticline. S_0 = bedding and S_1 = cleavage.

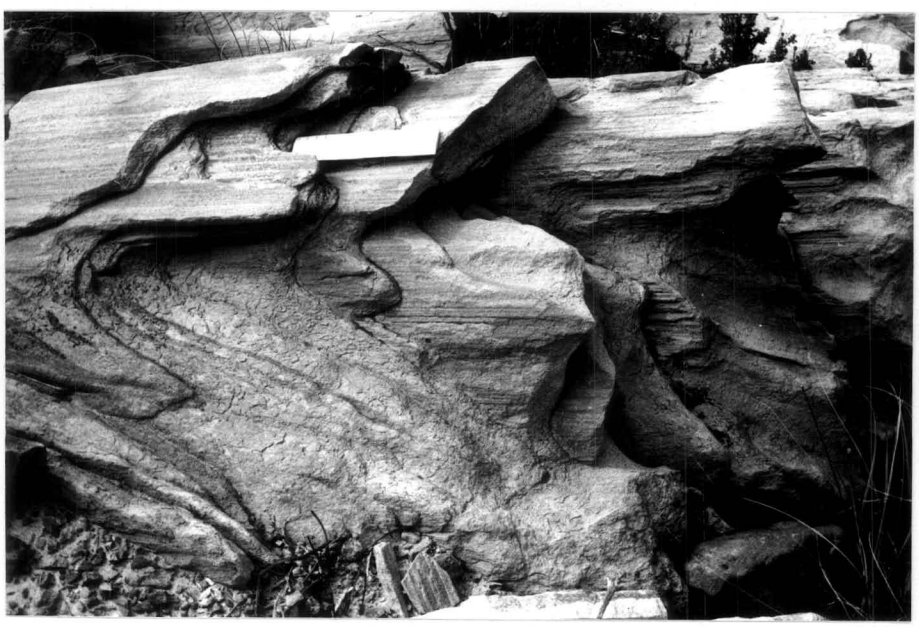

Figure 3.2
Prominent penetrative lineation (L_B) developed sub-parallel to fold axes in Witteberg rocks (scale bar 15 centimetres).

Stellenbosch University http://scholar.sun.ac.za

southern Cape Fold Belt, where thrusting in cover rocks still only occurred on a limited scale. Major faults in the area are of the normal type with near-vertical fault-planes, well-developed fractures and a small strike-slip component. Downthrow is normally to the south-west and the north-east. At least some of these faults are thought to be related to the break-up of Gondwanaland. The brittle behaviour of the rocks is manifested by breccia and closely-spaced joints along fault zones. Slickensides with quartzfibres on fracture planes usually support a vertical displacement sense. Faulting becomes more intense towards the southern part of the Ceres syntaxis around Swaarmoed. The NW-trending faults, which become more numerous toward the northern part of the study area, appear to represent a continuous, gradual change in direction from the WNW trend in the south (Map 1). Evidently more work needs to be done in order to prove this.

3.2 LINEAR STRUCTURES

3.2.1 Lineations

Two main types of lineations occur in deformed sediments of the Ceres Syntaxis, namely those approximately parallel to the local fold axes and those approximately perpendicular to it. The first type is ubiquitous in Witteberg rocks but absent in all other units excluding the Peninsula Fold Zone (Blignault, 1970), while the second type occurs throughout, indicating appreciable bedding-plane slip. Rare lineations parallel to

Stellenbosch University http://scholar.sun.ac.za

the tectonic a-direction occur in highly rotated short limbs of Witteberg megakinks.

A striking and very prominent feature of intensely-deformed Witteberg rocks is a linear fabric (L_B) parallel to the local fold axes (Figure 3.2). A penetrative grooving and rodding, sometimes related to minute wrinkling of intra-bed laminae, but commonly present in undisturbed, subparallel laminae, were produced in the rocks. The lineation is best developed in impure, thin-bedded sandstones, but also occurs on a penetrative scale in coarse, pure quartzitic sandstone. In the latter case it closely resembles current lineation, but may be distinguished by its penetrative character and local subparallelism to the fold axes, a feature which also sets it apart from cross-lamination/ bedding plane intersection lineations. Minor faults, either parallel to or cross-cutting this penetrative B-lineation, may impose a further linear fabric on the rocks. Interference between minute wrinkles that intersect each other at low angles is also commonly present on folded bedding planes.

The linear fabrics mentioned above are the same as those described by Bell (1981) in Witteberg rocks of the southern Cape Fold Belt, where their development was attributed to slump deformation of plastic, waterlogged sediments in water deeper than the base of the grounded Dwyka ice. The so-called "Miller-diamictite" was interpreted as a debris flow deposit related to subaqueous slumping. Similar, possibly debris flow deposits are present below uppermost Witpoort Formation

Stellenbosch University http://scholar.sun.ac.za

quartzitic sandstones in the Swartruggens Range, but the B-lineations are present everywhere in intensely-folded Witteberg rocks. If this lineation formed early in a soft-sediment state, it has an important bearing upon the rheology of Witteberg rocks at the time of initial folding.

Microscopical investigation of the lineation showed no elongation or preferred orientation of the quartz grains. Original grain boundaries are rarely visible in the pure quartzitic sandstones, because of the low initial clay content that would have provided the necessary mineralogical contrast. Only in one sample from Zeekoegat could the penetrative B-lineation be related to intersection with an incipient fracture cleavage, while all other samples showed a dense quartz mosaic of irregularly shaped grains in sections cut both parallel and normal to the linear fabric.

Lineations perpendicular to the local fold axes are of two kinds, namely, real slickensides on silty bedding interfaces and "slickenfibres" resulting from growth of fibrous quartz parallel to the slip direction. A faint streaking on cross- and parallel laminae, ubiquitous in many Witteberg sandstones, reveals the presence of minute quartz fibres on closer examination. Geometric analysis of these minute fibres generally indicates very variable slip directions that may be oblique to the local fold axis. As a result, a clear separation of these lineations from those on bedding planes is necessary to avoid confusion in outcrops that show fold interference structures. Whereas the slickenfibres and

Stellenbosch University http://scholar.sun.ac.za

slickensides generally indicate the approximate attitude of the fold axis in interference structures of low amplitude, the minute fibre lineations could not be used.

Stellenbosch University http://scholar.sun.ac.za

4. FOLDS AND FOLD STYLE

The fold style of the two major NNW - SSE and NE - SW trends is the same. Fold style in various stratigraphic units of the cover sediments, however, differ markedly. This is primarily the result of competency contrasts, differences in bed thickness, the ease with which bedding slip could take place, and stratigraphic considerations.

4.1 THE TABLE MOUNTAIN GROUP

The main structures of the Ceres syntaxis are the Hansiesberg and the Hex River mega-anticlines. The former dictates the NW fold trend of the cover in the west and the latter that of the NE folds in the south-east. Both structures display near-vertical axial planes and limb dips of 30 to 50 degrees at the level of Cedarberg shale exposure. The Hansiesberg mega-anticline, with an interlimb angle of approximately 90 degrees, is a "tighter" structure than the Hex River mega-anticline (interlimb angle is 120°).

The wavelengths of the western megastructures are of the order of 10 kilometres, while the amplitude is about 1 kilometre. The form of the mega-anticlines approximates Class 1C of Ramsay (1967). Second-order folds commonly occur in the outer arc (Nardouw Subgroup) of the mega-structures, above the Cedarberg shale. These folds generally have a kink form and are best developed in the Goudini Formation, probably because of its silty interbeds and proximity to the Cedarberg shale which

Stellenbosch University http://scholar.sun.ac.za

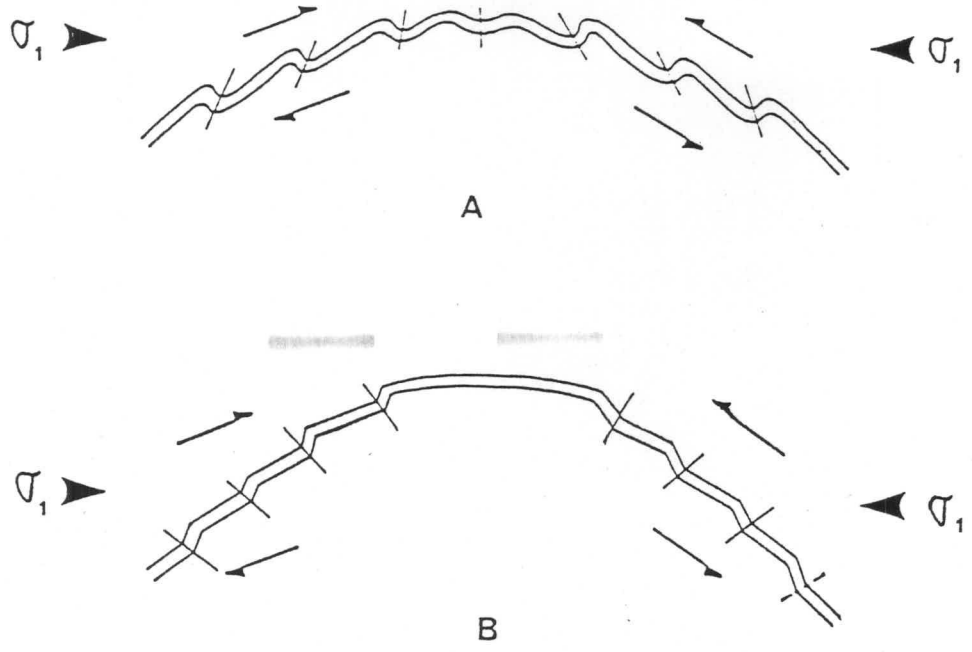

Figure 4.1
Difference in axial plane orientation between drag and kink folds on the limbs of a megastructure, given the same shear directions (σ_1 = direction of maximum compression).

Figure 4.2
Kinks in the Nardouw Subgroup on the southern limb of the Hex River mega-anticline.

Stellenbosch University http://scholar.sun.ac.za

clearly acted as a major décollement horizon in the megastructures. Such kinks are well-displayed in basal Goudini quartzites on the southern limb of the Hex River mega-anticline (Figure 4.2). Tighter megastructures like the Hansiesberg mega-anticline, exhibit even more second-order structures in the Skurweberg and Rietvlei Formations. The kinks display an opposite sense of vergence to that of common drag folds on the limbs of megastructures, that is, the short limb faces away from the mega-anticlinal axial plane and not towards it (Figure 4.1A and B). This property of kink folding has been well documented by Reches and Johnson (1976), who attributed the phenomenon to different combinations of layer-parallel shear and shortening, which apparently depend upon initial fold amplitudes, slope angles of layers relative to maximum compressive stress, strength of contacts between layers and sequence of deformation (see also Ramberg and Johnson, 1976).

Reches and Johnson (1976) concluded that monoclinal folds with one dominant vergence direction, develop when the principal stresses are inclined to bedding at more than 5 degrees. This suggests that the kinks in Figure 4.1 developed either simultaneously with, or later than the megastructure, with compression being horizontal throughout. Slight back-rotation of beds adjoining the monoclinal kinks (Reches and Johnson, 1976, p.326) sometimes led to the formation of second-order folds with one slightly rounded long limb and a short, straight limb. This type of fold was seen on the eastern limb of the N-S striking Witzenberg mega-anticline.

Stellenbosch University http://scholar.sun.ac.za

However, a large second-order fold of approximately kink form and very low amplitude, with opposite vergence to those described above, occurs in Peninsula quartzites on the same limb of the Witzenberg mega-anticline. This could indicate that the shear sense may have been reversed below the Cedarberg shale and that the interpretation of kinks in terms of megastructures in the Table Mountain Group is not all that simple.

That the so-called "Fold Zone" in the uppermost Peninsula Formation resulted from penecontemporaneous folding as shown by Blignault (1970) and Hälbich (1983), is evident from the overall style of these folds, combined with the intense fracturing and quartz veining that occur in them, in both the Hansiesberg and Hex River mega-anticlines. The presence of penetrative lineations parallel to the fold axes provides further evidence of a soft-sediment state during initial folding, very similar to that in some Witteberg rocks (see section on lineations). In the Skurweberg mega-anticline, folds of the "fold zone" show interlimb-angles of approximately 135 degrees. Amplitudes are of the order of 40 metres and wavelengths of 100 metres on average. The folds are sinusoidal and rounded in profile with axial planes that dip at 60 degrees towards the megastructure axial trace.

Table Mountain Group fold styles are illustrated in the Witzenberg and Hex River Mountains structural profiles which accompany the section on orientation analysis (Figures 5.2 and 5.4).

Stellenbosch University http://scholar.sun.ac.za

4.2 BOKKEVELD GROUP

Folding in this stratigraphic entity is of the open, upright, symmetrical type and folds mostly belongs to class 1B of Ramsay (1967). Few second-order folds developed in the western part of the Ceres syntaxis. Bokkeveld folds in the Baviaanshoek, as well as in the Ceres intermontane valley, display wavelengths of 0,5 to 2 kilometres (1 kilometre on average), and amplitudes of a few metres to a few tens of metres. Fold axial planes are normally vertical, but exceptions occur to the north in the Baviaanshoek (Map 1) brachi-anticlinorium. The approximately sinusoidal form of the buckle folds was controlled by the competent sandstones in the succession, while incompetent units reacted by thickening, without cleavage formation. As most of the Bokkeveld Group consists of incompetent mudrock and shale (Table 2.1), this thickening resulted in a fan of fold axes with Ceres situated at the centre of divergence. This deformational pattern, as well as the low fold intensity, prohibited the formation of interference folds on a meso-scale.

The general appearance of a typical fold in Bokkeveld lithologies is depicted in Figure 4.3. Hinge dilation commonly results in thick, short quartz veins between silty and quartzitic beds. In competent beds the hinge area displays (a-b) quartz veins approximately parallel to the axial plane in the crest. These veins are reoriented towards the bedding attitude near the bottom of the beds. Unfilled short fractures that are oblique to the axial plane, occur on the limbs. Some

Stellenbosch University http://scholar.sun.ac.za

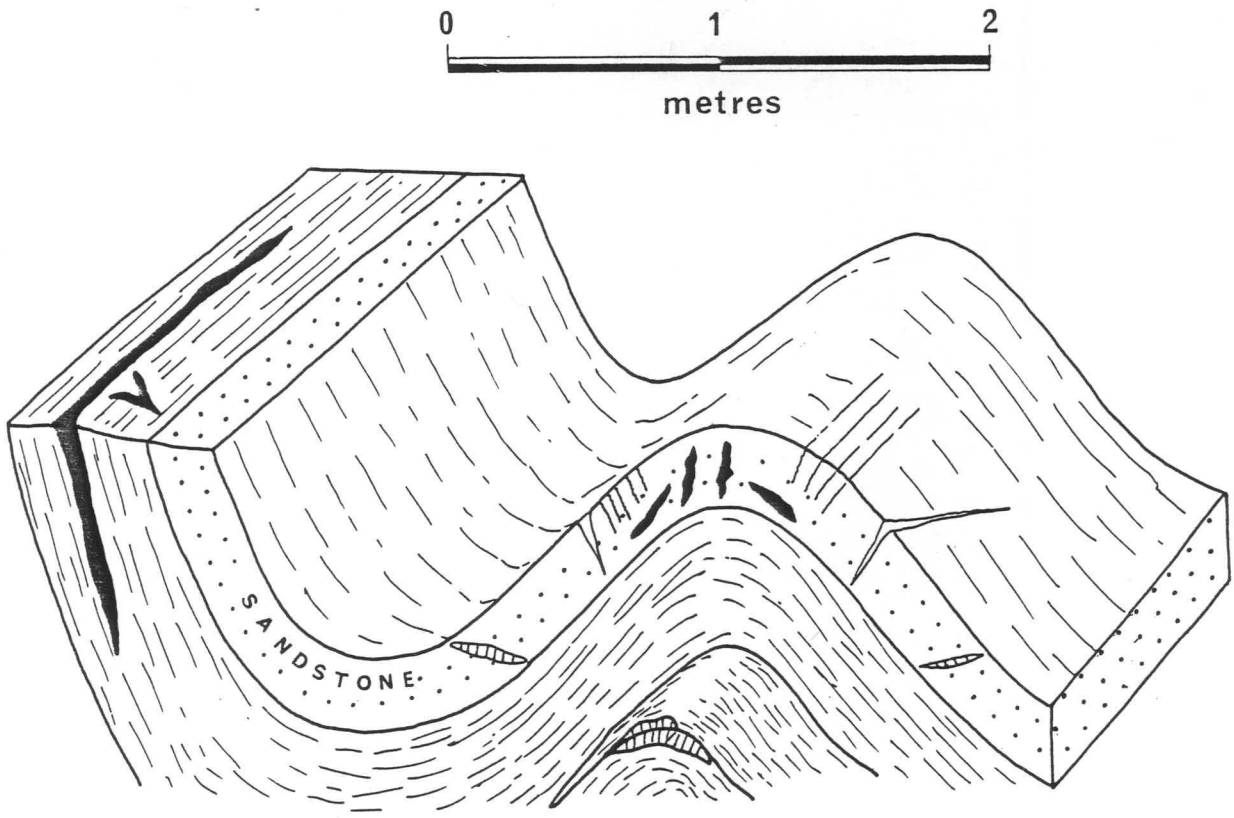

Figure 4.3
General character of Bokkeveld folds. The quartz in some veins is massive (black), while other veins contain fibrous infillings. Other late fractures in the sandstone near the fold crest are unfilled.

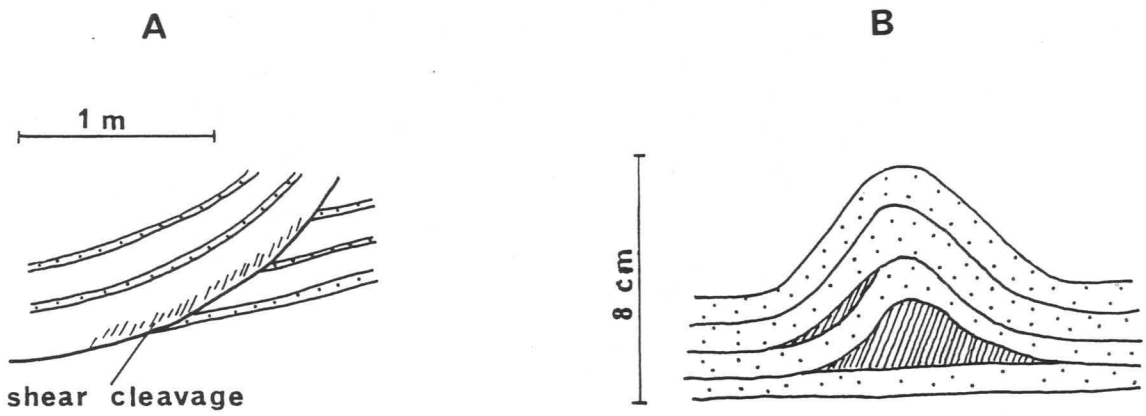

Figure 4.4
A: Faint shear cleavage developed in shale near slip plane on sedimentary channel contact.
B: Massive quartz filling of dilational spaces that developed during folding.

Stellenbosch University http://scholar.sun.ac.za

bedding-parallel, dilational quartz veins in silty layers often display quartz fibres that grew approximately parallel to the local fold axis. Some small listric faults that originated on bedding or cross-laminations are frequently encountered.These faults may be either unfilled or lined by quartz fibres that grew parallel to the slip direction. Sometimes, a mild shear cleavage developed adjacent to some slip planes (Figure 4.4A). Some small folds (Figure 4.4B) contain large massive quartz segregations that formed in voids, due to bedding plane décollement and elastic folding.

The open, sinusoidal fold style in Bokkeveld sediments is compatible with deformation of a sequence which had almost zero contact strength between the layers, as well as high competency contrasts (Honea and Johnson, 1976). These properties of the Bokkeveld Group are very different from that of the overlying Witteberg Group and are mainly responsible for the difference in fold style as outlined below.

4.3 WITTEBERG GROUP

Large folds in the Witteberg Group are never sinusoidal, they rather approach the form of complementary kinks with rounded hinges (box folds). Abundant slickensides on bedding planes and constant bed-normal thicknesses, indicate that they are flexural slip folds. These structures, in which bedding maintains a near constant orientation between adjacent hinges, and the hinges are very narrow with respect to limb lengths, are characteristic of the Witteberg Group. Lone monoclinal

Stellenbosch University http://scholar.sun.ac.za

"megakinks" and conjugate sets of megakinks affecting hundreds of metres of sediments, occur from the base of the Witteberg Group to the Floriskraal sandstone at the top. Sometimes, the uppermost Bokkeveld sandstone (Osberg Formation) also conforms to basal Witteberg (Wagendrift Formation) megakinking by showing long, straight limbs and narrow hinge zones. This feature can be seen in the Baviaanshoek area, just east of Wamakershoogte (Wagenmakers Hoogte 270). The kink-like fold style is believed to have been entirely a response to the character and configuration of Witteberg lithologies.

One major "anticlinorium" of Witteberg rocks can be demarcated in the Ceres Syntaxis. Only the Baviaanshoek (Map 1) "brachi-anticlinorium", which has Bokkeveld beds exposed in its core, can be termed a "first-order" structure. This structure, which has a half-wavelength of about 11 kilometres and structural relief of the order of 700 metres, has smaller kink folds on its limbs. All other major kink-like folds in the Witteberg rocks of the Ceres Syntaxis have a size approximately similar to that of these second-order structures on the limbs of the Baviaanshoek megastructure. Conjugate megakinks are rarely cylindrical, because hinge-lines are seen joining each other in a conical fashion in many instances (Map 1). Single sets of kinks (monoclines), with similar vergence directions, also join in the same fashion. Complexities such as doubly plunging and en-echelon folds, abrupt termination of folds, and changes in fold trend, occur throughout. It is remarkable how these intricate Witteberg kink patterns faithfully recorded the complex local stress variations that existed in the Ceres

Stellenbosch University http://scholar.sun.ac.za

Syntaxis. The largest folds in the area are more than 12 kilometres long and involve units on formation-scale (tens to hundreds of metres). Similar styles of folding were described by Faill (1973) in the Appalachians, Laubscher (1976) in the Jura, and Rixon et al. in New South Wales.

Although deformation intensity in the Witteberg Group appears to be higher than that of the Bokkeveld Group, the shortening in the former was confined to narrow zones, and it is believed that no major structural discontinuity exists between the two stratigraphic entities. The absence of major thrust ramps that underlie steep monoclines or megakinks, supports this statement. Kink and conjugate folds may form in layered or laminated rocks at small to moderate values of shortening (Ghosh, 1967; Ramsay, 1967). Megakinking in the Witteberg Group is typified by the Baviaansberg structures (Figure 4.5), which will be described below.

Baviaansberg, situated on the farms Tolsberg 275 and Baviaansberg 274 (3319BA), displays a large conjugate pair of megakinks. The kinks face towards each other, thus forming a synclinal mega-box fold that affected about 1200 metres of Witteberg and uppermost Bokkeveld beds. Bedding in the southern kink dips nearly 80 degrees to the north, while that in the northern kink dips about 60 degrees south. The structure as a whole thus suffered a slight clockwise rotation and is not strictly upright. Orientation data of the structure are given in Figure 4.6. All structural elements lie more or less along a well-defined great circle and small fold axes plot

Stellenbosch University http://scholar.sun.ac.za

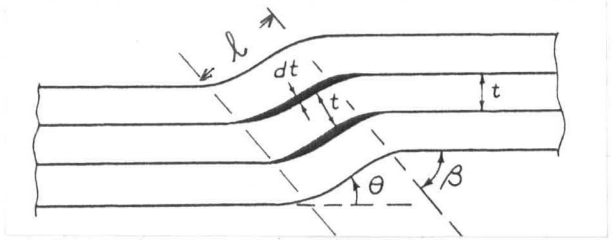

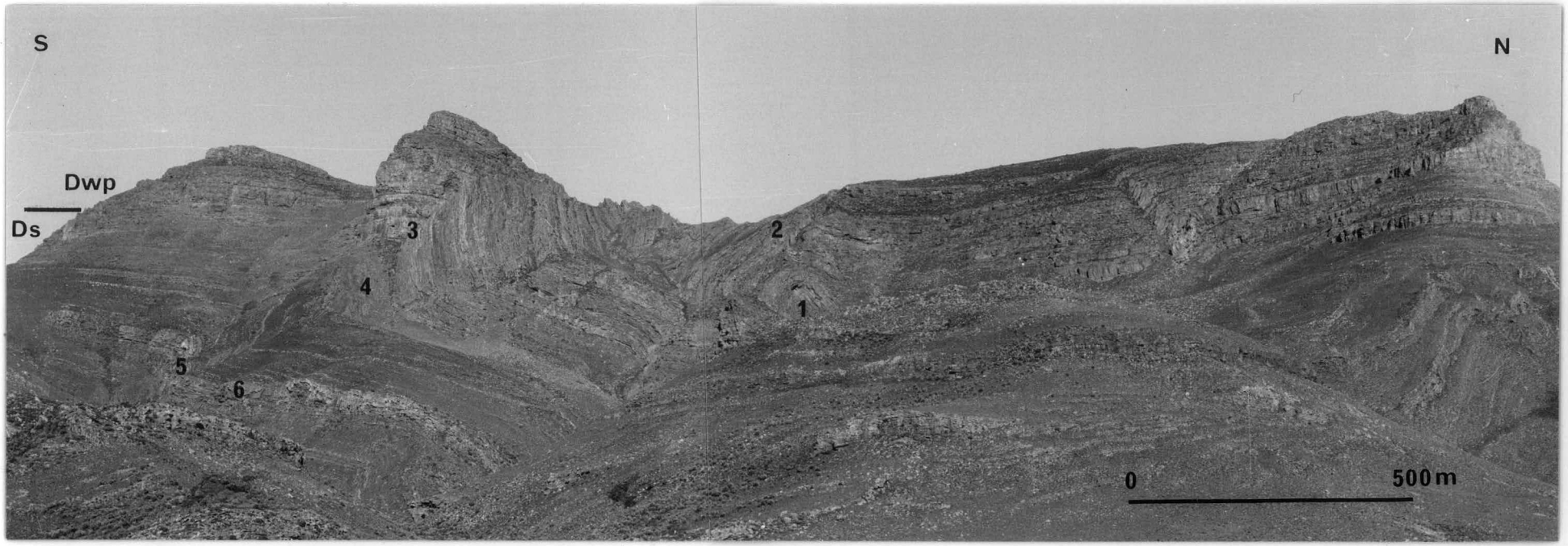

Figure 4.5
The Baviaansberg conjugate megakink. Numbers refer to text and scale to steep cliffs in background. Inset from Reches and Johnson (1976), where: t = bed thickness; dt = dilation; l = width of kink band; Θ = angle between bedding inside and out-side kink; ß = angle between bedding outside kink and kink axial plane. Dwp = Witpoort Fm., Ds = Swartruggens Fm.

Stellenbosch University http://scholar.sun.ac.za

near the two kink axes at 080/0 and 078/0, thus indicating near-cylindrical geometry.

The characteristics of the two kinks are not the same. The southern kink shows a sudden, sharp bend of horizontal quartzitic sandstone beds in the Witpoort Formation and bedding stays parallel throughout the kink, without any signs of buckle folding. It also retains its kink form downwards into beds of lower competency. The northern kink, in contrast, displays upper straight kinked beds and sinusoidally folded lower beds (1, Figure 4.5) in the same Witpoort quartzites affected by the southern kink. As a result of the disharmony between the upper beds and the immediately underlying beds, the kinked limb appears to "die out" in the lower strata. A smaller subsidiary kink of lesser intensity formed just south of the northern megakink in the slightly northward-dipping, intermediate limb that connects the two megakinks. This smaller kink extends down into underlying incompetent beds.

Growth of the anticline in the lower part of the northern kink was probably stimulated when dextral slip along the beds inside the kink also spread to the foliation outside the megakink (Reches and Johnson, 1976; Stubley, 1989). Though it most probably existed only as a small " pucker" right from the time when the kink was initiated (Reches and Johnson, 1976), excessive growth of the anticline probably also resulted from adjustments that were necessary to accommodate hinge and interlayer dilation while bedding in the upper, relatively straight part of the kink was undergoing rotation and

Stellenbosch University http://scholar.sun.ac.za

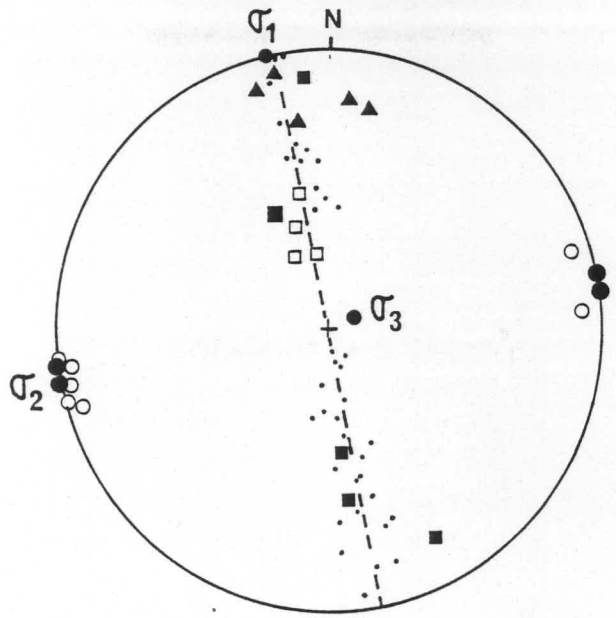

Figure 4.6
Orientation data for the Baviaansberg megastructures.
• = bedding poles; ○ = small fold axes; ● = megakink axes; □ = slickenfibres; ■ = kink plane poles; ▲ = cleavage near kink plane; σ_1, σ_2 and σ_3 = principal stress axes.

Figure 4.7
Southern megakink plane in the upper competent sandstones. Height of the section is approximately 100 m.

Stellenbosch University http://scholar.sun.ac.za

concomitant dextral bedding-parallel shear. It is also possible that the removal of material from that part of the northern kink which underlies asymmetric "shear folds" higher up, provided the space for the anticlinal upright fold to form.

It is important to note that this large anticlinal fold is upright and rounded, while smaller folds higher up in the kink display strong asymmetry and axial planes that dip steeply south (2, Figure 4.4). The vergence of these asymmetric folds is consistently towards the north, which indicates northward movement of beds over one another during continued rotation of the kink limb. The latter also corroborates a dextral shear sense inside the kink. The sense of movement described here is also consistent with that of oblique thrusting that would have occurred during continued rotation of the kink (Laubscher, 1976), if the sinusoidal folding had not occurred. The anticline is probably upright, because the external direction of maximum compression was near the horizontal (see later).

The differences between the southern and northern megakinks are evidently attributable to heterogeneous slip and sticking in the northern kink during rotation of the kink segment, combined with disharmonic folding which made use of slightly less competent units. In the southern megakink, homogeneous, well-distributed, bedding- parallel slip occurred.

The southern megakink has straight boundaries that dip 36 degrees and 20 degrees to the south respectively (Figure 4.5). This non-parallelism of the kink boundaries causes them to

Stellenbosch University http://scholar.sun.ac.za

converge downwards upon one another. The kink segment therefore attains a maximum width (ℓ" in Figure 4.5) of 100 metres in the upper competent Witpoort quartzitic sandstone, and becomes progressively narrower in lower, less competent Swartruggens beds. The ratio of hinge to kink limb width is about 1:20, which demonstrates the highly angular fold style.

Considering the scale of the structures, Witteberg kink boundaries are amazingly smooth when viewed from a distance. Closer inspection of the southern megakink hinge (Figure 4.7), however, displays a number of features related to hinge dilation and expulsion of redundant material which must take place on the concave side of such structures (Laubscher, 1976). Slightly asymmetrical, open concentric folds with their axial planes oriented subparallel to the southern kink boundary, occur in less competent layers (3, Figure 4.5 and Figure 4.8). The folding is accompanied by severe fracturing in the more competent layers and intense shearing of incompetent siltstone beds. The fractures are of the open, unfilled type and may enclose slightly rotated segments of bedding similar to that observed by Laubscher (1976) in the Jura. A crude axial plane cleavage (Figure 4.9) is sometimes observed in intensely disharmonic small folds which fill these hinge dilations.

The effects of dilation and expulsion of redundant material in the angular hinges were probably minimized by the presence of many so-called "subsequences"in the multilayer. In these subsequences, the competent beds with high contact strength would have resisted bedding-parallel shear to a large extent.

Stellenbosch University http://scholar.sun.ac.za

Figure 4.8
Severe fracturing and slightly asymmetric minor folds in the kink hinge zone (rod = 1,8m).

Figure 4.9
Crude cleavage in silty interbeds at the kink boundary (upper left hand side of photograph).

Stellenbosch University http://scholar.sun.ac.za

On the other hand, shearing would be concentrated in the incompetent layers due to their lower contact strength, and buckles could form in the dilational space in the hinge. The extent to which this would happen, depended largely upon interlayer competency contrast. The existence of many such subsequences in the Witteberg rocks had the effect of distributing the strain more evenly through the multilayer. This gave rise to the relatively smooth kink plane at the level of the competent Witpoort Formation.

The rotated short limb of the southern megakink shows unfolded, straight beds in the upper competent part (Witpoort Formation) of the multilayer and intense folding, accompanied by compressional faulting in incompetent layers of the Swartruggens Formation below (Figure 4.5). This difference in deformational behaviour is again mainly attributed to differences in competency contrast and interlayer strength. Buckling in the kink limb would only have been possible while the layers were still inclined at less than 45 degrees to the direction of maximum compression (σ_1). During later stages of development the resistance to layer-parallel shear and folding would have largely increased due to σ_1 operating subperpendicular to the bedding.

In the competent quartzites, the layers rotated passively while making use of thin interbedded siltstone and shale to accommodate the shear. The high shear modulus between quartzite beds prohibited much intra- and interbed movement, thus the bedding remained parallel.

Stellenbosch University http://scholar.sun.ac.za

The net strain in the competent Witpoort Formation, therefore, probably consists of syn- and post-compaction, layer-parallel shortening, followed by passive rotation and slip on silty layers during kinking. It seems unlikely that sideways migration of the kink boundaries (Ramsay, 1967) acted as a growth mechanism for megakinks in these competent quartzitic sandstones. It is more likely that the kink boundaries were already fixed at the onset of kinking as depicted by model 2 of Ramsay (1967, p. 452).

Less competent beds of the Upper Swartruggens Formation that underlie the competent, straight kink limb (4, Figure 4.4), display intense disharmony. A train of numerous small folds with nearly equal wavelengths and amplitudes developed in these beds. The axial planes of the folds are subparallel to the kink boundaries. Folding quickly dies out across the kink boundaries. These folds were formed, because competence contrast in the silty beds was higher than in the overlying pure sandstone, thus passive rotation in the quartzitic sandstone was accompanied by buckle shortening in the incompetent beds (while σ_1 was still favourably oriented towards bedding). This is the probable mechanism whereby wide kinked segments become narrower in incompetent beds, and eventually die out in the Witteberg multilayers.

The folds described in the previous paragraph thus represent a major décollement below the competent quartzitic sandstones whereby dilation perpendicular to, and shear parallel to bedding (Laubscher, 1976) were relieved. The above-mentioned

Stellenbosch University http://scholar.sun.ac.za

disharmony disappears abruptly lower down in the kink limb, where relatively pure siltstones deformed mainly by thickening and volume loss (expelling of pore fluids).

However, 160 metres below the base of Witpoort Formation, the upper one of two prominent quartzitic sandstone units in the Swartruggens Formation, again displays intense folding and reverse faulting in the short, kinked limb (5, Figure 4.5 and Figure 4.10). The width of the kinked segment here, as measured along the enveloping surface of the folds, is only 50 metres. The quartzitic unit is embedded in less competent layers (Figure 4.11). More buckle shortening therefore occurred at this level within the southern megakink. The sense of asymmetry displayed by the folds show that they resulted from left-lateral layer-parallel shear. This is consistent with the right-lateral (clockwise) external rotation of the southern megakink as a whole. The southern and northern folds in Figure 4.10 have axial planes that dip 78 and 75 degrees north, respectively. The former axial plane is markedly curved and is cut by a reverse fault (Figure 4.12). The apparent displacement on the fault, which steepens out of bedding along the northern limb and cuts across the southern limb at an angle of 70 degrees, is about 7 metres. Quartz fibres on the fault plane indicate dominantly north-south movement. The absence of multiple fractures subparallel to this fault, indicates that movement occurred under relatively hydroplastic conditions. A crude axial plane cleavage accompanies bulging and thickening of shale in the fold crest. In this part of the kink, the folds developed mainly because of a high contrast in

Stellenbosch University http://scholar.sun.ac.za

Figure 4.10
Intense folding and faulting in Swartruggens sandstones, surrounded by incompetent beds at (5) in Figure 4.5. Height of the section is approximately 80 m.

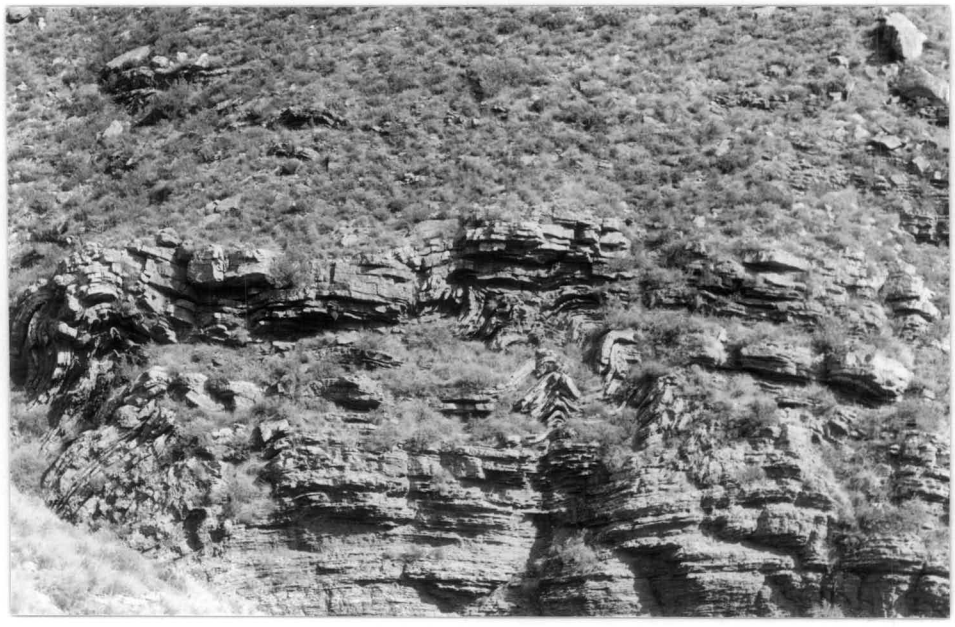

Figure 4.11
Incompetent, thin-bedded siltstones below the sandstones of Figure 4.10. Note severe disharmony of folding. Height of the section is about 30 m.

Stellenbosch University http://scholar.sun.ac.za

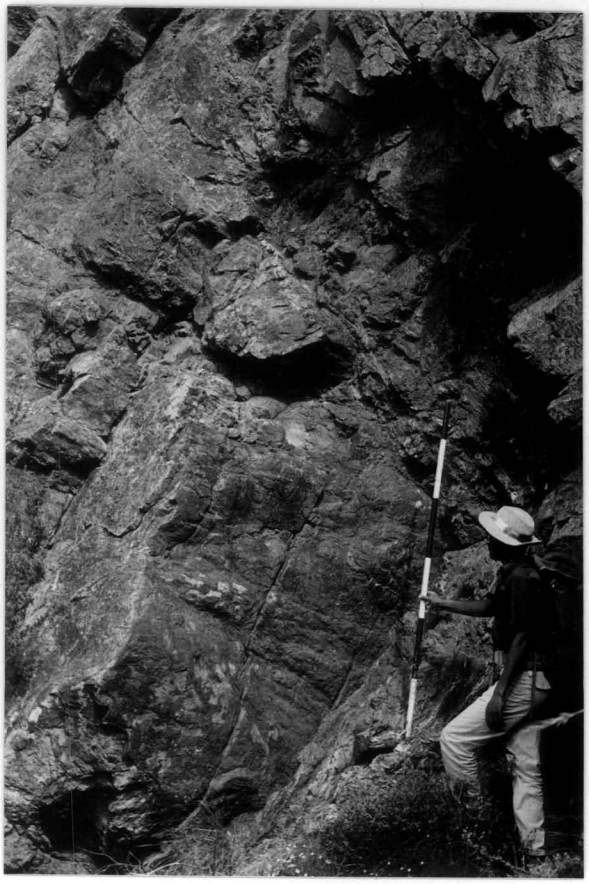

Figure 4.12
Reverse fault running from upper left hand side to lower right hand side of photograph. Locality at upper fold in Figure 4.10. Length of scale rod is 1.8m.

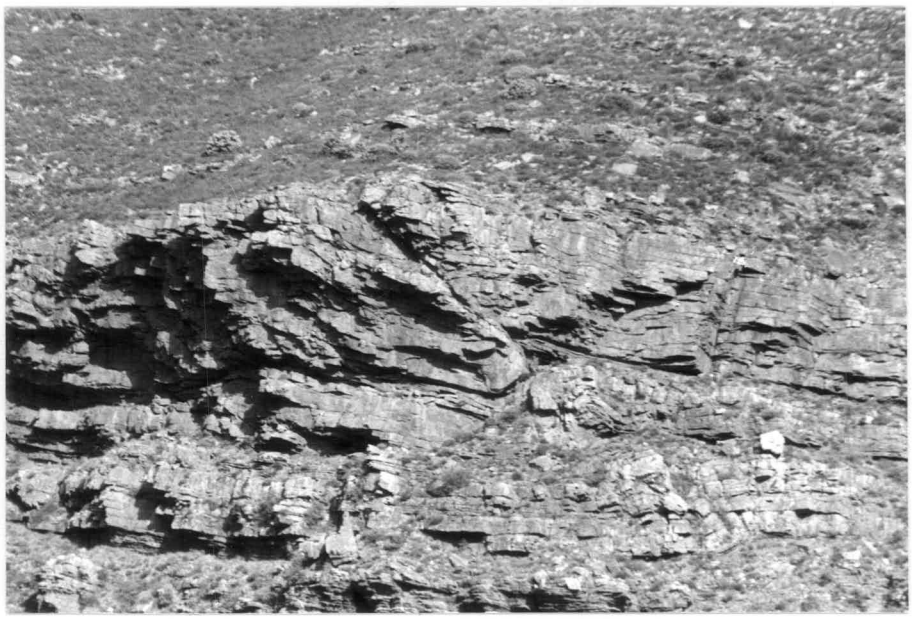

Figure 4.13
Local disharmonic folds and reverse fault developed in flat lying limb of the quartzites depicted in Figure 4.10 north of the southern megakink. Height of section is about 70m.

Stellenbosch University http://scholar.sun.ac.za

competency, because the quartzitic sandstone beds were embedded in incompetent layers (Ramberg, 1964).

Bedding-parallel compression during initial rotation of the kink produced the folds and reverse faults, while the subsequent bedding-normal attitude of σ_1, resulted in additional flattening of the folds. The character of the reverse faults indicates that the beds were still unlithified, which, in turn points to their early formation. Thus, by folding and faulting, the width of the kinked segment could have been reduced to half of its original width as displayed in the upper competent Witpoort quartzitic sandstones.

The flat-lying limb north of the kink zone also shows local reverse faulting and asymmetric folding in this competent sandstone unit (6, Figure 4.5). Small disharmonic, upright folds that developed above thinly laminated siltstones, become progressively more asymmetric in overlying layers and eventually die out in competent beds as a reverse fault (Figure 4.13). The vergence of these asymmetrical folds is again consistently towards the south, as would be expected for right-lateral kinking at the southern kink.

The so-called "locking angle" of kinks has received widespread attention in the literature (Dewey, 1965; Ramsay, 1967; Reches and Johnson, 1976; Collier, 1978). This locking of the fold is likely to occur at limb dips somewhere between $60° \leq \Theta \leq 80°$ (Θ = angle between bedding inside and outside the kink).

Stellenbosch University http://scholar.sun.ac.za

The main problems in estimating the value of this angle for a specific sequence, lie in estimating the amount of dilation ("dt" in Figure 4.5) that occurred in the kink. As stated earlier, bedding-parallel shear strain diminishes rapidly when the kink boundary becomes inclined at angles of more than 45 degrees towards the maximum compression. The kink band will then lock, due to an increase in compression normal to the layers. If the angle ß (Θ and ß as in Figure 4.5) is smaller than that predicted by the equation ß = (90 -Θ/2), there will be thickening of layers ("dt" in Figure 4.5) within the kink (For a full explanation of theory, see Reches and Johnson, 1976). This will compensate for the rise in normal stress due to continued rotation and increase the locking angle (Θ) of the layers. The southern megakink at Baviaansberg displays angles of 36 degrees and 80 degrees for ß and Θ respectively. Substitution of these values into the above equation, shows that dilation in the kink limb must have occurred during the later stages of rotation.

On the other hand, there will be thinning of layers within the kink band, thereby causing the layers within the band to lock at lower angles. However, the narrow spacing of bedding surfaces in the sequence and the substantial width of the kink band, resulting in low t/ℓ (Figure 4.5) values Ramsay (1967), would have further facilitated rotation of the multilayer beyond the theoretical locking angle. The observed limb dip inside a kink is also dependent on the level of exposure of the structure, because it decreases as the folding dies out towards the top and bottom. Although some kinks in the Witteberg Group

Stellenbosch University http://scholar.sun.ac.za

of the Ceres Syntaxis display locking angles of almost 90 degrees, the angle varies mostly between 30 and 60 degrees Because the locking angle is related to prevailing stress conditions, it can also be modified later by increasing the stress ratio (Reches and Johnson,1976).

Because of the conjugate character of the Baviaansberg megakinks the external direction of maximum compression must have stayed within ± 5 degrees of the original attitude of bedding. Conjugate kinks may be used to determine the orientation of the principal stresses, σ_1, σ_2, and σ_3 (Ramsay, 1962). The derived orientations of these are shown in Figure 4.6. The overall asymmetry of the box fold which formed, indicates that the bulk shear sense was right-lateral (Reches and Johnson, 1976, p.324), with σ_1 inclined towards the north at a low angle. Conjugate megakinks similar in size to the Baviaansberg structures, are uncommon in the Ceres Syntaxis. Instead, large kinks are usually of the lone, monoclinal type. This implies that σ_1 was only rarely oriented at a low angle to bedding on a mega-scale. Smaller conjugate structures, however, are quite common.

Stellenbosch University http://scholar.sun.ac.za

5. REGIONAL ORIENTATION ANALYSIS

Two main structural trends developed in the Ceres Syntaxis. The western and northern parts of the area are dominated by N-S to NNW-SSE trending structures, while the NE-SW trend prevails over much of the southern and central sector (Figure 5.1, Map 1). Northerly oriented structures die out east of the investigated area in Ecca Group sediments, while north-easterly oriented structures disappear abruptly near the northern boundary of the syntaxis (Map 1). Interference of the two main trends result in many minor structures of intermediate orientation. The extent to which one or the other trend predominates, largely controls outcrop patterns of the Witteberg Group subunits. The Bokkeveld Group outcrop pattern, on the other hand, is mainly controlled by that of the underlying thick arenitic Table Mountain Group and consequently displays no "real" interference effects. The Baviaanshoek brachi-anticlinorium is an exception to the rule in so far as it clearly shows short, curving, fold axes. Real interference between the north-westerly and north-easterly trends occurs between conjugate or single megakinks with their associated smaller-scale structures, which intersect one another at varying angles in the Witteberg Group. Subareas for the orientational study are shown in Figure 5.1.

5.1 BEDDING

Composite structural profiles will be used to illustrate the regional variation of structures from west to south-east across

Stellenbosch University http://scholar.sun.ac.za

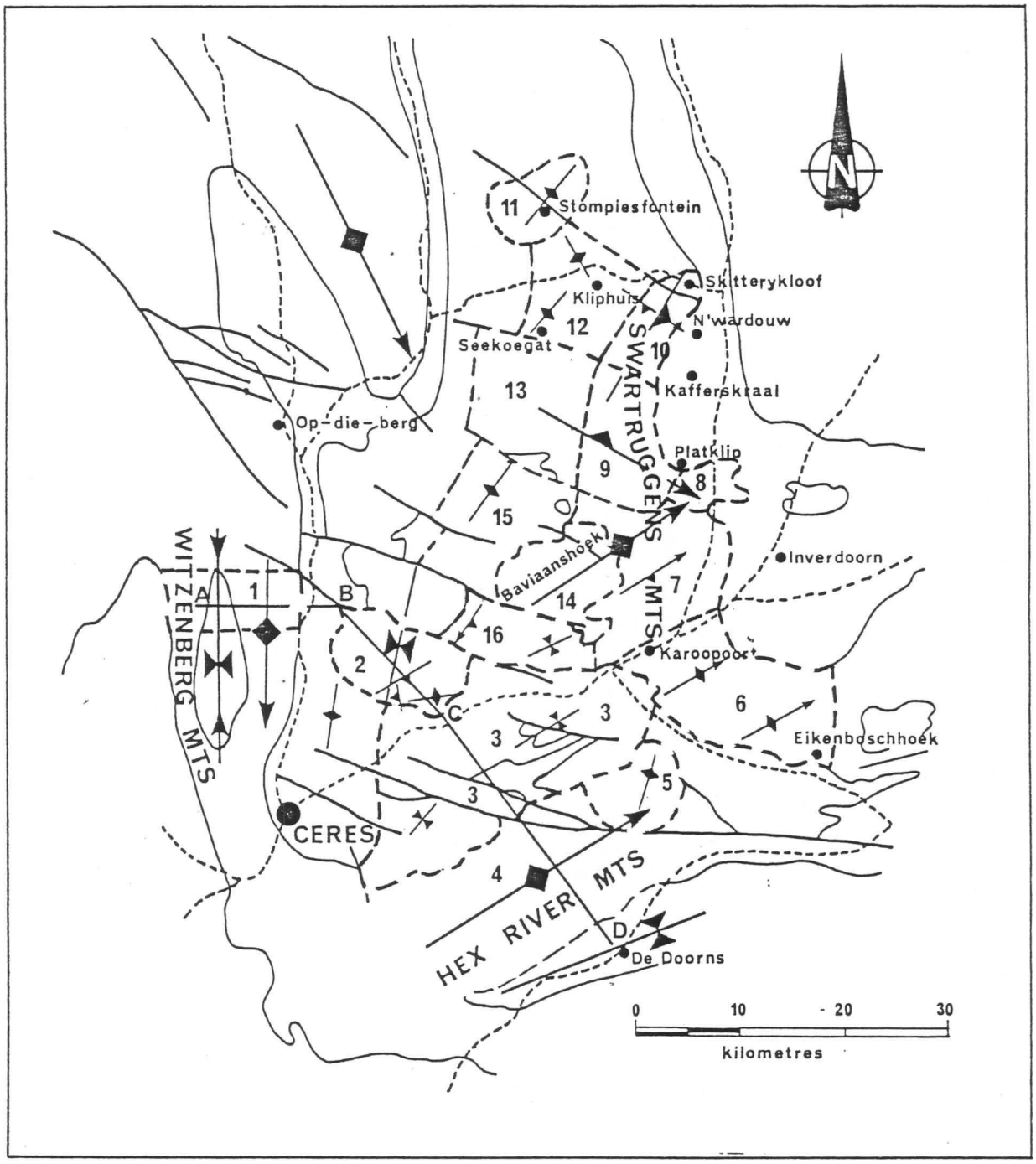

Figure 5.1
Structural domains in the Ceres Syntaxis. Domain boundaries are indicated by thick broken lines that follow lithological boundaries and faults. Section lines AB, BC and CD relate to Figures 5.2, 5.3 and 5.4, respectively.

Stellenbosch University http://scholar.sun.ac.za

the southern Ceres Syntaxis. Profiles AB, BC and CD were drawn perpendicular to the average fold axis trends of subareas 1,2,3, and 4. Bedding-poles for Subarea 1 in Figure 5.2 define a great circle with pole at 190/6 for the western Witzenberg megastructures. The bedding is slightly steeper on the eastern limb of the Hansiesberg mega-anticline than on the western limb, but the axial plane is nearly vertical. Bedding-poles from the Bokkeveld, Nardouw and Peninsula beds, all lie along the same great circle. This is not surprising for the Bokkeveld folds and the Nardouw kinks, but it is certainly peculiar that bedding poles of folds in the Peninsula "Fold Zone" (Blignault, 1970) also coincide with this same great circle. This general parallelism between older and younger deformational trends probably points to some form of basement and/or tectono-sedimentary control, as suggested by Hälbich (1983).

Profile BC (Figure 5.3) for Subarea 2, covers portions of the central part of the syntaxis which is mostly underlain by Lower Witteberg Group rocks. The two girdles on the bedding pole diagram with poles at 020/8 and 078/0, indicate that the fold trend varies from slightly east of north to slightly north of east. The non-cylindricity of symmetric and asymmetric conjugate folds and single monoclines, sometimes with crossing axes, as well as the variable axis attitudes, result in a rather wide spread of bedding poles along the great circles.

Profile CD (Figure 5.4) transects the Ceres intermontane valley (Subarea 3) and Hex River Mountain mega-anticline (Subarea 4).

Stellenbosch University http://scholar.sun.ac.za

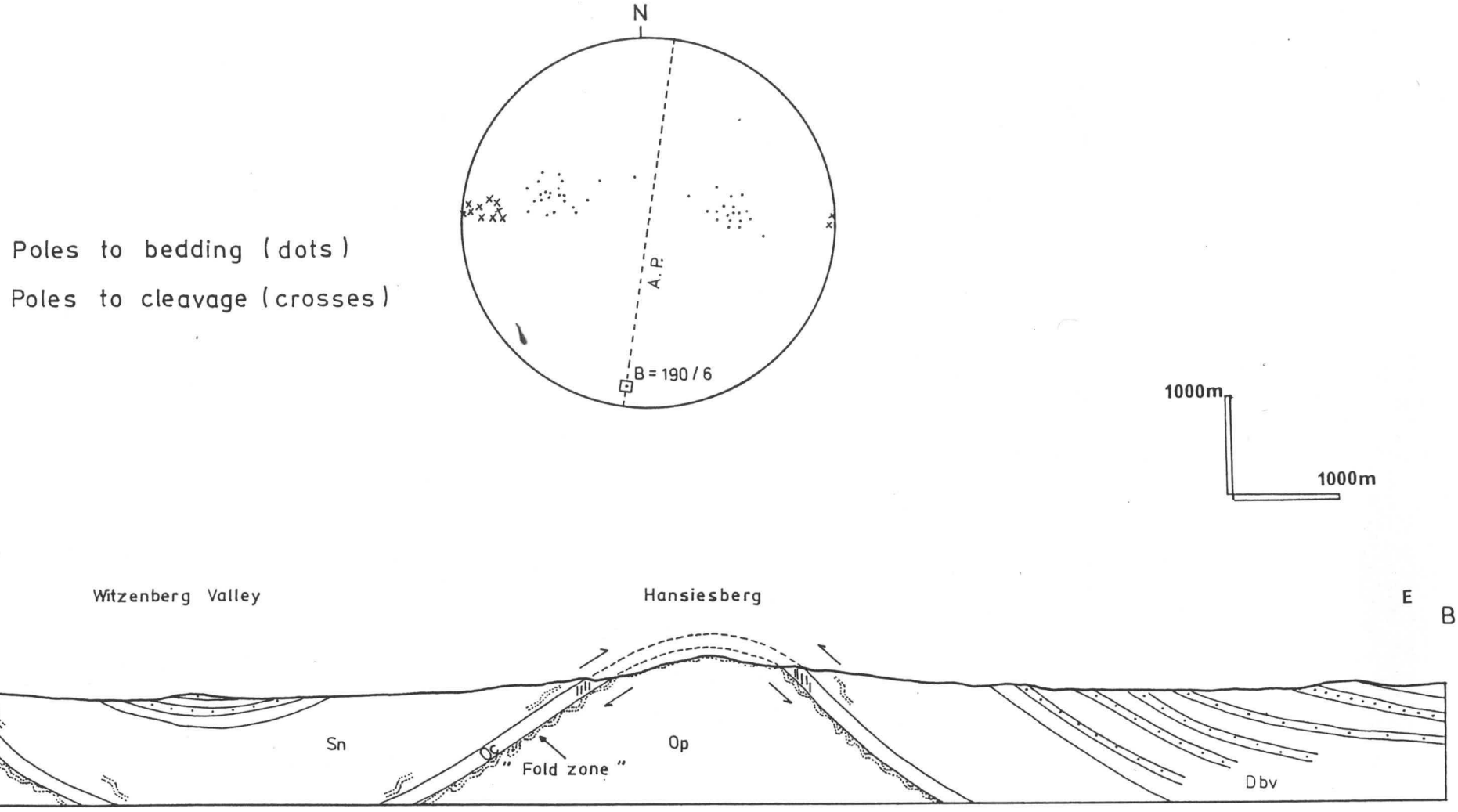

Figure 5.2
Profile AB depicts the western Ceres Syntaxis from the Witzenberg Valley in the west to north of Gydo Pass in the east. Note the kink vergence directions and cleavage orientation. Op = Peninsula Formation; Oc = Cedarberg Formation; Sn = Nardouw Subgroup; Dbv = Bokkeveld Group (sandstones are stippled).

Stellenbosch University http://scholar.sun.ac.za

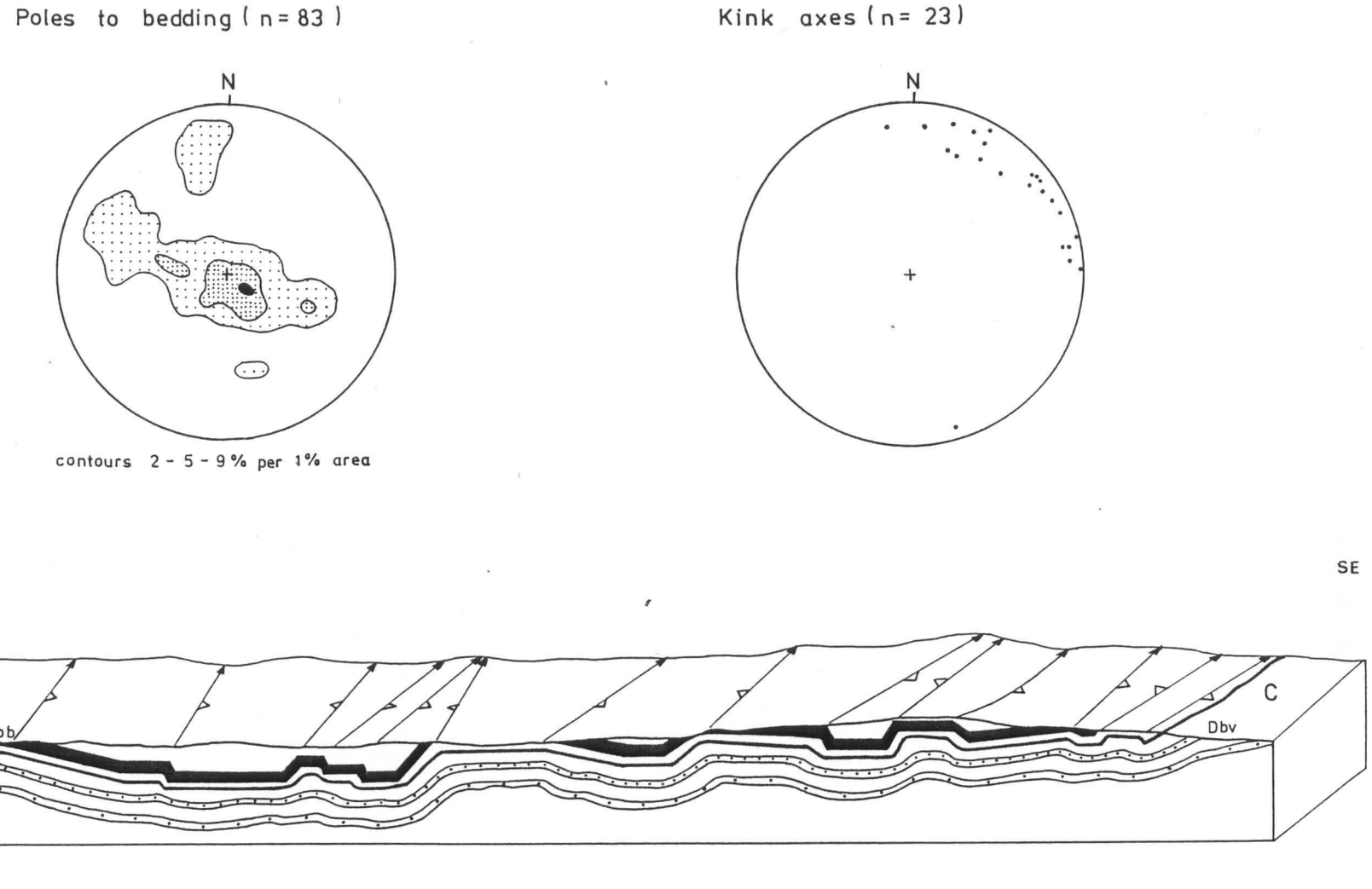

Figure 5.3
Profile BC from north of Gydo Pass to Theronsberg Pass. Thick black line is base of Witteberg Group, Dbb is Blinkberg Formation, Dbv is Bokkeveld Group.

Stellenbosch University http://scholar.sun.ac.za

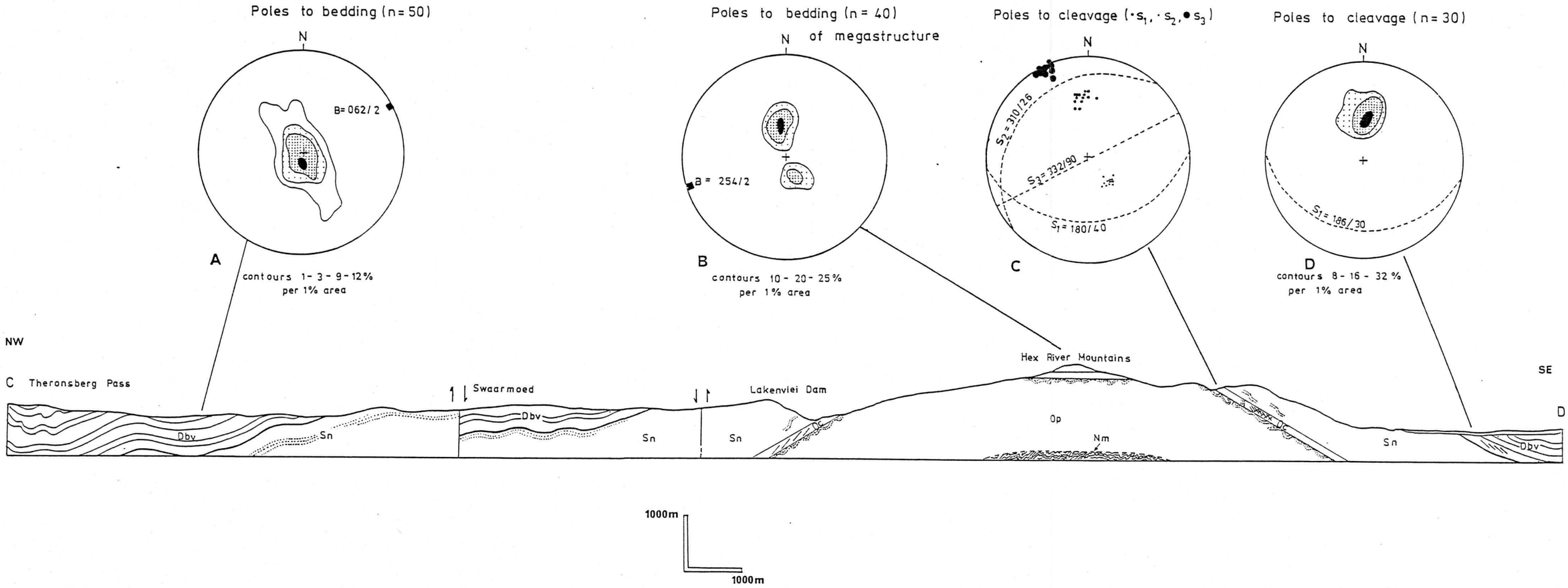

Figure 5.4
Profile CD from Theronsberg Pass to the Hex River Valley. Symbols the same as in Figure 5.3. For further description, see text.

Stellenbosch University http://scholar.sun.ac.za

Bokkeveld bedding poles from Theronsberg Pass to Swaarmoed, define a great circle with pole at 062/2. The fold limbs dip between 0 and 45 degrees. Axial planes are near vertical over most of the area.

Bedding poles of the Hex River Mountain mega-anticline describe a great circle with pole at 254/2, very similar to the attitude of the Bokkeveld Group north of it. The axial plane of the structure is nearly upright and the interlimb angle is 117 degrees. The above values only hold for the sector along the megastructure where the fold axis is nearly horizontal. Near its north-eastern termination, the bedding abruptly changes dip to steeply north-east and the anticline becomes double- crested. Bedding poles at the northern closure (Subarea 5, Figure 5.5A) best fit a great circle with pole at 028/28, though there is a slight tendency towards a small circle. The axis of this closure trends more towards the north, while the southern closure (not plotted), trends almost E-W. The northern closure may have formed, due to local NE-SW directed compression, related to the N-S structural trend in the Ceres Syntaxis.

Subarea 6 (Figure 5.5B), which includes Bokkeveld, but mostly Witteberg beds, shows a fairly broad great circle distribution due to variable fold axis trends and non-cylindrical folding. The pole to this great circle lies at 072/15, which is compatible with the attitude of beds on the north-eastward extension of the Hex River Mountain mega-anticline. The plunge of this pole is primarily the result of large plunging folds

Stellenbosch University http://scholar.sun.ac.za

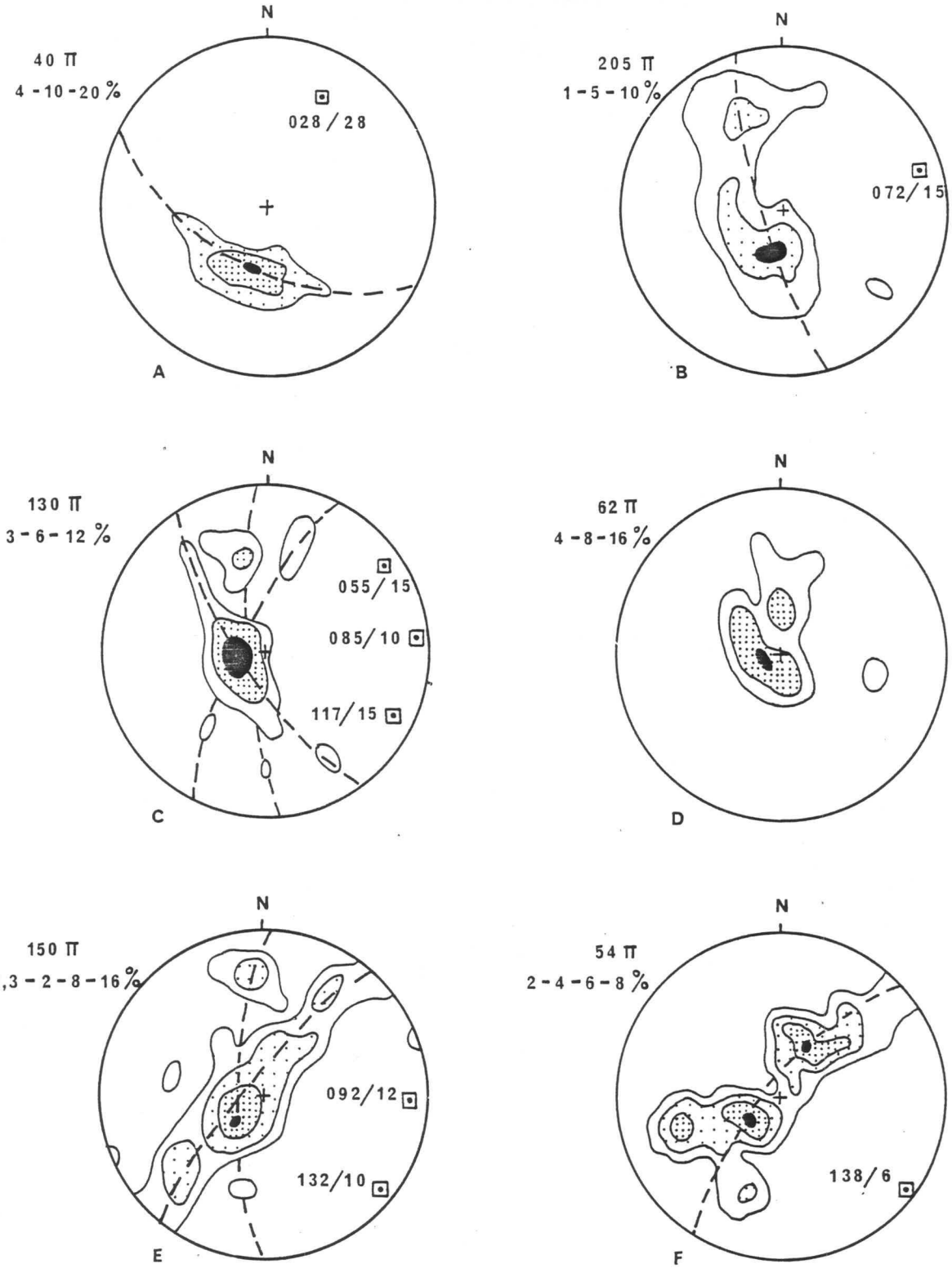

Figure 5.5
Bedding pole data for Subareas 5 to 10 (number of poles indicated as 40π, 205π, etc.- see Ramsay and Huber, 1987) All contours per 1% area.

Stellenbosch University http://scholar.sun.ac.za

measured in the western part of this subarea. A few poles lying in the south-eastern quadrant of the synoptic diagram are related to a rare north-trending kink axis at Waboomshoek.

Subarea 7 (Figure 5.5C) stretches from Karoopoort to Grootkloof, west of the Ceres-Calvinia road, and includes Witteberg rocks of the Swartruggens Mountain Range. The synoptic diagram clearly demonstrates the effect of the various south-easterly and north-easterly structural trends. Although the north-easterly trend (055/15) dominates the diagram, two other subsidiary trends are also present. An easterly oriented pole at 085/10 and an east-southeasterly pole at 117/15 are indicated. The low dips towards the east reflect the eastward regional dipslope of Witteberg rocks where they dip beneath the Karoo Sequence (the so-called "monocline" of Söhnge, 1983). The contours indicate that the trend related to the 117/15 pole is still very weak compared to that of the other trends. However, just north of the subarea boundary, this situation changes dramatically. Significantly, this change takes place across the WNW-ESE trending Winkelhaak Fault (Map 1). The synoptic diagram further indicates that kinks have no preferred vergence direction for NE trending structures, but that east-trending structures mostly verge to the south, that is to say, their axial planes dip steeply north. This is not a result of selective sampling, as virtually all structures were included in the survey.

The bedding-pole data of Subarea 8 (Figure 5.5D), which represent Floriskraal sandstone exposures at the closure of the Baviaanshoek anticlinorium at Platklip, show the result of

Stellenbosch University http://scholar.sun.ac.za

interference between the NE and NW trends. Although there are vague indications of east and north-east trends, no obvious great circle can be drawn through the poles.

Bedding pole data in Subarea 9 (Figure 5.5E) display the dominance of NW trending structures from Platklip to Kafferskraal. The switch from dominantly NE to NW trending structures is very sudden and only a weak subsidiary great circle with pole at 092/12 is present. The NE trend is again strongly present west of Subarea 9 in Subarea 12. The NW trend shows strong maxima along a great circle with pole at 132/10. No refolding relationship emerges from the synoptic diagram, because the two trends occur as intersecting, linear kinks with smaller parasitic folds. Crossing kinks commonly have the same vergence direction and only a few conjugate structures were observed.

Subarea 10, stretching from Kafferskraal to Skitterykloof, was analysed in detail because it was hoped that a clear age relationship between NW and NE trending folds could be determined. Separate bedding pole diagrams were constructed for the two trends and care was taken to ensure that poles belonged to only one fold trend. Figure 5.5G thus defines a pole at 047/8 for NE fold-related structures and Figure 5.5F one at 138/6 for the NW trend. In the area between N'wardouwskloof and Skitterykloof, an intermediate N-S trend also occurs. This trend, with axis at 005/0 (Figure 5.5H), was only rarely encountered to the south of Subarea 10. The

Stellenbosch University http://scholar.sun.ac.za

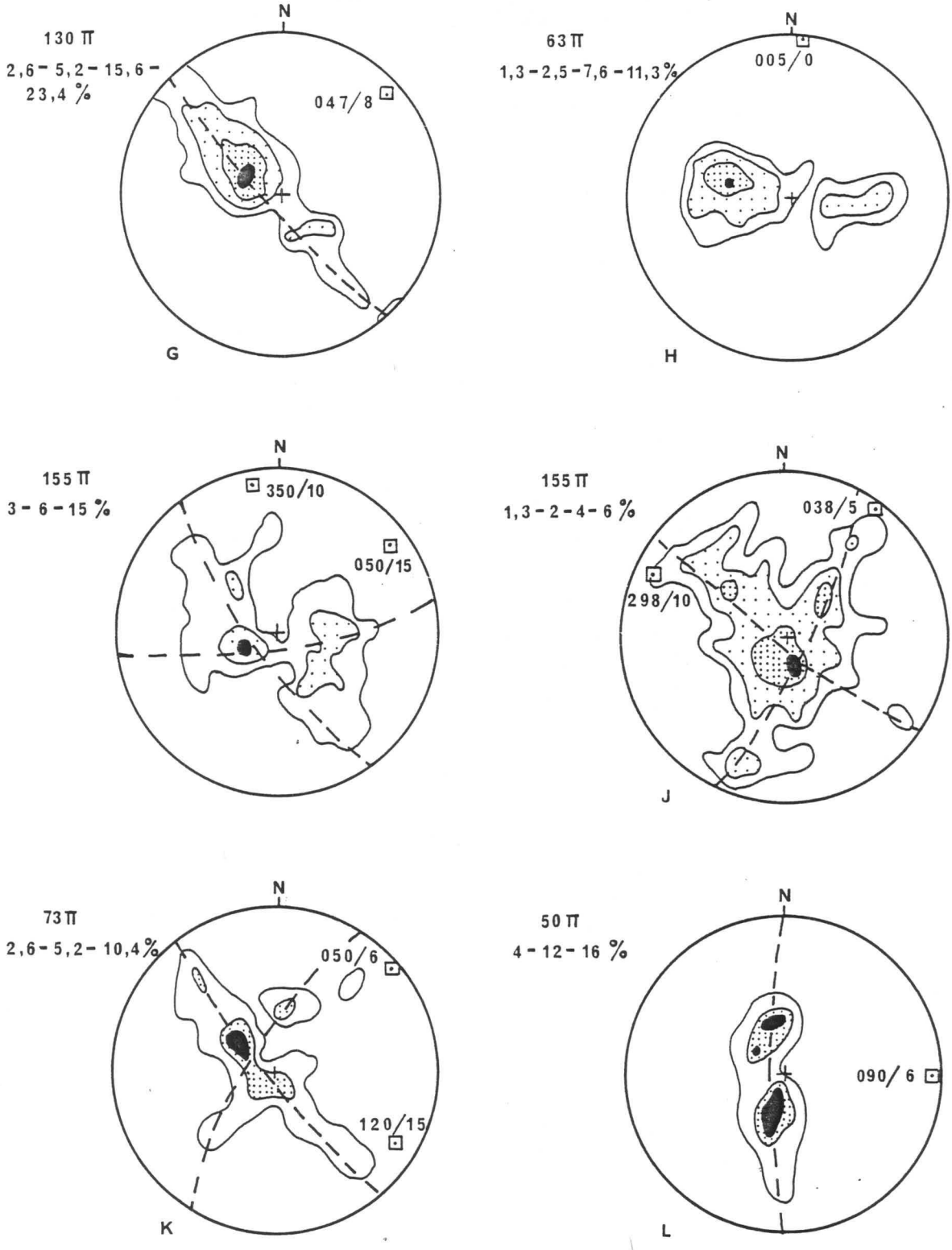

Figure 5.5 (continued)
Bedding pole data for Subareas 10 to 14. All contours per 1% area.

Stellenbosch University http://scholar.sun.ac.za

interrelationship of the three structural trends will be dealt with in more detail in the section on fold interference.

Subarea 11 (Figure 5.5I), situated on the plateau formed by resistant Witpoort Formation quartzitic sandstones, has a very low fold density. Open folded, undulating or horizontal beds, affected by mild NW trending structures, are cut by long, narrow and linear NE trending fold zones. Apart from these zones of high deformation, the effects of the NE trend are practically nil elsewhere. These narrow fold zones, which are spaced hundreds of meters apart, represent the last signs of the NE oriented structures in the Ceres Syntaxis. Cover sediments of the Cape Supergroup to the north of Subarea 11 display only NW trending structures. The geometry of these fold zones will be discussed later. Though the bedding poles of Figure 5.5I suggest interference of the NW and NE trends, this is mainly the effect of the relatively small angle between the two axial directions. It is nevertheless possible to fit two separate poles at 350/10 and 050/15 to the great circles if one uses measured fold axes as guidance.

Subarea 12 is characterized by linear zones of both NW and NE fold trends. These zones, which trend nearly perpendicular to one another, divides the area into rectangular blocks within which bedding attitude slopes at low angles in four directions towards the intensely folded border zones. The bedding pole distribution in Figure 5.5J reflects this structural architecture very clearly. They define two great circles with poles at 038/5 and 298/10. The narrow parts along the great

Stellenbosch University http://scholar.sun.ac.za

circle distributions represent intensely folded beds on the borders of the rectangular blocks, while the proliferation of bedding-poles near the centre of the diagram results from low dips in four opposite directions inside these blocks. The north-westward plunge of the π-pole at 298/10, as well as the low plunge of the north-easterly oriented π-pole is the result of the two deformational trends being almost of the same intensity. Subarea 12, therefore, experienced finely balanced deformational stresses in contrast to almost all other subareas where one trend tends to dominate over the other.

In Subarea 13, the dominance of the NE trend is again clear (Figure 5.5K). Bedding data for this trend define a great circle with pole at 050/6, reflecting the decrease in average plunge of folds from east to west over the Swartruggens Mountain Range. The few NW trending structures that occur, describe a great circle with pole at 120/15.

Subarea 14 comprises the Bokkeveld exposures in the core of the Baviaanshoek brachi-anticlinorium. Bedding poles were taken mostly from the central part of this area in outcrops composed of the sequence between the Tra-Tra and Wuppertal Formations. The diagram (Figure 5.5L) shows a pole to the great circle at 090/6. This π-pole is clearly more easterly-oriented than the main trend (055/15) in the adjoining Subarea 7, which contains mostly Witteberg rocks. A subsidiary trend in Subarea 7 at 085/10 is also slightly more northerly than the main axis of the Bokkeveld Group in the Baviaanshoek. However, the upper Bokkeveld exposures of the Klipbokkop, Osberg and Karoopoort

Stellenbosch University http://scholar.sun.ac.za

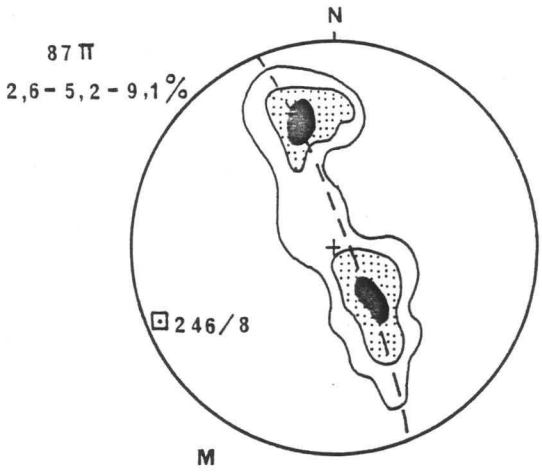

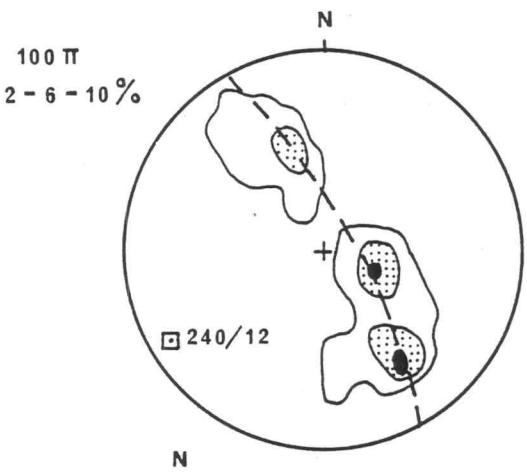

Figure 5.5 (continued)
Bedding pole data for Subareas 15 and 16. All contours per 1% area.

Stellenbosch University http://scholar.sun.ac.za

Formations show a gradual change towards the main (north-easterly) Witteberg trend.

Subarea 15, west of the Baviaanshoek, displays bedding poles (Figure 5.5M) that describe a great circle with pole at 246/8. This clearly reflects the dominance of the NE trend in Witteberg rocks of the central Ceres Syntaxis. The low plunge of the π-pole is repeated in Subarea 16 to the south.

Subarea 16 is situated between two WNW trending faults south-west of the Baviaanshoek area. The great circle with pole at 240/12 (Figure 5.5N) indicates that fold axes have a considerable plunge to the south-west. Although this may be the effect of a bigger displacement along the southern bounding fault than the northern one, this plunge is also believed to be related to a regional effect of the NW-SE trend. In the adjacent Subarea 2, bedding poles lie along a great circle with a pole that plunges NNE (Figure 5.3). This may indicate that the 240/12 pole of Subarea 16 is primarily related to the faulting.

5.2 CLEAVAGE

Due to the low deformational intensity over most of the Ceres Syntaxis, cleavage is only found in Subarea 4 (NE related) and very locally in Subarea 1 (N-S related).

Stellenbosch University http://scholar.sun.ac.za

In Subarea 1 (Figure 5.2), a near-vertical, spaced solution cleavage developed at the base of the Cedarberg shale in the Hansiesberg mega-anticline. On the eastern limb of the structure, this cleavage strikes 010 and dips 75 degrees to the east on average. Although exposures of shale on the western limb of the mega-anticline are poor, cleavage appears to strike vertically and trends 010. The east dipping limb of the Witzenberg mega-anticline displays the same cleavage attitude, but rare Cedarberg exposures here are severely weathered, making statistically significant measurements impossible. The attitude of cleavage in these N-S striking megastructures, therefore, is near axial-planar.

Cleavage in Subarea 4 developed in Bokkeveld beds of the Hex River valley syncline, and particularly well in the Cedarberg shale on the southern limb of the Hex River mega-anticline. On the northern limb of the latter though, its intensity approximates that in the Witzenberg megastructures. North of the Hex River Mountain, Bokkeveld beds show no cleavage as a result of lower deformation intensity. Cleavage in the Bokkeveld beds of the Hex River valley, dips at 30 degrees towards 186 degrees (Figure 5.4), slightly steeper than the local bedding attitude (25 degrees south). Exposures at the entrance to Sanddriftkloof display the intensity of cleavage formation in the southern limb of the Hex River mega-anticline. Figure 5.4 shows the relationship between the cleavages in the Cedarberg shale at this locality. S1 dips at 40 degrees towards 180 degrees, while the crenulation cleavage S2 dips at 26 degrees towards 310. The latter approximates the attitude

Stellenbosch University http://scholar.sun.ac.za

of second-order kink axial planes in the overlying Goudini Formation. A faint fracture cleavage (S3), which takes the appearance of closely-spaced joints, strikes 242 degrees and is vertical. Its attitude thus nearly coincides with the axial plane of the megastructure (Figure 5.4). The upper part of the Cedarberg shale was detached from the overlying Goudini sandstones on a grand scale. Rotated blocks of shale in which S1 and S2 have anomalous attitudes, bound by some thick quartz veins of shear and dilational origin, form a ramifying network in the outcrops.

Cedarberg shale at the Lakenvlei Dam on the northern limb of the Hex River mega-anticline, displays only one cleavage (S1), too faint to measure in the field. Oriented thin sections show that it dips about 40 degrees to the north-west.

A near-vertical cleavage strikes parallel to a fault in Bokkeveld shales near Swaarmoed. The cleavage developed only close to the fault plane and its presence is thus related to ductile strain along the fault. A pervasive shear cleavage was observed in siltstones along the short limb of a large megakink in Witteberg rocks east of Gydo Pass. The cleavage anastomoses slightly, but stays more or less subparallel to bedding in the vertical beds.

5.3 FOLD AXES

The fold axes given in this section, were either measured in the field, or determined stereographically, (depending on size

Stellenbosch University http://scholar.sun.ac.za

of the structure) by using not less than 10 bedding poles per fold. The planar limbs of many Witteberg kinks allowed the use of less poles than where a sinusoidal Bokkeveld Group fold had to be analysed.

In Subarea 1, the megafold axes of the Hansiesberg anticline and Witzenberg Valley syncline, trend and plunge at 190/6 (Figure 5.2). Second-order kinks on the limbs of the former anticline and also on that of the Witzenberg anticline to the west, all possess fold axes coaxial with the parent megastructures. Fold axes in the "fold zone" of the Peninsula Formation approximate the same general trend and are horizontal.

Subarea 2, in Witteberg beds directly north-east of Ceres, displays a variety of fold axis attitudes (Figure 5.3). Trends vary by as much as 90 degrees, while plunges are of the order of 0 to 20 degrees. Though fold axes tend to develop different trends at slightly different stratigraphic levels in the sequence, this relationship is not consistent. Crossing kink axes resulting from a heterogeneous stress field in this part of the syntaxis were encountered on Gydo Mountain and south of Driefontein. The vergence, that is, the facing direction of the short kinked limb on such crossing axes, is often the same. Thus many are not conjugate structures but crossing monoclinal kinks resulting from time- dependent instability of the stress vectors.

Stellenbosch University http://scholar.sun.ac.za

Fold axis trends in Subarea 3 are much the same as that of the main Hex River mega-anticline and no crossing trends occur.

In Subarea 4, the Hex River mega-anticlinal axis at 254/2 (Figure 5.4) parallels second-order kink axes (not shown) in the Goudini Formation on the limbs of the megastructure. This is different from areas to the south and southeast of the Hex River valley, where kink axes in the Nardouw Subgroup are slightly oblique to the megastructure axes (Newton, 1973). The double-crested structure contains a northerly anticlinal axis with attitude 028/28 (Figure 5.5A), while the southern nose trends due east and is cut by many faults.

Subarea 6, from Karoopoort to Eikenboschhoek, shows a fold axis maximum near 070/15 in Figure 5.6A, though trends vary by as much as 40 degrees and a few westerly plunging axes also occur. The majority of axes have low north-easterly plunges, because the subarea lies on the extension of the Hex River mega-anticline closure. Instability in stress vectors is again indicated by an anomalously-oriented kink axis at 018/20 in Figure 5.6A. No NW trending axes occur. The NE trending axes on the eastern side of the subarea curve and ultimately merge with E-W trending folds of the Southern Cape Fold Belt near Touws River.

In Subarea 7, between Karoopoort and Platklip (Figure 5.6B), fold axis trends vary between 045 and 135 degrees, while plunges stay in the order of 0-20 degrees east. The ESE trend occurs mainly as mesokinks, with megakinks oriented mainly

Stellenbosch University http://scholar.sun.ac.za

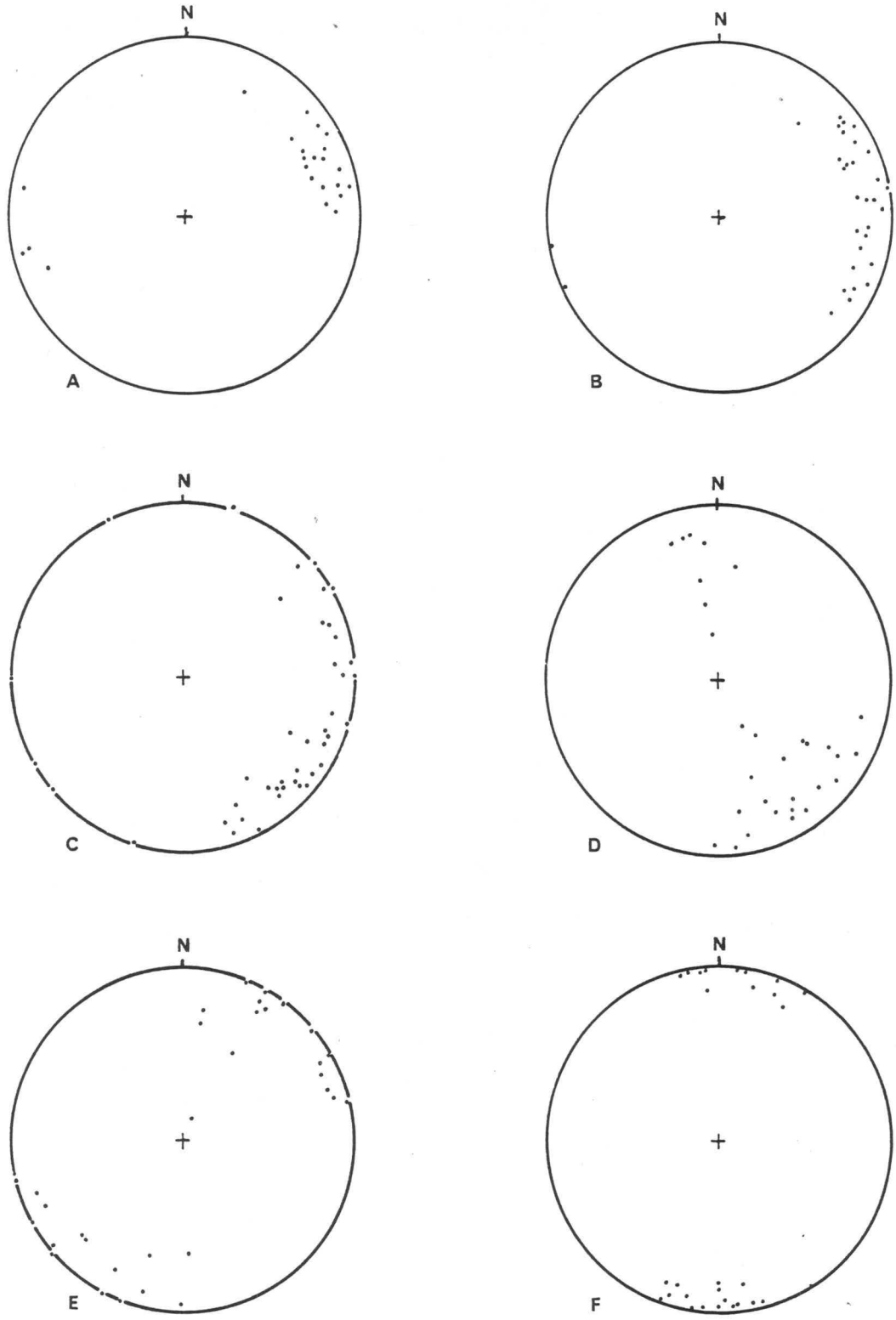

Figure 5.6
Fold axes for Subareas 6 to 10 (excluding subarea 8).

Stellenbosch University http://scholar.sun.ac.za

northeasterly to easterly. Abrupt changes in kink axis trend as depicted by the curvature of the Witpoort Formation outcrops, occur immediately north of Rooifontein (Map 1).

In Subarea 8, Kweekvlei shale and Floriskraal sandstone are folded about nearly horizontal axes which trend due east (Map 1).

From Platklip to Kafferskraal (Subarea 9), south-east-plunging fold axes dominate the diagram (Figure 5.6C). Trends vary between 040 and 165 and plunges from 0-25 degrees. In the field, the north-easterly folds are limited to isolated mesokinks with dominant south-east vergence.

Subarea 10 (Figures 5.6D,E and F) is characterized by a complex relationship between NW-SE, SW-NE, and on a lesser scale, N-S trending fold axes. In this subarea, the former two trends are nearly perpendicular to each other and of approximately the same intensity. These two factors contributed towards the forming of an intermediate N-S fold trend from Hartnekskloof to Skitterykloof. Fold axes of the three trends were plotted separately for clarity. The NW-SE trend (Figure 5.6D) displays much variability in trend and plunge, especially in the south-eastern quadrant of the diagram, due to interference with the NE-SW trend. The latter is in essence a monoclinal flexure of which the short limb faces towards the south-east. NE-SW folds (Figure 5.6E) in the subarea occur as minor structures on this short limb and plunge only at low angles. The steeper-plunging axes are situated on the limbs of NW-SE trending

Stellenbosch University http://scholar.sun.ac.za

kinks. It will be demonstrated later that the relationship between NW-SE and NE-SW folds are dependent on slight age difference. Fold axes of the N-S trend (Figure 5.6F) are nearly horizontal.

In Subarea 11 (Figure 5.6G), NE trending fold axes are confined to narrow fold zones which trend mostly between 030 and 040 degrees. The NW-SE trend shows greater variability than the NE-SW trend, but fold axes are generally subhorizontal. There is no longer an orthogonal relationship between the two trends in this subarea, largely because the NE-SW folds change trend towards NNE-SSW and ultimately die out north of this subarea.

Fold axes in Subarea 12 (Figure 5.6H), situated on the plateau formed by resistant Witpoort quartzitic sandstone, again show a near-orthogonal relationship as in Subarea 10 to the east. However, both NW-SE and NE-SW axes are now nearly horizontal due to the absence of a significant regional slope of the enveloping sequence. Apparent E-W and N-S trends on the diagram are subsidiary effects of the equally prominent NW-SE and NE-SW trending folds.

In Subarea 13 (Figure 5.6I), the NE-SW trend swings towards ENE-WSW, but NW-SE folds have generally the same trend as those in Subarea 12 to the north. The fold axes of both trends, however, are subhorizontal. The NW-SE trend is well-developed in the northern part of the subarea, but south of Champignons-Berg (Map 1) these folds are rare, and the structure is

Stellenbosch University http://scholar.sun.ac.za

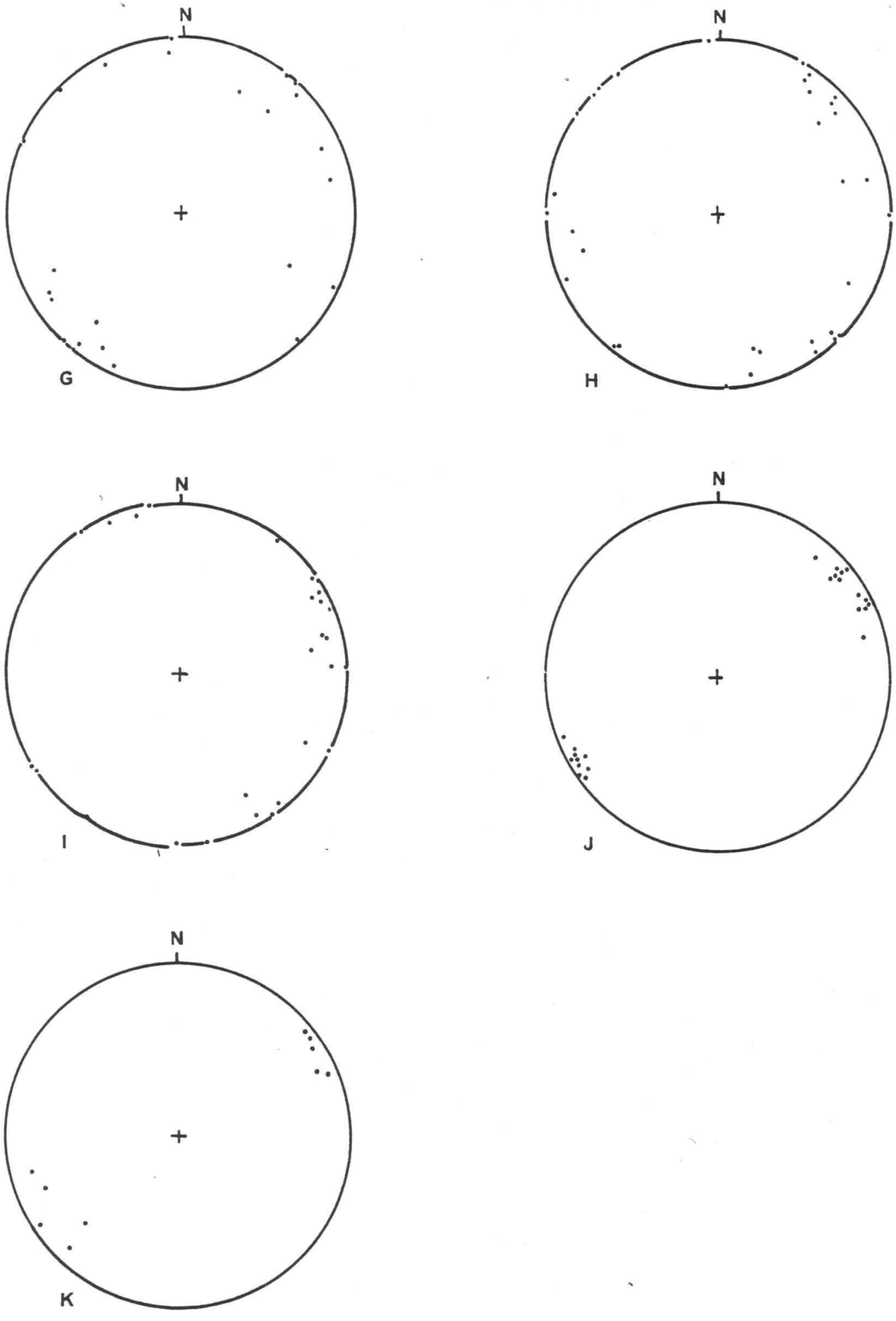

Figure 5.6 (continued)
Fold axes for Subareas 11 to 16 (excluding subarea 14).

Stellenbosch University http://scholar.sun.ac.za

dominated by NE-SW trending megakinks, which continue for several kilometers.

Subarea 15, west of the Baviaanshoek farming community (Figure 5.6J), is characterized by horizontal megakinks with an average trend of 050 degrees. Northwest trending folds are completely absent and only appear to the west of the subarea, near the N-S trending Table Mountain Group megastructures (Map 1).

Subarea 16, farther south (Figure 5.6K) displays the same fold trend as Subarea 15. Anomalous fold plunges in the south-western quadrant of this diagram are probably related to south-westward downthrow on the Odessa-Baviaansberg Fault (Map 1).

Stellenbosch University http://scholar.sun.ac.za

6. THE FOLD ZONES OF SUBAREA 11

The unusual fold style of these structures, which developed in the domain where NE-SW trending folds eventually disappear, warrants special attention. The narrow fold zones display the following features:

(1) The zone of intense shortening is bound by near-vertical, curving planes of structural discontinuity, but neither breccia, nor slickensides/ slickenfibres are present on or close to these planes.
(2) The zones are from 100 to 300 metres wide.
(3) The zones are typically hundreds of metres to kilometres apart. Between these, bedding remains essentially horizontal.
(4) Immediately overlying strata are horizontally bedded and appear totally undisturbed.
(5) Within fold zones the fold style is indicative of semi-soft sediment deformation, at least at the onset of buckling.

At Stompiesfontein (Figure 5.1), near the northern corner of Groenfontein (3219DC), relatively pure quartzitic sandstones of the Witpoort Formation are intensely deformed in such a NE-SW trending zone. The best outcrops occur on the eastern side of the kloof (Figure 6.1). Though the trend of the linear zone is 030 degrees, and many folds within the zone possess the same trend (Figure 6.1C), some elements of the NW-SE regionally penetrative trend can also be recognised. Bedding pole data

Stellenbosch University http://scholar.sun.ac.za

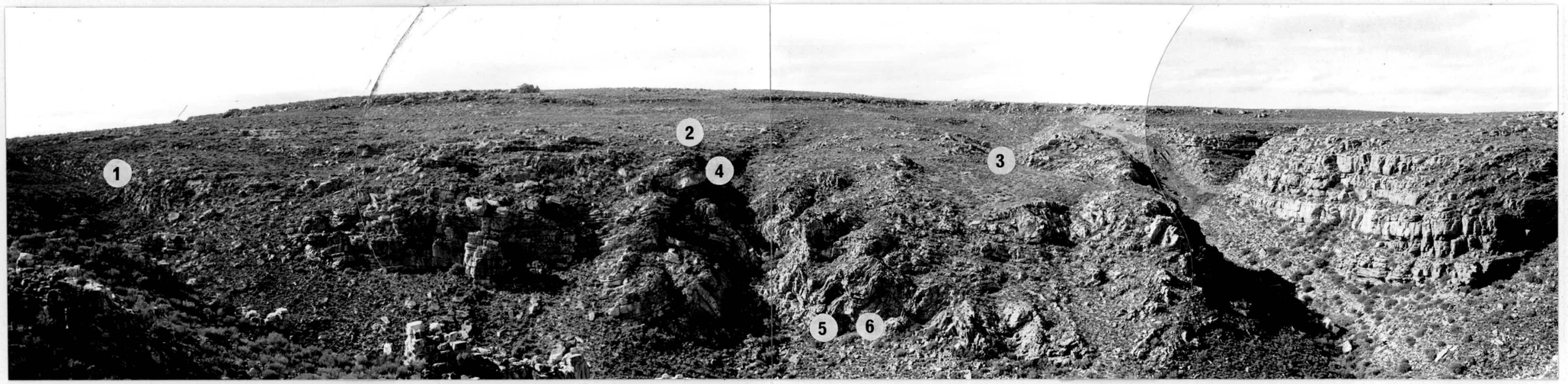

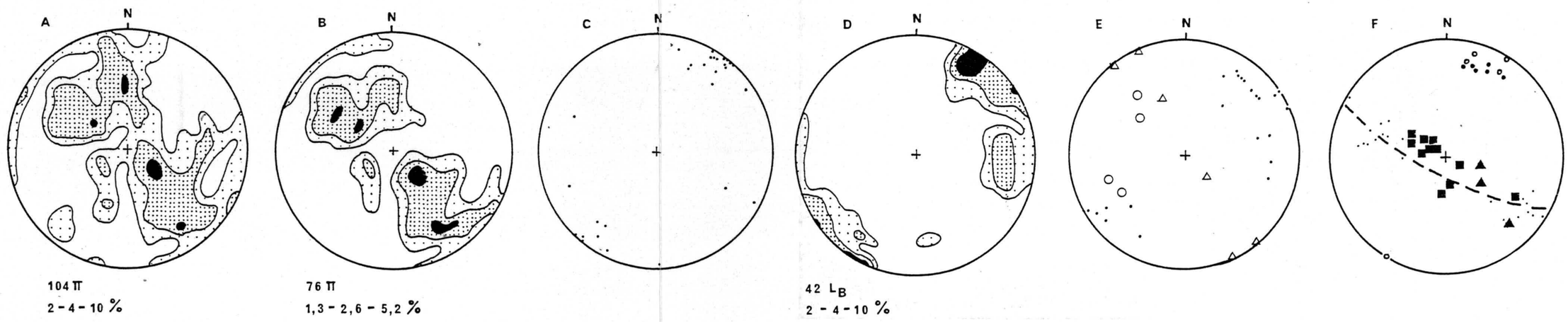

Figure 6.1 The Stompiesfontein fold zone, looking NE. Attitude of structural elements as measured inside Stompiesfontein fold zone. Figure 6.1A and B: All bedding poles and bedding poles of only NE folds; Figure 6.1C: All fold axes; Figure 6.1D: All L_B

Figure 6.1E: Structure at the northern zone boundary; · = L_B ○ = L_{qf}; △ = fold axial planes; Figure 6.1F: Data of folds in Figure 6.5. · = S_o; ∘ = axes of small wrinkles; • = L_B ; ■ = poles to tension fractures; ▲ = shear planes.

Stellenbosch University http://scholar.sun.ac.za

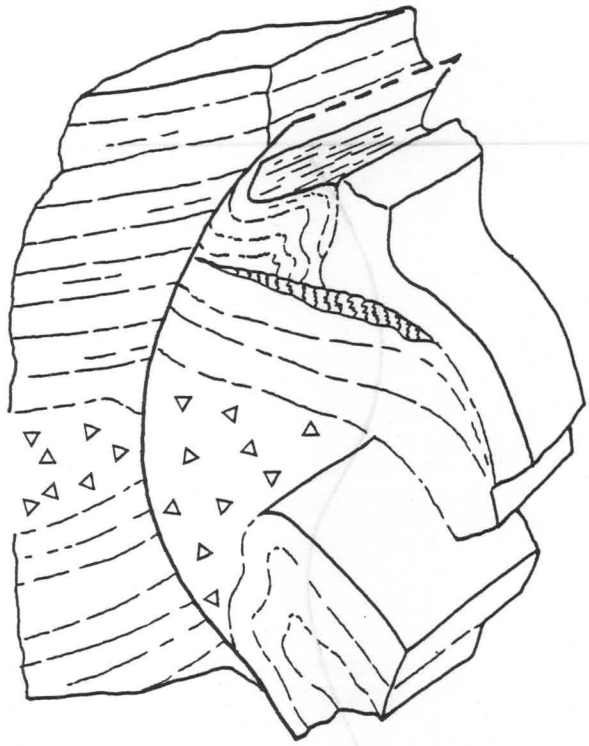

Figure 6.2
The northern fold zone boundary on the eastern side of Joubertskloof. Structural elements here are depicted in Figure 6.1E. Height of the section is about 40 m.

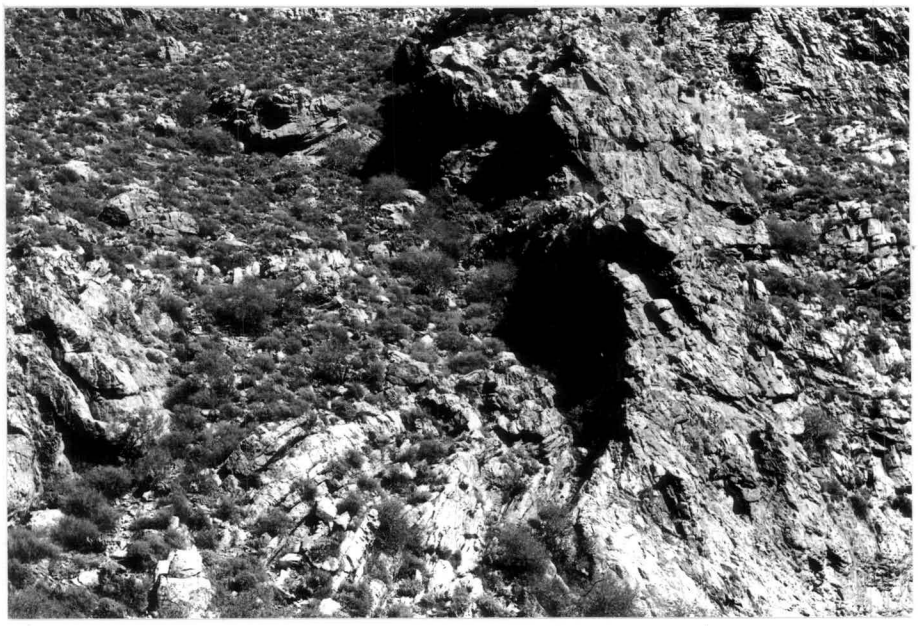

Figure 6.3
Isoclinal folds with their axial planes dipping towards the central fold zone occur at the northern boundary on the western side of the kloof. Height of section is approximately 30 metres.

Stellenbosch University http://scholar.sun.ac.za

(Figures 6.1A and 6.1B), as well as the attitude of B-lineations (L_B) within the zone (Figure 6.1D), show the effects of the minor NW-SE trend on the main NE-SW trending structures. A monocline with axis 352/0 and axial plane dipping 48 degrees east, occurs immediately north of the zone (1, Figure 6.1). A smaller monocline with axis at 138/0, is also present in essentially horizontally bedded sandstones immediately north of the fold zone (2, Figure 6.1) and somewhat higher up in the succession. The lower part of the fold zone is dominated by intense NE-SW trending folds, but as the intensity decreases upwards, "relict" and highly irregular NW-SE trending folds appear (3, Figure 6.1C).

The north-western boundary of the fold zone is sharp and defined by a curving, almost vertical planar discontinuity (4, Figure 6.1). Listric thrusting and reclined and isoclinal folds occur immediately south-east of this discontinuity, inside the fold zone (Figures 6.2 and 6.3). The axial planes of the isoclinal folds are either vertical or inclined towards the middle of the zone and well-developed B-lineations trend almost subparallel to the zone boundary (Figure 6.1E). Instabilities arising from horizontal shear parallel to the zone boundary, and related to nearby folding along NW-SE trending axes, together with an inhomogeneous piling-up process of differently reacting layers, probably caused the spread in attitude of L_B and slickenfibres (L_{qf}).

The fold-zone style is variable, but most folds are transitional between concentric Class 1C, similar Class 2, and

Stellenbosch University http://scholar.sun.ac.za

Class 3 types (Ramsay, 1967). Multi-hinge and isoclinal forms with flat to steeply dipping axial planes are common towards the zone boundaries, where more shortening has occurred than in the middle. The latter may indicate that the northern zone boundary was already fixed at the onset of deformation. In order to determine the characteristics of these structures, they were investigated along a short fold profile as indicated on Figure 6.1 (5 to 6).

Two anticlines and an intervening syncline were selected for detailed description (Figures 6.4 and 6.5). The attitude of bedding (S_o), small wrinkles on bedding and L_B are shown in Figure 6.1F. The measured axial planes of the anticlines both have attitudes of 017/90, while that of the syncline is 027/90. The wavelength and amplitude of the folds are 6 and 4 metres respectively. Their fold style changes from concentric to similar along the axial planes. Severe wrinkling of bedding produced higher order parasitic folds on the limbs of these folds. Substantial thickening of some beds occurred in the hinge zones of the folds and also in the northern limb of anticline 1 as a result of hinge collapse. When traced from left to right (north to south) along the profile, bed A thickens from 2,6 meters to 3 metres, from 1 to 2 metres, and from 1 to 1,5 metres in successive hinges. The maximum thickening occurs in the synclinal hinge of fold 2, where the orthogonal thickness actually doubles. Local transport of material is indicated by listric thrusting, intralayer wrinkles and shear veins (Figure 6.5). Small intralayer wrinkles inside an upthrusted block of bedding, indicate how thickening is

Stellenbosch University http://scholar.sun.ac.za

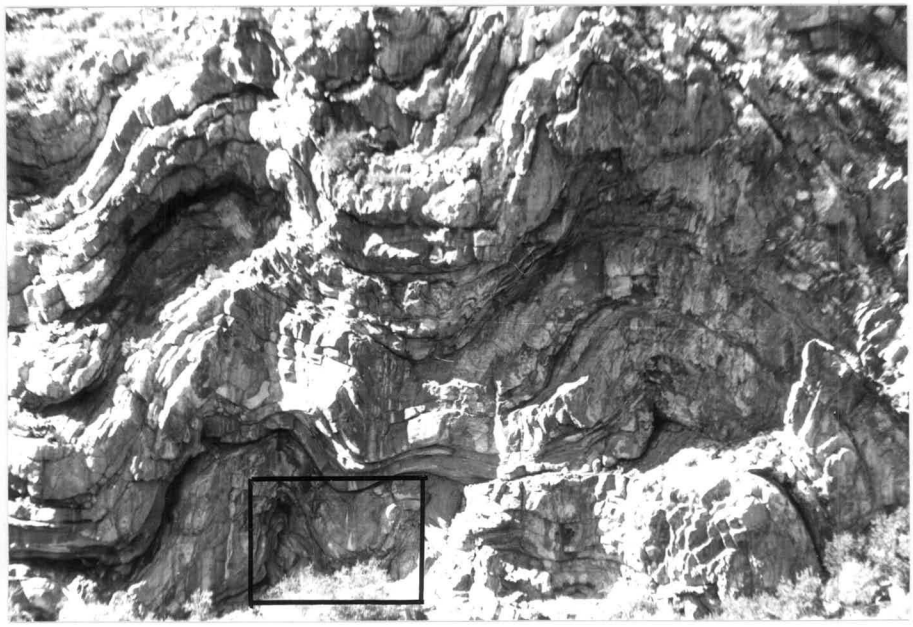

Figure 6.4
Location of the detailed fold profile in Figure 6.5. Height of the section is about 40 m.

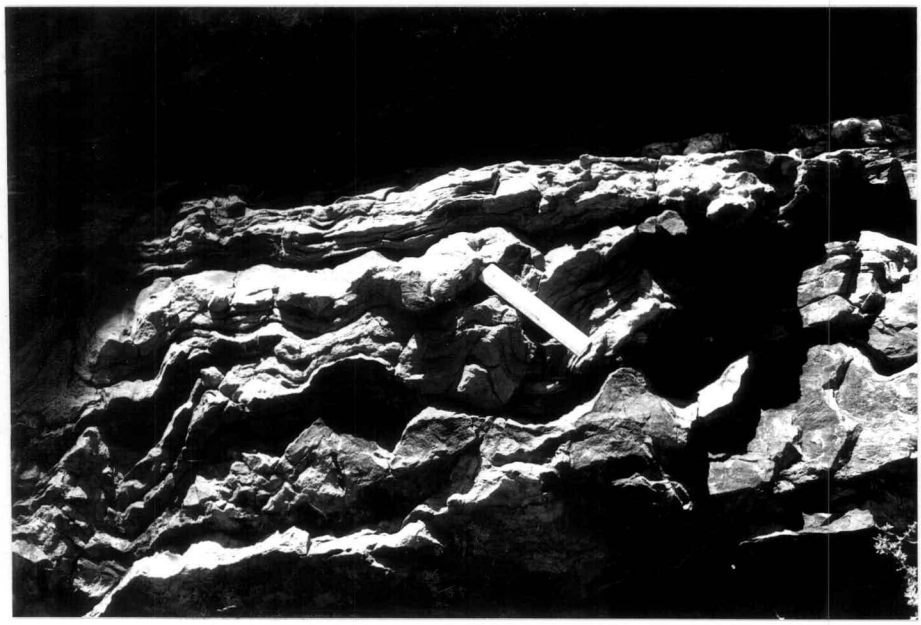

Figure 6.6
Severe folding in thin beds towards the right hand side of Figure 6.4. Length of scale bar is 15 centimetres.

Stellenbosch University http://scholar.sun.ac.za

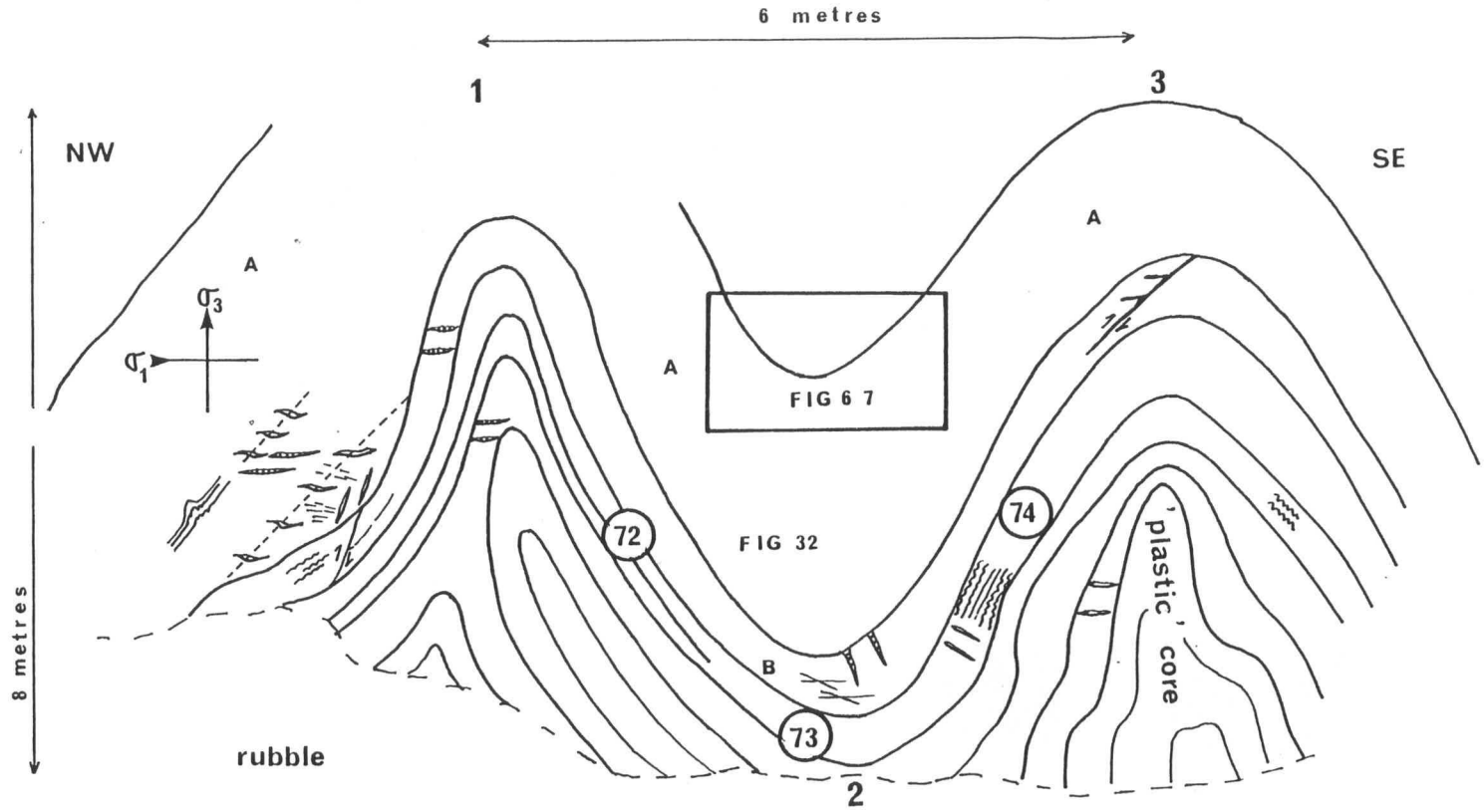

Figure 6.5
Detail of three selected folds from the Stompiesfontein fold zone, of which the structural data are given in Figure 6.1F. For further description, see text. Encircled numbers refer to sample localities for microfabric analysis.

Stellenbosch University http://scholar.sun.ac.za

accomplished in the bedding bulge of layer A in fold 1. The necessary space was provided by intense flattening to almost isoclinal forms, of thinner beds (Figure 6.5) in the core of anticline 1.

Individual cracks in the en echelon crack arrays of bed A (to the left of Figure 6.5) are approximately parallel to the σ_1 direction at their tips, while deviation from this is caused by rotation within the shear zones, which are approximately parallel to the top bedding surface. This same bedding-parallel shear produced many small wrinkles near the bedding surface. In the highly thinned vertical limbs of the nearly isoclinal anticlines (bed B), tensional veins are horizontally disposed. This indicates that little movement occurred on these bedding surfaces after initiation of the fractures, otherwise they would have shown rotational strains at their tips (close to the bedding surfaces). Tensional veins occur near the inner arc of a 50 cm thick bed (Bed B) in the synclinal hinge(fold 2). The latter seems anomalous at first glance, because near the inner arc of a bed in the fold hinge, compression, rather than tension, would be expected. This apparent discrepancy can be explained by the severe stretching on the limbs of bed B, and also by decoupling between beds A and B, but not between B and the beds below it.

It is sometimes difficult to distinguish between a sedimentary parting lineation and the tectonic B-lineation in Witteberg rocks. Outcrops at Stompiesfontein demonstrate the difference (Figure 6.7). The parting lineation clearly bends around the

Stellenbosch University http://scholar.sun.ac.za

hinge, while the tectonic lineation parallels the fold axis. The parting lineation stays in the same plane if followed around the hinge zone, which confirm a similar (Class 2) fold geometry.

A less intensely deformed zone of NE-SW trending folds occurs some 3 kilometres south of the Stompiesfontein one (Map 1). Between the two zones, bedding is essentially horizontal. The next zone occurs 8 kilometres farther south along the Katbakkies-Skitterykloof road. South of this road, the spacing of NE-SW trending fold zones decreases to between 800 metres and 2 kilometres. Intervening areas are dominated by NW-SE trending kinks and open box folds of low amplitude. Where NE-SW trending fold zones cross NW-SE trending kinks, the latter structures are almost obliterated. Data for the fold zones just south of Stompiesfontein and south of Kliphuis are given in Figures 6.8A and B. Steeply plunging small folds inside the Kliphuis zone indicate inhomogeneous strain that probably resulted from simultaneous compression subparallel to the fold zone boundaries.

The low viscosity contrast between beds, together with high interlayer strength in Witteberg quartzitic sandstones, enabled horizontal beds to transmit compressive stress over large distances without buckling. Buckle deformation of the multilayer was probably initiated along early linear anisotropies such as thinning and thickening of beds or master joints in the basin floor (Jaroszewski,1984). Deformation rate was probably a maximum immediately after the onset of buckling

Stellenbosch University http://scholar.sun.ac.za

Figure 6.7
The primary flow lineation stays in a plane as it bends around the synclinal trough, indicating Class 2 geometry. The tectonic lineation coincides with the local fold axis. Thickness of lower bed is 1 m.

Stellenbosch University http://scholar.sun.ac.za

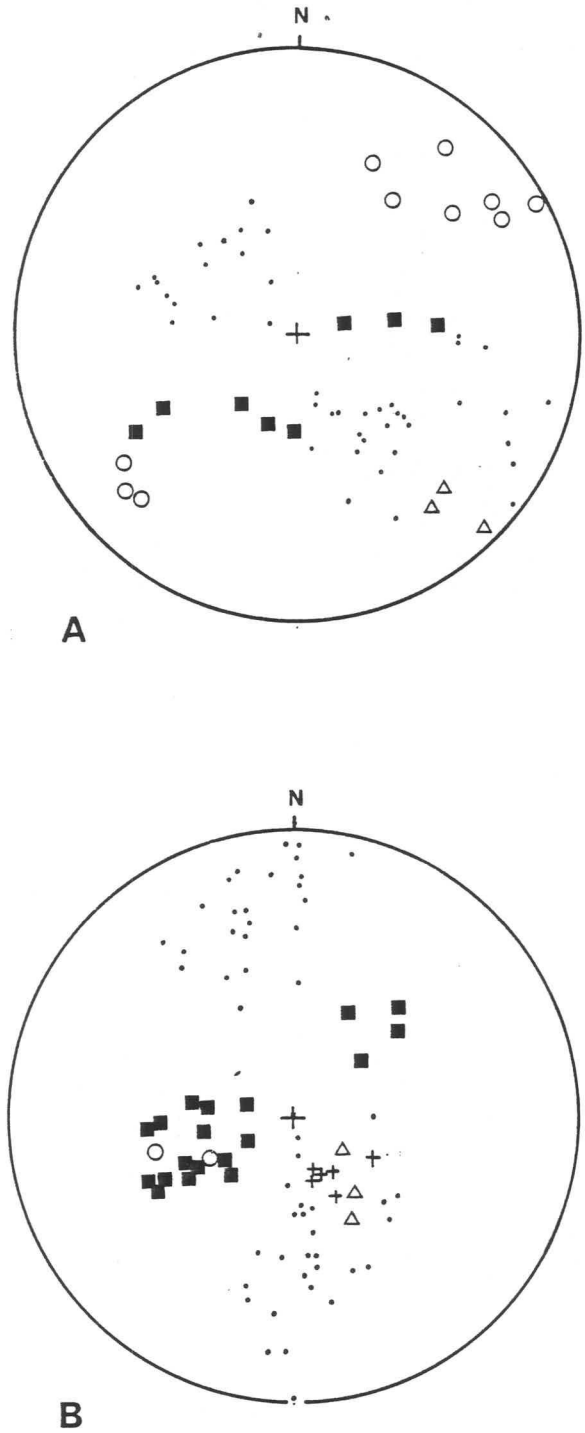

Figure 6.8
Orientation data for structures at the fold zones south of Stompiesfontein (A) and south of Kliphuis (B).
• = NE fold bedding poles; ■ = NW fold bedding poles;
○ = slickenfibres of NW folds; △ = slickenfibres of NE folds;
+ = poles to extension fractures.

Stellenbosch University http://scholar.sun.ac.za

adjacent to the northern zone boundary, hence somewhat chaotic folds developed here. This high deformation rate could probably not be sustained, due to the distance from the source of compression to the south. Therefore, the central fold zone displays much more open folds. The fact that folds at the southern boundary of the Stompiesfontein fold zone are as chaotic as those at the northern boundary, indicate that the interim period of low deformation rates was followed by high deformation rates of the next shortening pulse. This process is analogous to stress build-up along fault planes. Conceivably, the periods of high deformation rate occurred when bedding-parallel shear stresses in the multilayered sequence were sufficiently high to overcome interlayer shearing strength on a grand scale. The magnitude of the latter would have been largely controlled by factors such as competency contrasts and pore pressures.

The occurrence of NW-SE trending folds and small monoclines adjacent to, as well as towards the top of the Stompiesfontein fold zone, indicates that the multilayer was actually shortened in two mutually perpendicular directions. The fact that essentially undisturbed beds often overlie the fold zones, may be explained by the general character of the average Witteberg multilayer, together with substantial bedding-parallel décollement immediately above the fold zones. Beds that appear thick-bedded from a distance, reveal many internal planar discontinuities upon closer inspection. Minute quartz fibres on these surfaces indicate that slip occurred incrementally

Stellenbosch University http://scholar.sun.ac.za

throughout the multilayer, as well as on wider-spaced bedding planes.

The bulk shortening of a multilayered sequence consists of a combination of internal layer and buckle shortening (Ramberg, 1964). Competency contrast is the main factor that will determine the amounts of these shortening components in the finite strain of a multilayer. A slight, but significant difference between viscosity contrasts in the overlying beds and that of the beds involved in the fold zone, could cause the former to shorten more (primarily?) by layer shortening (thickening), opposed to dominant buckle shortening in the latter (Ramberg,1964). Higher shear strength between bedding surfaces in the overlying sequence, would have inhibited buckling instabilities (Honea and Johnson, 1976). In the part of the sequence that was involved in the fold zone, buckling became important after only a slight amount of layer-parallel shortening had occurred.

The general fold style within the fold zones are believed to have resulted from deformation of relatively unlithified beds. Dewatering of these beds may have been inhibited by the presence of some silty interbeds, as well as the proximity of the Kweekvlei shales above. The absence of brittle deformation indicators like penetrative fracturing, breccia and general scarcity of slickenfibres, especially on the northern planar fold zone boundary, confirm that most of the deformation occurred in a ductile (plastic) state. Elastic folding would certainly have produced more dilational spaces between folded layers of such intense curvature. Microstructural evidence, which supports some of the above, will be presented in a later section.

Stellenbosch University http://scholar.sun.ac.za

7. CROSS-FOLDING RELATIONSHIPS

7.1 GENERAL

One of the main aims of the study was to find coexisting crossing fold axes from which a possible age relationship between the Cedarberg and Southern Cape Fold Belt could be established. Crossing folds were recognized for the first time during this study, excluding the so-called en-echelon folds south of the Hex River Valley, described by De Villiers (1956) and Newton (1975). In the writer's opinion, the latter structures do not reflect age relationships as such, but rather the effects of rotational stress as registered in units above the Cedarberg shale (i.e. Nardouw Subgroup and higher).

Söhnge (1983) suggested that Bokkeveld and Witteberg Group subunit exposures might indicate "mild cross-folding" in the Ceres area. This statement is one of the more ambitious ones relating to the syntaxis, but it also points out one of the main problems concerning its geometry, namely: Does the NE-SW structural trend in the northern syntaxis represent the western continuation of the arcuate E-W striking southern Cape Fold Belt, or is it supplementary to the NW-SE and E-W trending fold directions? This question will have to be answered before cross-folding in the Ceres Syntaxis and the age relationship between the southern Cape Fold Belt and the folds in the western Cedarberg ranges can be described. A number of features relating to this problem are outlined below.

Stellenbosch University http://scholar.sun.ac.za

1. Folds of the north-east trend do not have a preferred vergence, but they become fewer northwards, until they ultimately die out beyond Katbakkies (Map 1).

2. Cleavage intensity in the Bokkeveld Group decreases progressively from the Koo near Montagu, towards the Ceres syntaxis. In the former area, a penetrative slaty cleavage developed, but in the Hex River Valley, this cleavage is very weak. Cleavage is absent from all Bokkeveld beds north of the Hex River mega-anticline.

3. As one goes north-westwards from Montagu, the number of second-order kinks on the limbs of the Table Mountain Group megastructures decreases steadily. This is clearly illustrated by a comparison between the northern limb of the Kwadouwsberg mega-anticline and the southern limb of the Hex River mega-anticline, as well as between the limbs of the latter megastructure.

It thus seems highly probable that the NE-SW trend of the Hex River Mountains is primarily related to the E-W trend, which occurs towards the south and east. For this reason, a direct comparison between the age of Cedarberg folds and that of the southern Cape Fold Belt on the grounds of intersecting fold axes in the Ceres Syntaxis, looked like a viable proposition.

The double closure of the Hex River mega-anticline west of Bokrivier, (3319 BC) is probably a manifestation of NE - SW directed compression in the Ceres Syntaxis. Bokkeveld Group

Stellenbosch University http://scholar.sun.ac.za

folds with short, curving northeast-trending axes in the Baviaanshoek (3319 BA) brachi-anticlinorium probably represent a domal structure on mega-scale. Significantly, this dome is situated on the straight line extrapolation of the Sneeukop mega-anticlinal axial trace (3219 CD) to the closure of the Hex River mega-anticline (Figure 5.1, Map 1).

Due to the absence of regionally penetrative cleavages related to the NW-SE and NE-SW fold trends in the Ceres syntaxis, cross-folding relationships can be described only in terms of bedding and fold relationships as observed at fold intersections. Folds in the Bokkeveld Group do not lend themselves to a rigorous investigation of this kind, because interference effects are rather subdued. The apparent lower intensity of the Cedarberg folding in areas underlain by Bokkeveld beds, such as the Ceres intermontane valley, also contributed towards the absence of cross-folds. The orientation of bedding in Bokkeveld beds is largely controlled by underlying megastructures of the Table Mountain Group. Consequently, the Bokkeveld folds north of Ceres, towards Gydo Pass, trend N-S, while those to the east trend NE-SW. The fold axes therefore fan out rather than cross one another.

In the Witteberg Group, however, the high sensitivity to local stresses resulted in kink axes crossing one another at varying angles. This, in itself, provides a problem, because deformation was concentrated in the kink zones, resulting in rather complex interference structures at their intersections. Some subareas are also characterised by fold trends that belong

Stellenbosch University http://scholar.sun.ac.za

neither to the NW-SE nor the NE-SW trend. Kink intersections in the Witteberg Group are rare in the southern Ceres Syntaxis (Subareas 6, 7, 13, 15 and 16), but increase towards the north where the NE-SW trend displays the same intensity as the NW-SE trend. Detailed investigations of crossing fold axes in the Witteberg Group were carried out between N'wardouw and Skitterykloof (Subarea 10) as well as at Seekoegat (Subarea 13).

7.2 N'WARDOUW TO SKITTERYKLOOF

This area of about 9 km² was selected for detailed investigation on a scale of 1:16 000 (Figure 7.1). Here, folds developed in a monotonous succession of Witpoort Formation quartzitic sandstones and minor siltstones, while the overlying Kweekvlei and Floriskraal Formations were only slightly affected. Three subareas, namely the N'wardouwskloof, Hartnekskloof and Skitterykloof subdomains, are distinguished on the grounds of fold trend. Their boundaries coincide with faults. This does necessarily imply that faulting and folding were contemporaneous. In the N'wardouwskloof subdomain, fold trends are almost exclusively NW-SE and NE-SW; consequently, a right-angle cross-folding relationship exists. The Hartnekskloof subdomain contains mainly NE-SW and N-S, as well as a few NW-SE trending fold axes. The Skitterykloof subdomain displays only NE-SW and a few NW-SE folds. The probable reasons for these differences will be discussed later.

Stellenbosch University http://scholar.sun.ac.za

Figure 7.1

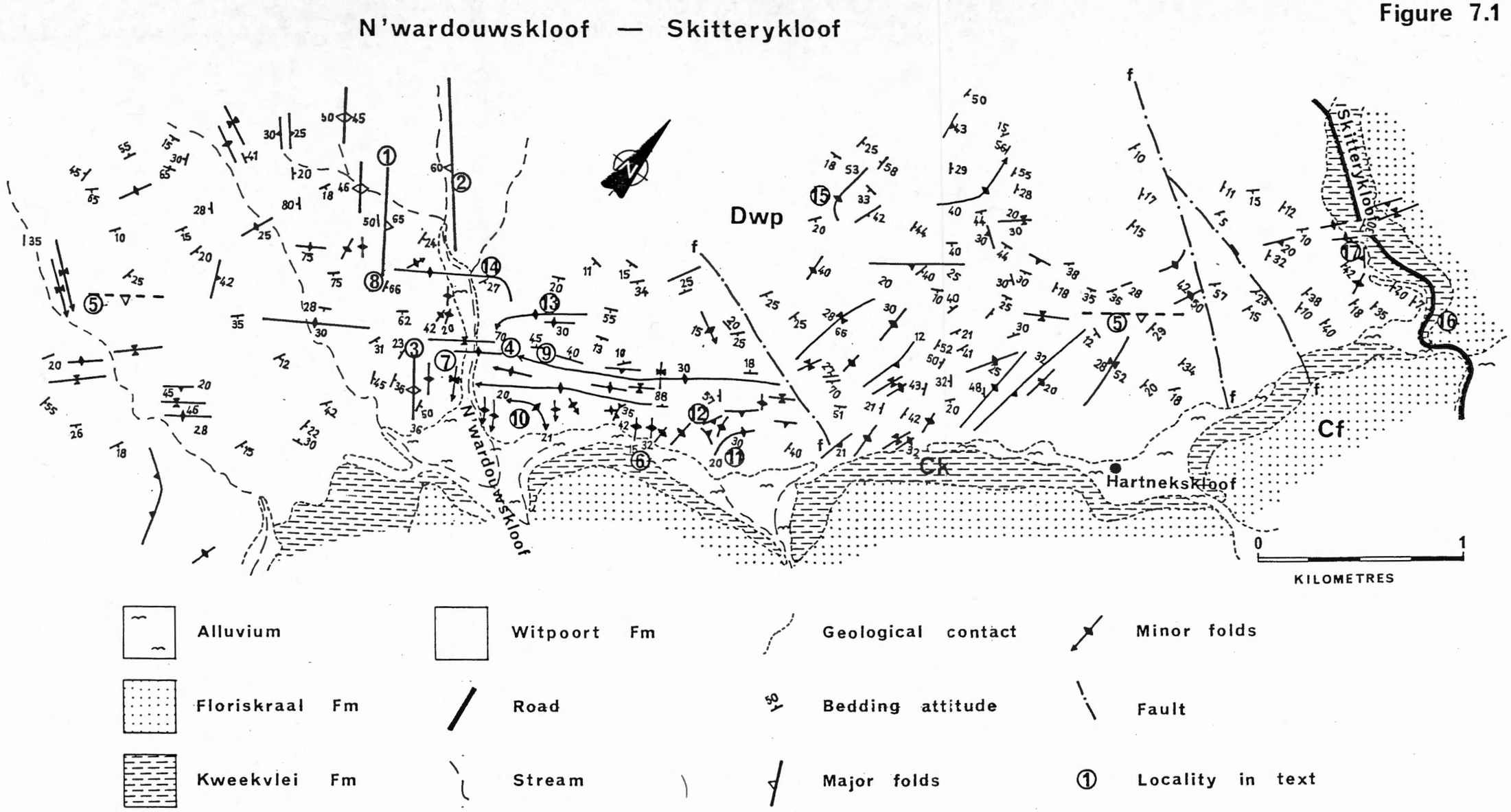

Figure 7.1
Map of the N'wardouw to Skitterykloof area, showing crossing fold trends. The N'wardouwskloof, Hartnekskloof and Skitterykloof subdomains are separated by faults.

Stellenbosch University http://scholar.sun.ac.za

7.2.1 N'wardouwskloof subdomain

Beds on the western side of the kloof were folded along dominantly NW-SE trending axes, while on the eastern side, NE-SW trending folds dominate. The main NW-SE trending folds are two megakinks with axes at 160/0 and 140/10 respectively (1 and 2, Figure 7.1). These two kinks have axial planes inclined at about 50 degrees to the west and east respectively, and thus form a conjugate, synclinal box fold. The hill immediately west of the kloof entrance consists of a broad anticlinal box fold with higher-order kink folds on its limbs (3, Figure 7.1, Figure 7.2). This box fold plunges nearly 36 degrees south-east, while parasitic kinks on the eastern limb of the structure have axial planes dipping to the south-west. The anticlinal box fold is situated along the south-eastward continuation of the synclinal trough between the two earlier-mentioned, NW-SE trending megakinks (Figure 7.1.), but involves stratigraphically higher beds than the latter structures.

On the eastern side of the kloof, NE-SW trending axes are dominant, until the fault trending 105 degrees is reached at the subdomain boundary. NE-SW folds developed preferentially in areas of low dip alongside NW-SE trending megakinks. On the western side of the kloof, intense NW-SE folding prohibited or inhibited them from forming. The NE-SW trending syncline-anticline pair (4, Figure 7.1, Figure 7.3) on the eastern hillside at the entrance to N'wardouwskloof, is situated on a large monoclinal flexure which runs for 15 kilometres from west

Stellenbosch University http://scholar.sun.ac.za

Figure 7.2
Large anticlinal box fold with smaller kinks on its limbs, west of entrance to N'wardouwskloof, N'wardouw.

Figure 7.3
Anticlinal NE cross fold on the eastern side of N'wardouws-kloof (4, Figure 7.1). Height of the hill is about 80m.

Stellenbosch University http://scholar.sun.ac.za

of Kafferskraal to Skitterykloof (Figure 7.1). The syncline is tightly appressed with an axial trend of 065/0, while the anticline is a typical box fold with nearly straight limbs and a slightly curved hinge area (Figure 7.3). Numerous higher order parasitic folds occur especially on the south-eastward dipping limb of this box fold. These small folds are commonly of isoclinal geometry with appreciable bedding-parallel shear (Figure 7.4).

Although the NW-SE folds are absent in the central part of the linear, NE-SW trending fold zone, they appear again at the southern edge of the hills, just below the base of the Kweekvlei shales (6, Figure 7.1). This has an important kinematic significance as will be discussed later on.

North of the north-easterly fold zone, the NW-SE trending fold axes are nearly horizontal, but they acquire a steep south-eastward plunge beneath almost vertical north-east striking beds, at the northern side of the hill (8, Figure 7.1). Crossing NW-SE and NE-SW trending folds are best displayed in the hills directly west of the entrance to N'wardouwskloof (7, Figure 7.1 and Figure 7.5). A detailed survey of the outcrops on the western hillside was undertaken in order to investigate the cross-folding relationships. Figure 7.6 is a schematic representation of the structures. The attitude of bedding in the three blocks, as well as that of L_B and slickenfibres, are shown in Figures 7.6A-D.

The northern part of the outcrops (Figure 7.7, Block A in Figure 7.6) displays the effects of the larger, synclinal,

Stellenbosch University http://scholar.sun.ac.za

Figure 7.4
Isoclinal folds formed by intense bedding parallel shear on the limbs of the anticlinal NE trending box fold shown in Figure 7.3.

Figure 7.5
Interference between the NW-trend and NE fold trends seen in the hillside directly west of the entrance to N'wardouwskloof. Length of the exposure is about 170 metres.

Stellenbosch University http://scholar.sun.ac.za

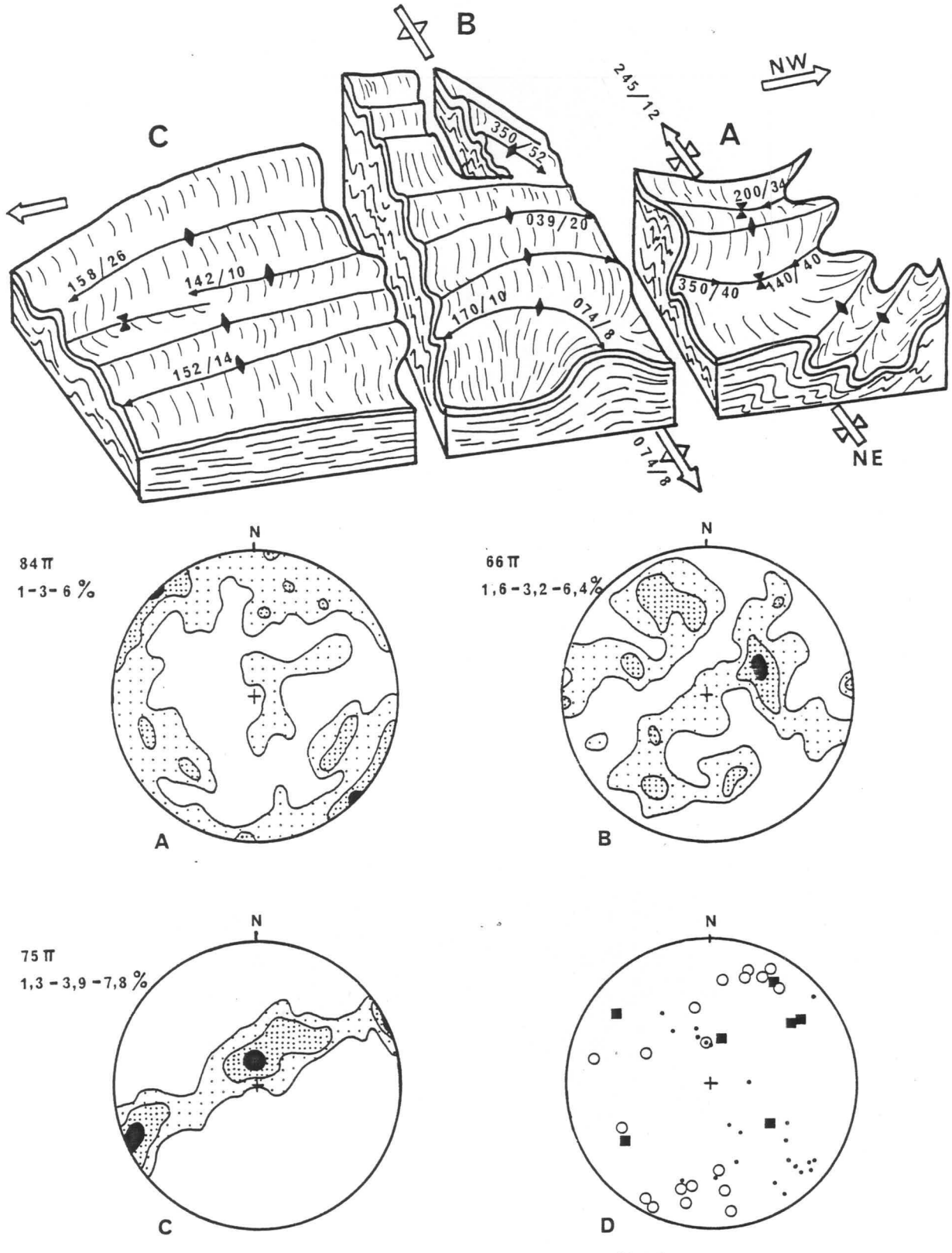

Figure 7.6
A schematic representation of the structures in Figure 7.5. Figures 7.6A to C are bedding pole diagrams for blocks A to C in the drawing (all contours per 1% area). Figure 7.6D: • = fold axes; ○ = B-lineations; ■ = slickenfibres.

Stellenbosch University http://scholar.sun.ac.za

Figure 7.7
NW trending folds affected by the NE synclinal cross-fold (block A in Figure 7.6). Distance from left to right in foreground is 70 metres.

Stellenbosch University http://scholar.sun.ac.za

NE-SW trending cross-fold, on initial NW-SE trending smaller folds. Fold axes of the latter plunge towards the cross-fold axis. At (1) in Figure 7.7, initial knee-folds with a "z" cross-section and axial planes dipping steeply south-west, were tightened to synclines and anticlines of which the axial planes are now curved and dip south at low angles. The upper synclinal structure (Figure 7.8A) displays a complex lineation pattern (Figure 7.8B). Horizontal lineations were not measured due to non-exposure of that part of the fold. The (local) axial plane at the top of this very tight, reclined syncline strikes 030 and dips 70 degrees south-east. By using only bedding poles from the approximately cylindrical part of the fold, a general axial orientation of 200/34 was determined north of the synclinal NE-SW cross-fold axis. The lineation plunges 30 to 40 degrees towards the south-west in the northern part of the refolded syncline. The general pattern of the lineation, which describes neither a small-circle, nor a great circle distribution, is typical of refolded or penecontemporaneously cross-folded structures in the area. The (pre-existing) NW-SE oriented lineation is deformed in conjugate shear zones south and north of the synclinal cross-fold axis (Figure 7.8A). This suggests that the NW-SE trending folds are locally slightly older than the NE-SW folds. Subhorizontal NW-SE trending wrinkles on steep bedding surfaces with steeply plunging lineations in the southern part of the syncline (Figure 7.8A), however, also illustrate that NW-SE folds were tightened till after the development of some NE-SW folds.

Stellenbosch University http://scholar.sun.ac.za

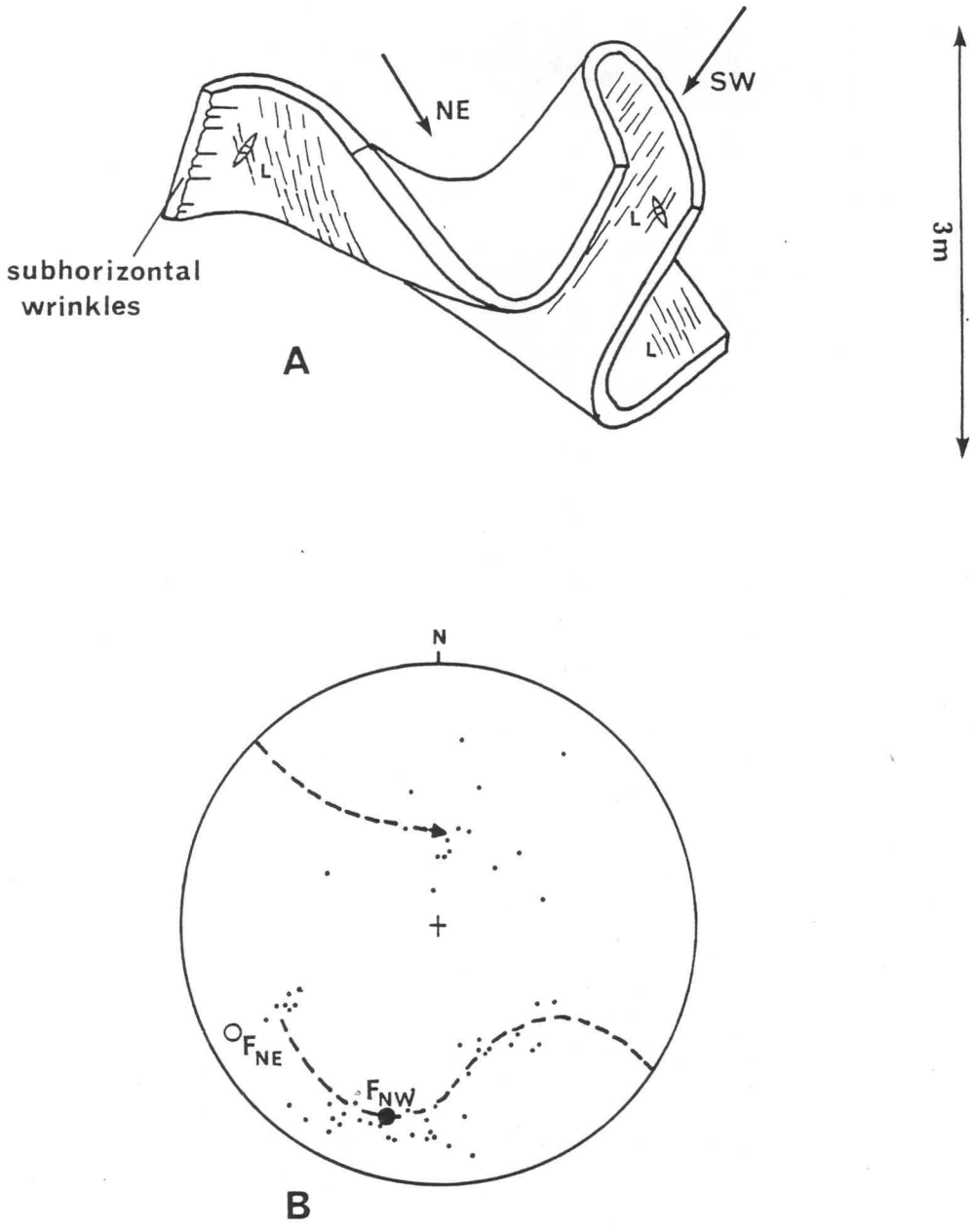

Figure 7.8
(A): Lineations subparallel to the (first formed ?) NW folds, complexly refolded by the NE synclinal cross-fold at (1) in Figure 7.7;
(B): Locus traced out by lineations in fold of (A) (path indicated from right hand side to left hand side of fold).

Stellenbosch University http://scholar.sun.ac.za

A NW-SE anticline - syncline pair is situated immediately below the tight syncline, at (2) in Figure 7.7. North of the NE-SW synclinal cross-fold axis, the anticline plunges steeply southward, but south of the cross-fold axis, it continues as a simple monocline plunging at 039/20 (Figure 7.6). The lower syncline (3), reacted differently to NW-SE directed compression, in that it was not tightened, but unfolded. The lowermost anticline (4) is also highly tightened, overfolded and underfolded north of the cross-fold axis, like the uppermost syncline (1). Some brecciation occurred along the fold hinge and bedding attitudes are highly irregular. Small folds, plunging to the south and north (Figure 7.6D) at between 20 and 70 degrees, occur towards the top of the hill (5, Figure 7.7).

Towards the middle of the outcrops (Figure 7.6, Block B and Figure 7.9), the adjacent anticlinal cross-fold had a seemingly milder affect on the NW-SE trending folds, but the bedding poles (Figure 7.6B) still reflect considerable interference. At (1) in Figure 7.9, about halfway up the rock face, NW-SE folds "ride" over a NE-SW anticline. The core of the NE-SW structure (2) is complex, with bedding poles describing a fold axis that changes orientation from 074/12 to 170/10. This feature demonstrates how beds gradually change attitude by oblique slip on bedding planes and on cross-cutting fracture planes to conform to one of the two mutually perpendicular fold trends. Slickenfibres which plunge 125/52 and 043/18 on consecutive bedding planes (Figure 7.10) confirm the occurrence of oblique slip and differential movement. Intense fracturing

Stellenbosch University http://scholar.sun.ac.za

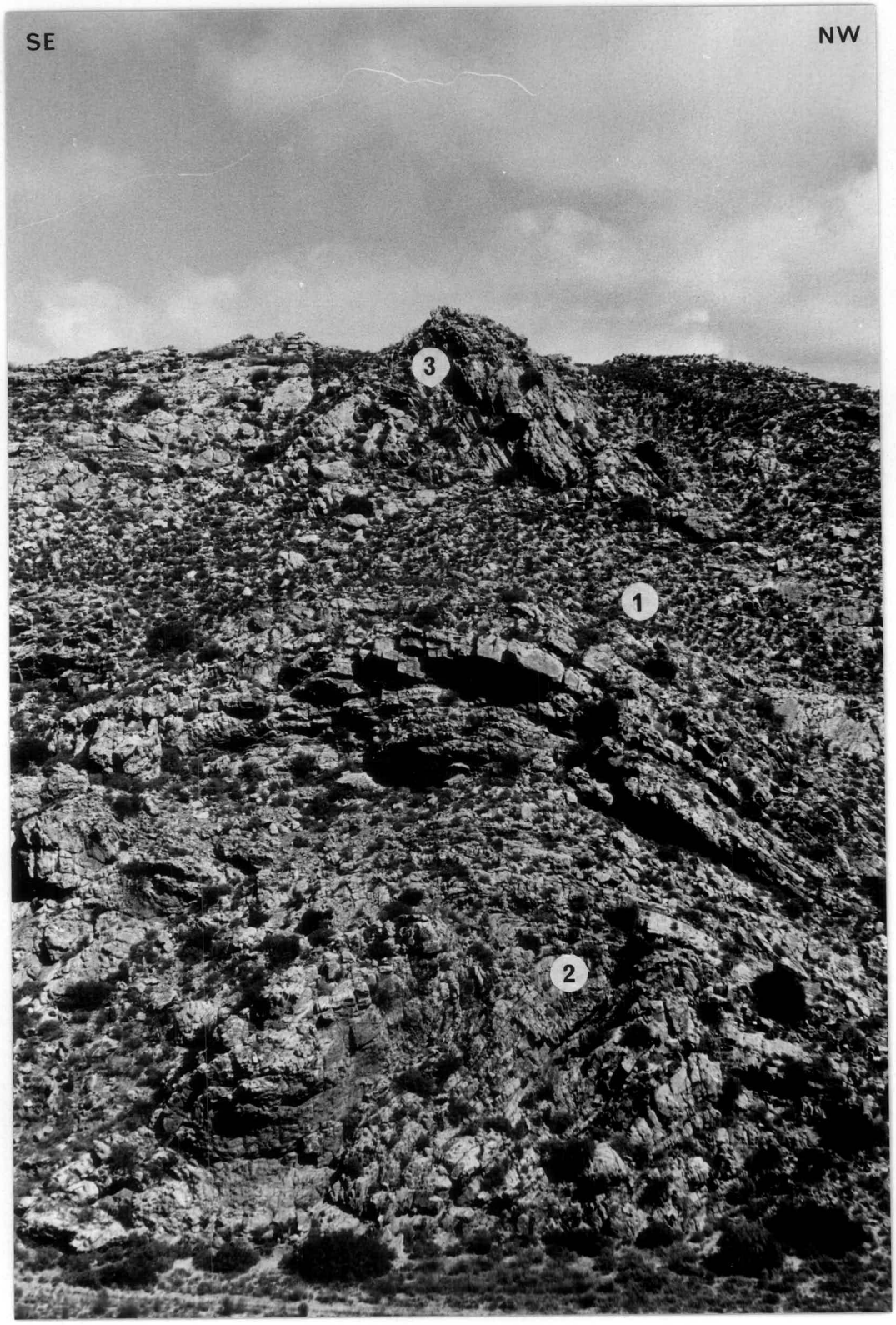

Figure 7.9
The folds of block (B) in Figure 7.6. Numbers refer to text. Distance from left to right in foreground is 40 metres.

Stellenbosch University http://scholar.sun.ac.za

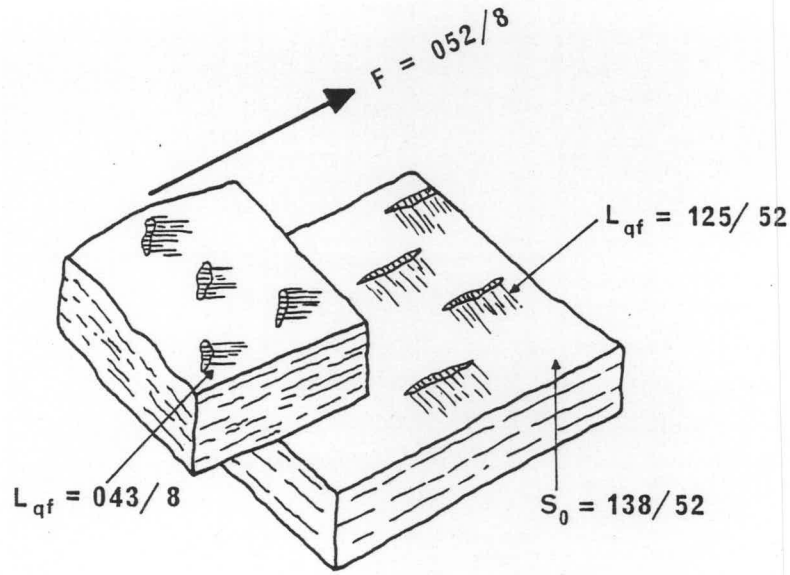

Figure 7.10
Dissimilar slickenfibre (l_{qf}) orientations on consecutive bedding planes (S_0) near fold at (2) in Figure 7.9.

Figure 7.11
Folds of the NW trend unaffected by the NE cross- folds towards the south-eastern side of the hillside (Block C of Figure 7.6). Height of the section is about 40m.

Stellenbosch University http://scholar.sun.ac.za

and complex folding occurred in the area to the left of Figure 7.9, which represents the continuation of the intensely deformed southern limb of the NE-SW anticline east of the kloof. The anticlinal cross-fold is also responsible for a fold axis plunging 350/52 at the top of the hill (3, Figure 7.9).

Towards the south-eastern end of the hillside, the bedding pole diagram (Figure 7.6C) indicates that fold axes plunge 146/10 outside the cross-folded zone. Individual fold axes, as determined from π-plots, are oriented 158/26, 142/10 and 152/14. A small NE trending monocline towards the lower righthand corner of Figure 7.11, reflects compression subparallel to these fold axes.

On the eastern side of N'wardouwskloof, NE-SW trending anticlines at the top of the hill are canoe-shaped (9, Figure 7.1 and Figure 7.12), with highly undulating fold axes. As NW-SE trending folds are absent from the centre of the NE-SW fold zone along the top of these hills, the canoe shape of the latter evidently resulted from either open NW-SE folds that were originally present, or from simultaneous NW-SE and NE-SW directed compression acting on horizontal beds. The relative tightness of NW-SE trending folds in the cliff section immediately west of N'wardouwskloof, as well as immediately south of the NE-SW trending cross-folds, shows that the former folds could not have been open structures. Canoe-shaped folds have been described from many areas where fold interference, due to superimposed deformational episodes, occur. They could, however, also evolve during contemporaneous cross-folding.

Stellenbosch University http://scholar.sun.ac.za

Figure 7.12
Canoe-shaped folds (at X) near (9) on Figure 7.1.

Figure 7.13
Refolding of an originally NE trending small anticline by its own fold trend. The anticlinal axis now plunges 70 degrees south-east (away from the observer).

Stellenbosch University http://scholar.sun.ac.za

Immediately south of the NE-SW fold zone, small NW-SE trending folds are again abundant. The two largest ones of these display hinge-lines that gradually curve towards the NE-SW trend (10 and 11, Figure 7.1). The axial plunge of one of these folds increases as it becomes more north-westerly orientated, but the other plunges in both directions. There are no indications that these folds were rotated to their present position by successive compressional events. No excessive stretching occurred in the limbs on the convex side of the curved, near-vertical axial plane. Remarkably, slickenfibres on bedding planes remain perpendicular to the local fold axes, notwithstanding intense curvature. Anomalous movements in limbs on either side of the axes of such folds, led to tightening or unfolding during progressive development of the structure. These folds are similar to the "accommodation structures" described by Bhattacharji (1959) and Rast and Platt (1957), who attributed their formation to synchronous cross-folding. Closely associated with these structures are smaller folds, rather similar to the "table-cloth" folds (12, Figure 7.1) of Ramsay and Huber (1987), which are expected to form in a constrictional stress field (Field 3 of Ramsay's diagram). Ghosh and Ramberg (1968), also produced such folds in laboratory experiments by simultaneous buckle-folding at unequal orthogonal compressions in the plane of the beds. Intersections and merging of these folds are typically unsystematic, like those in Figure 7.1.

A small anticline (13, Figure 7.1), with a wavelength of about 5 metres and an amplitude of 2 metres, near the northern

Stellenbosch University http://scholar.sun.ac.za

boundary of the NE-SW trending fold zone, displays some important features as far as the age of the main trends at N'wardouwskloof is concerned. The fold axis plunges 15 degrees towards 210 degrees, approximately perpendicular to the NW-SE trending folds along the kloof. Where unaffected by interference, the anticline has a straight axis. However, as the structure tightens to the west, the axis curves sharply towards the south and its plunge gradually steepens until it ultimately plunges at 70 degrees below beds belonging to the NE-SW trending syncline (13, Figure 7.1 and Figure 7.13). This "cannibalistic" way in which the original anticline is refolded by its own trend, may be explained as follows:

(1) The NW-SE trending part existed before the NE-SW extension formed. The previously tilted beds thus controlled the swing in the latter structure.

(2) NW-SE and NE-SW related folds formed contemporaneously, thus the NE-SW fold axis could not have developed in an area where compression subparallel to its trend exceeded compression perpendicular to its trend.

Although it is clear that during cross-folding by a flexural mechanism, the shape and orientation of the cross-folds will be determined by the initial slope of bedding produced by the first-formed fold trend (Bhattacharji, 1959; Ghosh and Ramberg, 1968; Skjernaa, 1975; Watkinson, 1981), the same could also be said of almost simultaneous cross-folding.

Ghosh and Ramberg (1968) stated that for simultaneous cross-folding, "A fold may die out when a differently trending fold lies across its way, or the two hinges might join in a

Stellenbosch University http://scholar.sun.ac.za

smooth arc." This smooth change in the trend of fold axes is common in the N'wardouwskloof subdomain. Also, the dip of beds at the closure of the plunging NW-SE trending megakink (just south of 14 in Figure 7.1) is less than 20 degrees south-east. This attitude would have been ideal for the development of NE-SW trending folds, if the NW-SE trending kink already existed. Notwithstanding these conditions, the small NE-SW trending anticline rather changes trend towards the south-east and becomes refolded. The field evidence therefore indicates that NW-SE and NE-SW trending folds were at one stage being formed simultaneously, resulting in confinement of the NE-SW anticlinal axis when it reached a zone dominated by the NW-SE trend. The NE-SW directed compression was just sufficient to prevent this fold axis from developing further into the NW fold zone. A similar structure can be seen about 100 metres up N'wardouwskloof (14, Figure 7.1), where another small anticline, trending 065 degrees, gradually merges with beds towards the closure of the NW-SE trending megakink and changes to a monocline with axis subparallel to the megakink (Figure 7.14).

The N'wardouwskloof subdomain, in summary, provides evidence in favour of slightly earlier NW-SE trending folds being refolded by NE-SW trending cross-folds, and of contemporaneous cross-folding in two mutually perpendicular directions. Some folds, displayed in the hillside west of N'wardouwskloof, are typical type 2 structures (Ramsay, 1967), with curved axial planes. They formed from kinks with steeply-inclined axial surfaces that were refolded at right angles to their axes. Though

Stellenbosch University http://scholar.sun.ac.za

Figure 7.14
Small NE trending anticline merging with a NW megakink near (14) in Figure 7.1. Height of the hill is about 200m.

Stellenbosch University http://scholar.sun.ac.za

Ramsay's models strictly apply to shear-type superposed folds, the similarity with flexural superposition is evident. Due to accommodation and compatibility constraints, pure flexural modes for type 2 interference patterns are impossible unless the fold is, or becomes, isoclinal (Watkinson, 1981). The latter has evidently occurred in the tight synclinal fold towards the top of Figure 7.7, locality 1 (See also Figure 7.8A).

Another feature of fold interference patterns, namely that perpendicular refolding of open concentric folds will produce type 1 patterns (basins and domes), is displayed locally by the syncline at locality 3 (Figure 7.7). Due to the fact that Witteberg folds developed mostly by kinking along linear zones, most kink intersections developed type 2 structures. Away from the intersections, however, basin and dome (type 1) structures invariably occur as a result of lower bedding dips (Ghosh and Ramberg, 1968).

The apparent refolding of existing NW-SE trending folds occurs only in the northern part of the western hillside at the entrance to N'wardouwskloof. Towards the centre of the area (Figure 7.6, block B), the NE-SW anticlinal cross-fold provides evidence of simultaneous cross-folding by displaying a curving axis similar to those described in the previous paragraphs. From the map (Figure 7.1), it is clear that purely NW-SE and NE-SW trending folds occupy certain areas, while "accommodation folds" and "table-cloth" folds, occupy others. Similar results were reported by Ghosh and Ramberg (1968) for simultaneous

Stellenbosch University http://scholar.sun.ac.za

buckle-folding by unequal compressions in two orthogonal directions when they stated that: "Only very rarely do divergent folds cut across each other." There is also a tendency for folds of the two trends to develop unsystematically at different levels in the multilayered sequence. The Stompiesfontein fold zone (Chapter 6) displayed only NE-SW trending folds in the lower and middle parts, while NW-SE trending folds developed towards the top. In beds where the two perpendicular main stress vectors were of approximately the same magnitude, curving fold axes resulted.

7.2.2 Hartnekskloof subdomain

This area is characterized by the absence of NW-SE trending folds. The dominant fold trend (Figures 5.5H and 5.6F) is almost N-S. A few NE-SW folds intersect the latter obliquely or gradually change trend towards N-S along strike.

Fold axes that curve from NW-SE towards NE-SW, are well displayed in a kloof west of the Hartnekskloof ruins (15, Figure 7.1; Figures 7.15 and 7.16). An anticline with axis 297/4 is situated on the right hand side of Figure 7.15 at (1). Poles to bedding (S_0), slickenfibres on bedding and on a small reverse fault parallel to the axial plane (l_{qf}), as well as the attitude of the fault and quartz-filled extension fractures (Figure 7.16A), suggest a cylindrical geometry for this part of the fold. A very faint lineation (L_B) on bedding planes coincides with the fold axis. Where the anticline starts curving towards the north-east, a small dome has formed and

Stellenbosch University http://scholar.sun.ac.za

Figure 7.15
Curved fold axes in the kloof west of the Hartnekskloof farmhouse. Note the high fold intensity in the NE trending folds and the almost undisturbed overlying beds. Length of section approximately 80 metres (in the middle ground).

Stellenbosch University http://scholar.sun.ac.za

bedding attitude changes dramatically (2, Figure 7.15). The fold axis now trends 328/0 and a basin structure was formed where there should have been a synclinal trough (3). The anticline at (4) deviates even more from its original trend as measured in outcrops on the opposite side of the kloof (not shown in photograph), because the fold axis changes from 160/14 (B1) to 018/0 (B2) along strike (Figure 7.16C). No stretching lineations or significant extension fracturing occur where the fold axis attains its maximum curvature, but a ramifying network of quartz-filled shear veins, trending tangentially to the outer convex arc of the structure, is seen in the stream bed below. An intensely deformed zone of folds trending 030/0 occurs on the northern side of the exposures (5, Figure 7.15). Isoclinal folds with flat-dipping axial planes, listric faults, bedding wrinkles, and a penetrative lineation parallel to the fold axes (Figure 7.16D) are characteristic of this zone. Buckle shortening and flattening are evidently a maximum at the south-eastern boundary of the zone where these folds meet with the curving axes of the NW-SE trend. The NE-SW trend dies out abruptly towards the northern side of the exposures. Immediately overlying beds are undisturbed, as at the Stompiesfontein fold zone (p. 52). However, kinks trending 009 degrees occur in stratigraphically somewhat higher beds.

The fact that fold axes remain subhorizontal at Hartnekskloof, clearly shows that the NE-SW and NW-SE fold trends developed simultaneously as a result of compression in two orthogonal directions. The change in trend of the NW-SE folds primarily result in the steepening and flattening of limb dips, thus

Stellenbosch University http://scholar.sun.ac.za

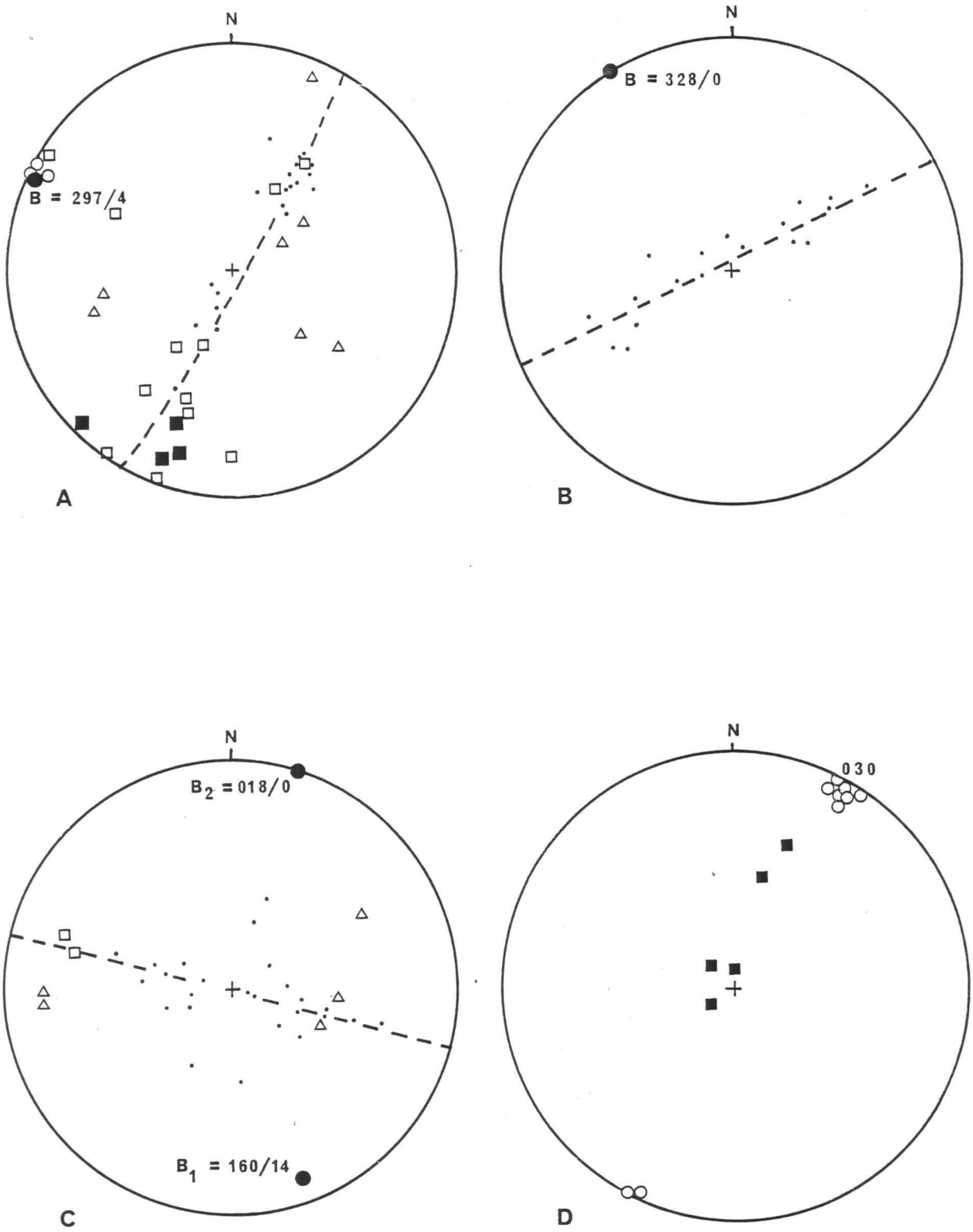

Figure 7.16
Orientation data for the folds in Figure 7.15. A, B and C: · = S_o; ● = fold axis; ○ = L_B △ = l_{qf}; □ = poles to extensional fractures (quartz-filled); ■ = poles to reverse fault. Figure 7.16D: ○ = L_B; ■ = axial planes to folds.

Stellenbosch University http://scholar.sun.ac.za

a typical type 1 (Ramsay, 1967) interference pattern was formed. This view is further supported by the development of only one lineation, parallel to either the NE-SW or the NW-SE trend, depending for its development on the intensity of folding.

N-S trending fold axes in the Hartnekskloof subdomain probably represent the resultant of an orthogonally constricted strain field with main strains directed NW-SE and NE-SW. The boundary faults probably also exerted some control on the distribution of strain in the subdomain. They do not show appreciable vertical or horizontal displacement of the Witpoort-Kweekvlei contact, but metre-wide brecciation occurred along the near-vertical fault planes. Apparent association of these faults with the N-S trend, suggests that they may have been initiated syntectonically. Stress reorientation by fault movements is now widely accepted (Stubley, 1989).It is highly probable that the faults have strike-slip displacements, but the absence of marker beds, together with broken outcrops, make this difficult to confirm. Evidently, more work is needed in this regard.

7.2.3 Skitterykloof subdomain

This area is situated at the north-eastern termination of the NE-SW trending monoclinal flexure which runs for nearly 15 kilometres from Vleiberg to Skitterykloof, subparallel to the lower slopes of the Swartruggens Range. North of Skitterykloof, the NE-SW trend had little effect on the contact

Stellenbosch University http://scholar.sun.ac.za

between the Witpoort and Kweekvlei Formations. Fold axes and bedding pole data are roughly the same as for the N'wardouwskloof subdomain. Kinked bedding in Kweekvlei shales (Figure 7.17), as well as Witpoort sand-dykes injected into shale (Figure 7.18), are seen along Skitterykloof Pass (16, Figure 7.1). The injected sandstone is structureless and displays a fine linear fabric subparallel to the dyke walls. The latter fabric resembles water-escape structures. The local fold axes in the Floriskraal and Witpoort Formations lie approximately in the planes of the Kweekvlei shale kink boundaries (Figure 7.19). The dyke was probably injected along a syntectonic longitudinal fracture. This is a clear indication of the rheology of the some of the sediments during at least the initial stages of folding.

A small dome occurs in brownish sandstone just below the Kweekvlei shale, immediately south of Skitterykloof Pass (17, Figure 7.1). An anticline with axis attitude 045/6 is transected by a south-westward facing monocline that trends approximately 125 degrees (Figure 7.20). The effect of this monocline is reflected in a cliff of Floriskraal sandstone south of Skitterykloof Pass. North of the monoclinal axis, L_B in NE-SW trending folds plunge 020/17 on average, whilst south of it, the lineation and a small fold axis plunge 217/10 (Figure 7.21). The relative tightness of the small folds and the NE-SW trending anticline, compared to the gentle NW-SE trending monocline and plunging B-lineations, suggest that the NW-SE trend is either younger, or that the two trends evolved approximately contemporaneously at some stage. Some small-

Stellenbosch University http://scholar.sun.ac.za

Figure 7.17
Kinks formed in thinly laminated shales of the Kweekvlei Formation at Skitterykloof.

Figure 7.18
Sand dyke, about 1m wide (at hammer), injected into Kweekvlei shales at locality 16, Figure 7.1.

Stellenbosch University http://scholar.sun.ac.za

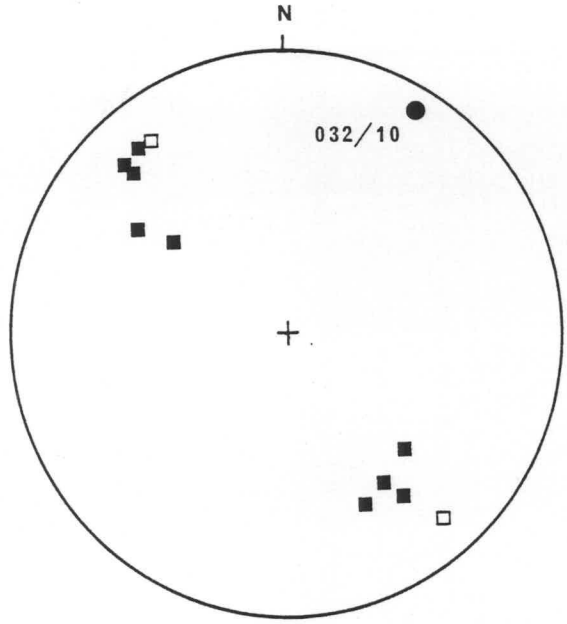

Figure 7.19
Orientation of kink planes (■), sandstone dyke bounding planes (□) and local fold axis (●) in Floriskraal sandstone at locality 16 of Figure 7.1.

Figure 7.20
Small dome (at X), formed by interference between a NE trending anticline and a NW kink, in river bed below Skitterykloof Pass.

Stellenbosch University http://scholar.sun.ac.za

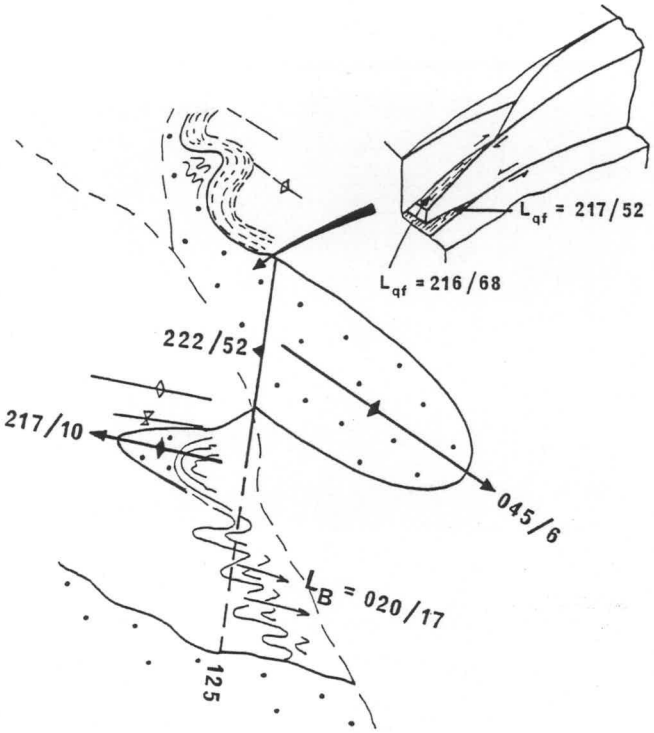

Figure 7.21
Sketch of the exposures around the dome depicted in Figure 7.20 (not to scale).

Figure 7.22
Small-scale listric faulting in beds above the NW kink axis in Figure 7.21. Orientation of slickenfibres (l_{qf}) is shown in Figure 7.21.

Stellenbosch University http://scholar.sun.ac.za

scale listric thrusting, related to compression that formed the NW-SE trending monocline, is evident in the beds immediately overlying the dome (Figures 7.21 and 7.22). Slickenfibres on these faults indicate NE-SW directed compressive slip.

In summary then, structures in the area between N'wardouwskloof and Skitterykloof appear to indicate that the two main fold trends are approximately synchronous. The overall similarity in fold styles further supports this argument.

7.3 SEEKOEGAT

Crossing NE-SW and NW-SE folds occur at Seekoegat (portion of the farm Nouga, Map 1). A NE-SW trending zone of intense folding intersects an equally intense NW-SE trending zone about 3 kilometres south of Katbakkies Pass on 3219DC Groenfontein (Figure 7.23). Both fold zones end against an E-W to WNW-ENE trending fault. The cliffs immediately north-east of the Seekoegat locality display NE-SW fold zones at different levels with unfolded or N-S to NW-SE folded beds sandwiched in between. The intense Seekoegat NE-SW fold zone dies out at the foot of the mountain, near the level of the river bed. Above this level, numerous N-S and NW-SE trending small kinks as well as one small, south-east facing, NE-SW monocline occur. The latter contrasts strongly with the wide NE-SW trending Seekoegat fold zone below. Towards the top of the cliffs, the NE-SW trending monocline gradually intensifies into the 300 metre wide fold zone south of Kliphuis (Map 1) of which the orientation data were presented in Figure 6.8B. Two intensely

Stellenbosch University http://scholar.sun.ac.za

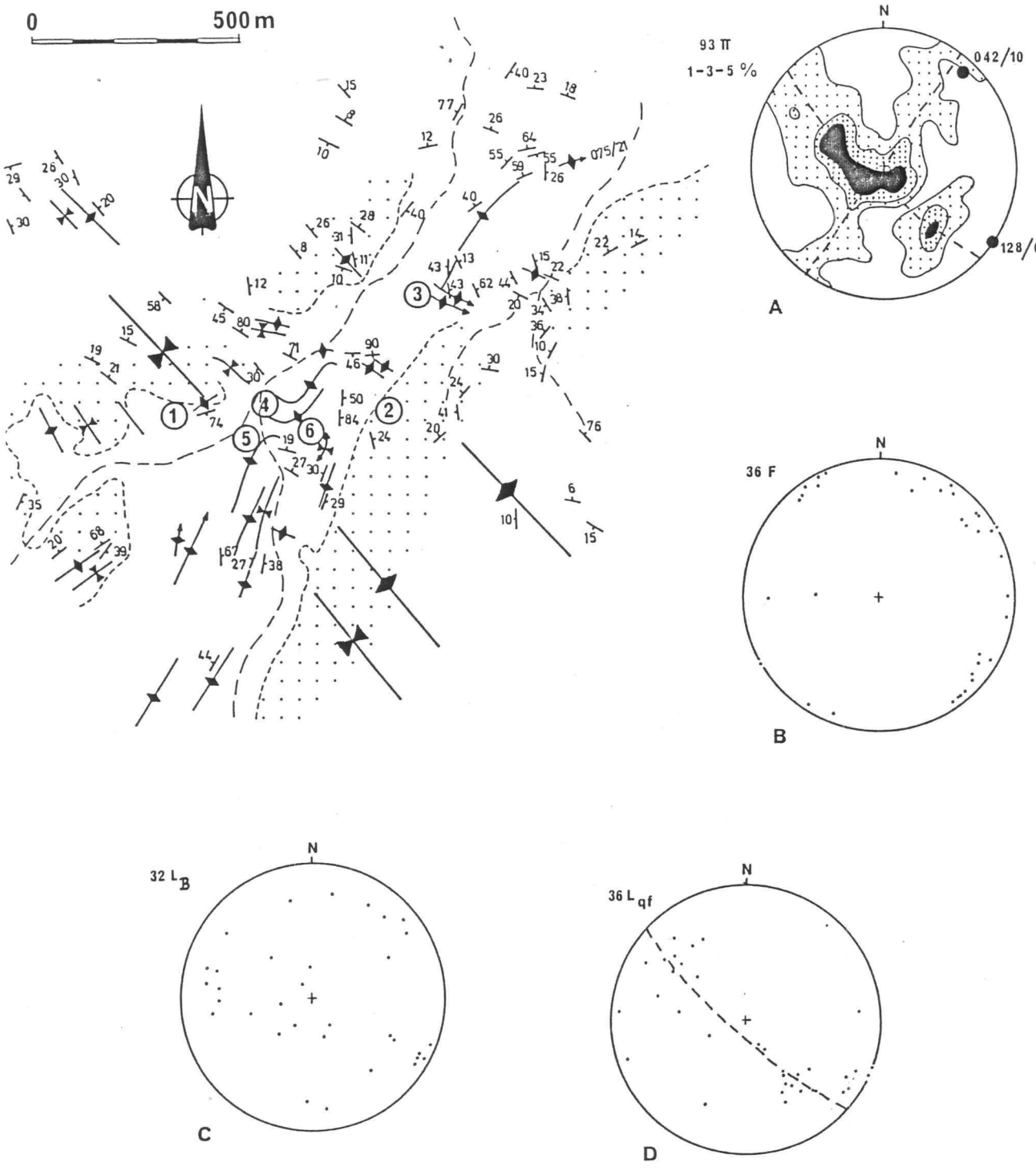

Figure 7.23

Crossing NW and NE folds at Seekoegat south of Katbakkies Pass. Major and minor folds are indicated as before, while the stippled area represents thick bedded sandstones and the blank areas are incompetent thin-bedded sediments. Circled numbers refer to the text. Bedding attitudes are indicated by the usual dip and strike symbols. Thin broken lines are stream beds. Figure 7.23A: Bedding pole diagram for all folds, with the main fold trends indicated. Contours per 1% area; Figure 7.23B: All fold axes; Figure 7.23C: L_B; Figure 7.23D: Slickenfibres (l_{qf}).

Stellenbosch University http://scholar.sun.ac.za

deformed zones of NE-SW trending folds are therefore stacked on top of each other. However, their trends change from 030 at Seekoegat to 085 south of Kliphuis.

Bedding poles at Seekoegat describe two main trends at 042/10 and 128/0 (Figure 7.23A). Fold axes (Figure 7.23B), and L_B (Figure 7.23C) display many different attitudes. Slickenfibre (l_{qf}) orientations appear to belong mainly to the NE trend (Figure 7.23D). The NW-SE folds are open box folds with numerous small parasitic folds on their steep limbs. The amplitudes of these folds are of the order of metres to a few tens of metres, with wavelengths of about 100 metres. The NE-SW folds are comparable in shape to the north-east trending Stompiesfontein and Kliphuis fold zones, and display concentric, similar and kink forms. Most north-east trending fold axes are subparallel to the fold zone boundary. At the Zeekoegat locality, thin-bedded, incompetent, silty sandstones are exposed in the north-east trending fold zone. Overlying competent, pure white quartzitic sandstones are folded penetratively by the north-west trend. The effects of the north-east trending folds in the competent beds are only visible at the boundaries of the fold zone, whilst interference between north-west and north-east trending folds occurs freely within the incompetent rocks of the zone. However, there is no convincing evidence that the north-west trend is older than the north-east trend.

At (1) in Figure 7.23, small folds trending 040 degrees, occur on the limbs of a north-west trending syncline near the

Stellenbosch University http://scholar.sun.ac.za

northern boundary of the zone of north-east trending folds. Kinks and isoclinal, north-easterly folds at (2) in Figure 7.23 (Figures 7.24A and B), occur in cross-bedded, competent, white sandstones that are folded into a broad, north-west trending anticline. Associated quartz-filled tension veins and slickenfibres, both inclined towards the south-east, are related to north-east folds in the underlying incompetent units. The fold axes plunging 120/20 at (3) in Figure 7.23, either represent tilted early north-west trending folds, or north-west trending folds tilted by simultaneous folding along north-east trending axes.

Curving fold axes and steeply-inclined lineations (L_B), developed characteristically at the intersection of north-west and north-east trending folds of equal intensity. At (4) in Figure 7.23, a gradual change in fold axis trend from north-west to north-east, and vice versa, can be observed. Approaching the outcrops from the west, north-east trending anticlines become isoclinally folded in their cores (Figure 7.23, at (5) and Figure 7.25) and simultaneously change trend towards the south-east where they meet with the intense north-west trending parasitic folds on the eastern limb of a large syncline.

In the central part of the outcrops (6, Figure 7.23), north-west trending isoclinal folds acquire steep south-eastward plunges, as indicated by a penetrative B-lineation plunging 152/65. Towards the north-east, a north-westerly trending fold changes its axial attitude from 150/15 to 050/10. This fold

Stellenbosch University http://scholar.sun.ac.za

Figure 7.24A
NE trending kinks in overlying thick-bedded sandstone at (2) in Figure 7.23.

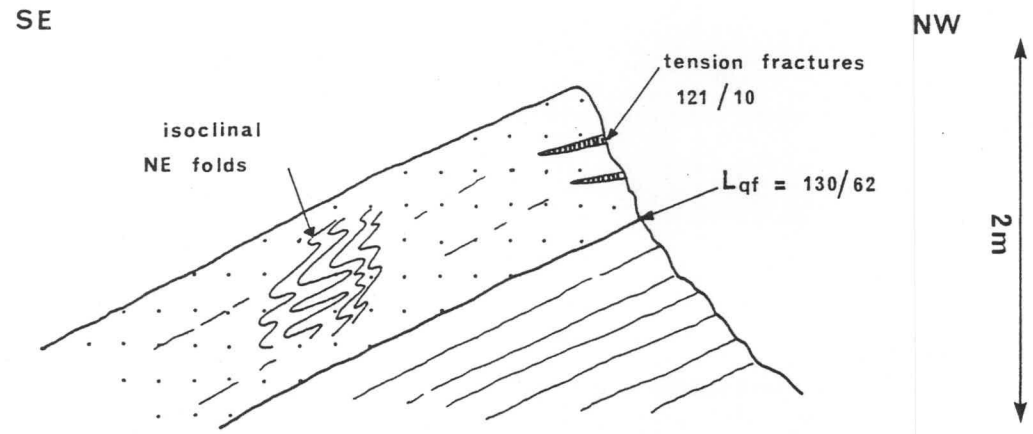

Figure 7.24B
Isoclinal folds, slickenfibres (l_{qf}) and tensional fractures relating to the NE fold trend at (2) of Figure 7.23.

Stellenbosch University http://scholar.sun.ac.za

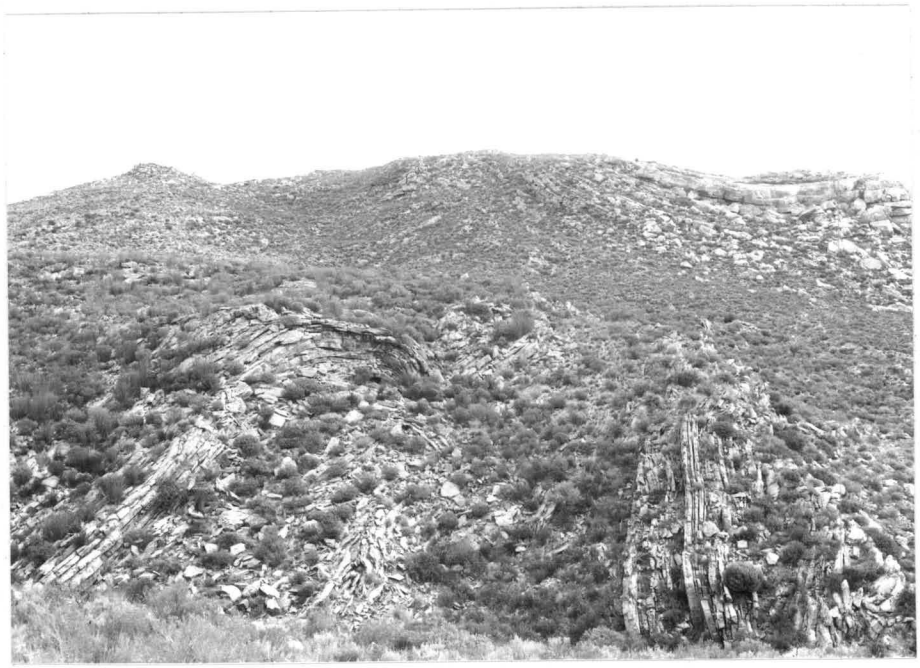

Figure 7.25
North-east folds with isoclinal beds in their cores at (5) in Figure 7.23. Note the thin-bedded character of the sediments. Height of fold on left is about 15 m.

Figure 7.26
Nearly isoclinal small fold with steeply plunging lineation parallel to the fold axis.

Stellenbosch University http://scholar.sun.ac.za

displays (a-b) tension cracks tangential to, and slickenfibres perpendicular to, the local fold axis. It is therefore apparent that the fold axis must have formed approximately in its present position. There are no intersecting B-lineations or differences in fold style between the two trends. Little fracturing resulted from the superposition of the two main stress directions. All these features indicate that the two fold directions are approximately synchronous. It may be argued that steeply inclined B-lineations of the north-west trend in the north-east trending fold zone, indicate refolding, but there are also steeply inclined northeast-trending B-lineations (Figure 7.23C).

The folded Witteberg sediments at Seekoegat provide evidence of a high water content during deformation. A prominent, reddish weathering, structureless, sandy unit is locally sandwiched between the upper competent and the lower incompetent part of the succession. All sedimentary structures therein were obliterated during deformation and the rock appears to be severely leached. The incompetent, thin-bedded succession below displays isoclinal small folds (Figure 7.26) that belong to both trends, together with highly contorted beds (Figure 7.27). The latter observations clearly indicate that these structures developed more or less penecontemporaneously in relatively unconsolidated sediments. As at N'wardouwskloof, the occurrence of steeply plunging, north-west trending folds near the boundary with the north-east crossing trend, may indicate that the former folds started to develop slightly earlier. This slight age difference around Seekoegat, is of

Stellenbosch University http://scholar.sun.ac.za

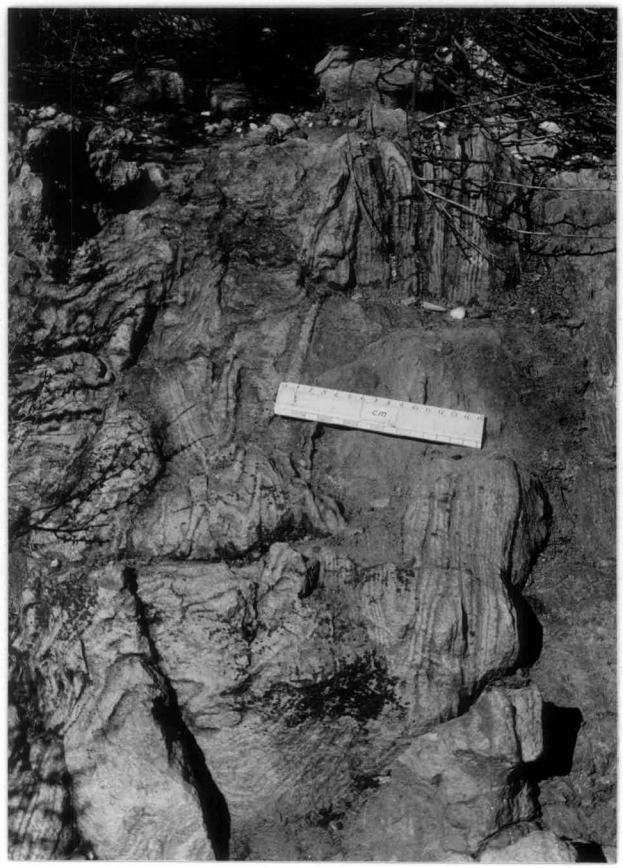

Figure 7.27
Highly contorted bedding laminae at locality (4), Figure 7.23. Length of scale is 15cm.

Stellenbosch University http://scholar.sun.ac.za

perhaps related to the proximity of this area to NW-SE megastructures in the Table Mountain Group.

7.4 EVIDENCE FROM THE PLATKLIP AREA

The axial traces of north-west and north-east trending folds intersect at an angle of 45-55 degrees at the Winkelhaak Fault immediately west of Platklip (3319BA). Immediately north of the south-easterly extension of the fault, south-east plunging fold axes dominate over the north-east plunging ones, while south of it, the situation is reversed (see Figure 5.1 and Map 1). On either side of the Winkelhaak Fault, both these trends swing towards the east - the north-west trend more so than the north-east trend. The lower intensity of north-west trending folds, compared to the north-east folds, is probably the main reason for this feature. The latter trend coexists with the north-west trend further north, but the north-westerly folds disappear south of the Winkelhaak Fault (Map 1). These features are best explained by simultaneous folding in two directions or, alternatively, by penecontemporaneous but separate pulses of the same orogeny.

7.5 SUMMARY OF CROSS-FOLDING RELATIONSHIPS

(1) There is no overall difference between the fold styles of the main trends.

(2) Plunging fold axes of each of the two trends, occur on limbs of megastructures related to both trends. In the south, for example, north-easterly fold plunges occur on

Stellenbosch University http://scholar.sun.ac.za

the regionally eastward dipping Witteberg rocks in the Swartruggens Range, whilst in the north, south-eastward fold plunges occur on the limbs of the north-east trending Kafferskraal-Skitterykloof monocline.

(3) According to Rast and Platt (1957), the thicker the fold prism, the more noticeable will the cross-folding be. Thus, Bokkeveld folds merely reflect the trend of Table Mountain Group megastructures as a conformable member of a structural lithic unit, but the overlying Witteberg Group displays true cross-folds.

(4) The two main trends in the Witteberg Group formed nearly simultaneously by interference of linear structures, each of which dominated in a specific area (see Whitten, 1969). The magnitude of compression for each trend also played a part in this.

(5) The abundance of slickenfibres on bedding planes indicates true flexural-slip cross-folding. The shape of early folds dictated the attitude of axes of buckling of the local (subsequently superposed?) folds. In interference structures, two different orientations of slickenfibres on the same, and on closely associated beds, indicate that structural accommodation of different trends occurred by oblique-slip. Shear folding occurred locally in incompetent beds due to space problems. The fact that cleavage cannot develop in the competent quartzites at low metamorphic grades, excludes superposed shear folding as a dominant mechanism.

(6) Steep fold axes and B-lineation plunges are not, as such, an indication of compressive phases separated by a long

Stellenbosch University http://scholar.sun.ac.za

time span, but may also be related to the continuously varying attitude of the bedding anisotropy, produced by concomitant tilting in all directions. Curved axial planes and lineations developed locally due to the pulsating character of compression with relation to the two fold trends.

(7) The criterion that early folds are usually more continuous than superposed folds (Skjernaa, 1975), does not hold for Witteberg structures, because the two trends developed zonally and penecontemporaneously.

(8) Folds of one trend often die out when a differently trending fold lies across its way. Two divergent folds very rarely cut across each other. However, at a later stage, patterns similar to that of superposed folds developed (N'wardouwskloof subdomain for example). These structures are characteristically formed where unequal compressions acted simultaneously at a large angle to each other (Ghosh and Ramberg, 1968).

(9) Interference folds of the first type (Ghosh and Ramberg, 1968), i.e. basins and domes, developed where open structures crossed each other (Skitterykloof and Hartnekskloof subdomains). Interference folds of the second type developed only locally where kinks were intersected by tight cross-folds (N'wardouwskloof, western hillside). However, real "wormlike" forms (Julivert and Marcos, 1973), were rarely encountered on a regional scale.

(10) The most regularly encountered "interference structures" are the so-called accommodation folds, where the two

Stellenbosch University http://scholar.sun.ac.za

trends share a common, curving axial plane. If these structures represented refolded, plane, cylindrical folds, strong shear strains (Ghosh, 1974) would have resulted in axial surface slides (Ramsay, 1967). Instead, the small reverse fault in the Hartnekskloof accommodation fold (p.72), occurs where the north-west trending anticline is still rectilinear. In the curved segment of the anticline, no sliding or conspicuous shearing is evident. The axes curve as a result of increasing or decreasing limb dips on the convex or concave sides of the arcs. The accommodation folds do not display marked fracturing perpendicular to the axial direction, or different ages of longitudinal veins indicative of hinge-migration (Odonne and Vialon, 1987). The fact that these accomodation folds are of the same size as folds with linear axes, and that they are either associated with right-angle cross-folds (Rast and Platt, 1957) or can occur alone, indicate penecontemporaneous cross-folding.

(11) The net movement picture of Witteberg cross folding consisted of two orthogonally opposed compressions affecting different parts of the multilayer simultaneously. Differences in the magnitude of strain, or in the local timing of fold initiation, produced refolding or transecting relationships.

Stellenbosch University http://scholar.sun.ac.za

8. ORIENTATION OF PRINCIPAL STRESSES

8.1 INTRODUCTION

Principal stress directions were determined from conjugate kink folds (Ramsay, 1962) in the Witteberg Group. The morphological and mineralogical differences between Witteberg sediments and the slate used by Gay and Weiss (1974) in their experiments, prevented the author from using monoclinal kinks for a stress orientation analysis. The analysis was carried out mainly on meso-scale structures, but the results are also regionally applicable. Separate diagrams of σ_1, σ_2 and σ_3 were prepared for all subareas where Witteberg rocks occur (Figures 8.1A to H).

8.2 RESULTS

One of the interesting points arising from the present study, is that the inclination obtained for σ_2 was always more than that of either kink axes (except where both kink axes were horizontal). The attitude of σ_3 varied between 45 degrees and vertical. The synoptic contoured diagrams (Figures 8.2A to C) for the whole area indicate that σ_1 of the two main trends stayed sub-horizontal and operated perpendicular to each other on a regional scale. Due to the plunging kink axes, the maxima for σ_2 display westerly and easterly shifts in relation to σ_1 maxima. The maximum for σ_3 is sub-vertical, as would be expected in an area of constrictional strain.

Stellenbosch University http://scholar.sun.ac.za

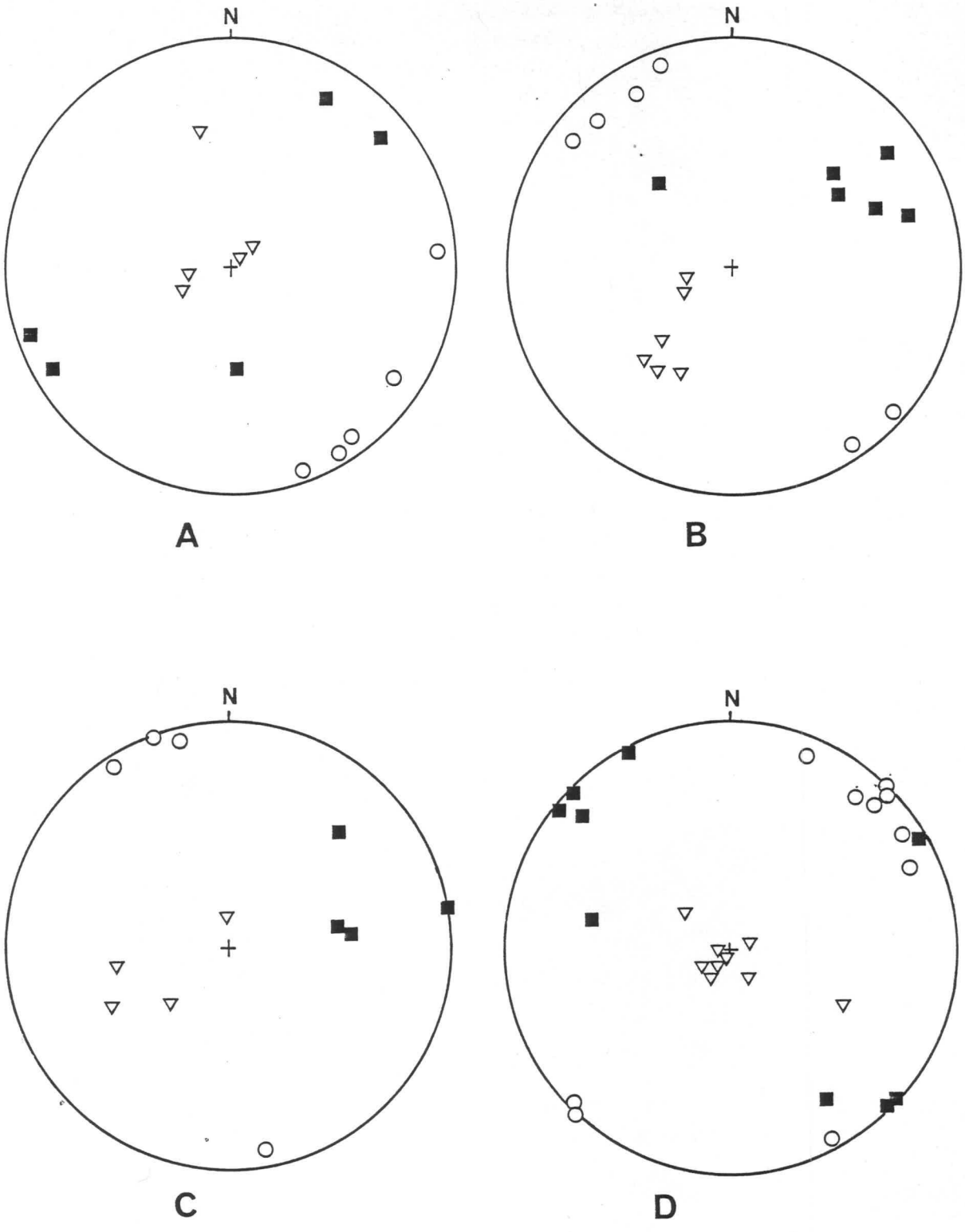

Figure 8.1
Attitudes of σ_1 (○), σ_2 (■) and σ_3 (▽) as determined from conjugate mesokinks for Subareas 2,6,7 and 9 (Figures A-D respectively).

Stellenbosch University http://scholar.sun.ac.za

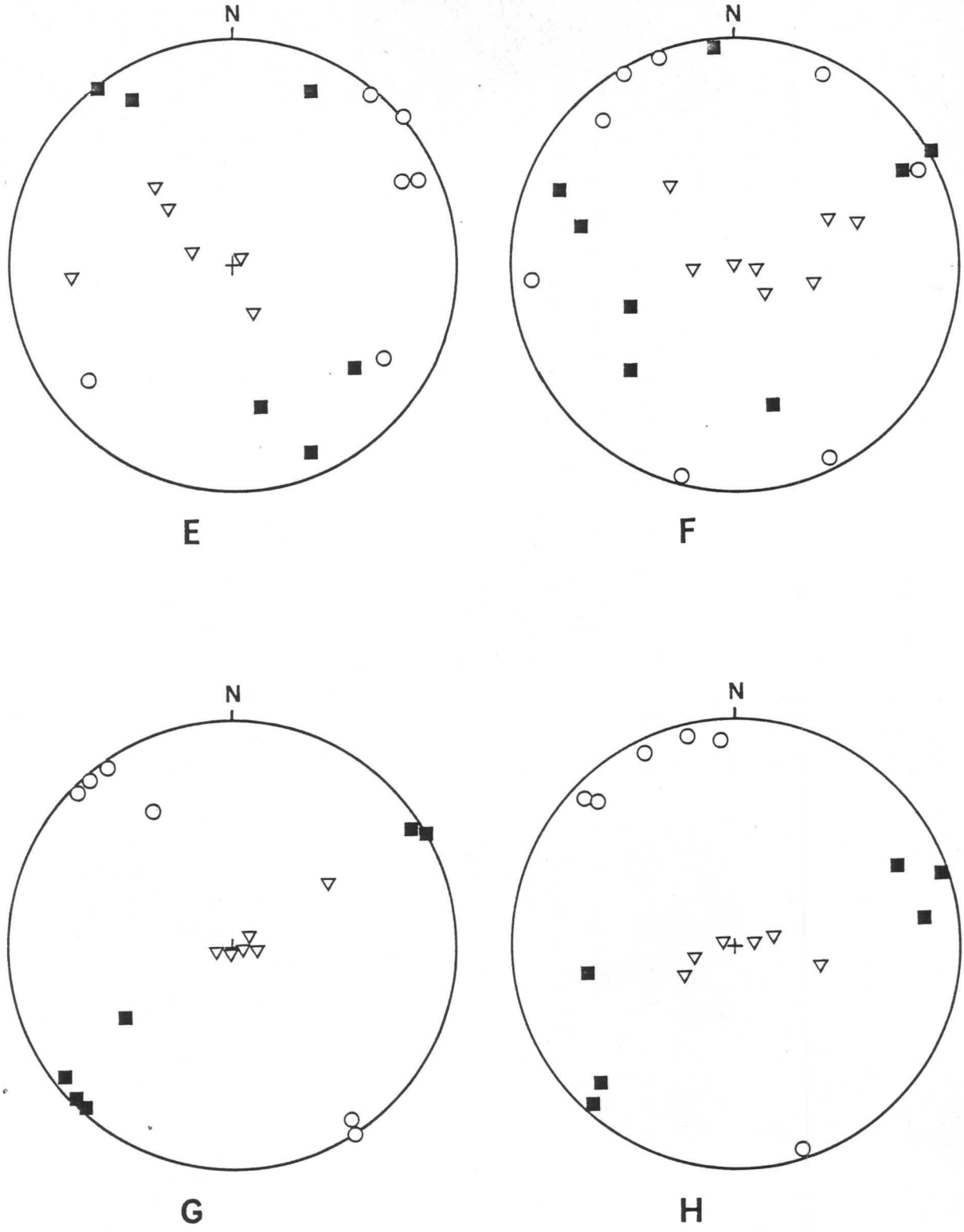

Figure 8.1 (continued)
Attitude of σ_1, σ_2 and σ_3 for Subareas 10, 12 and 13 (Figures E to G, respectively), as well as 15 and 16 combined (Figure H).

Stellenbosch University http://scholar.sun.ac.za

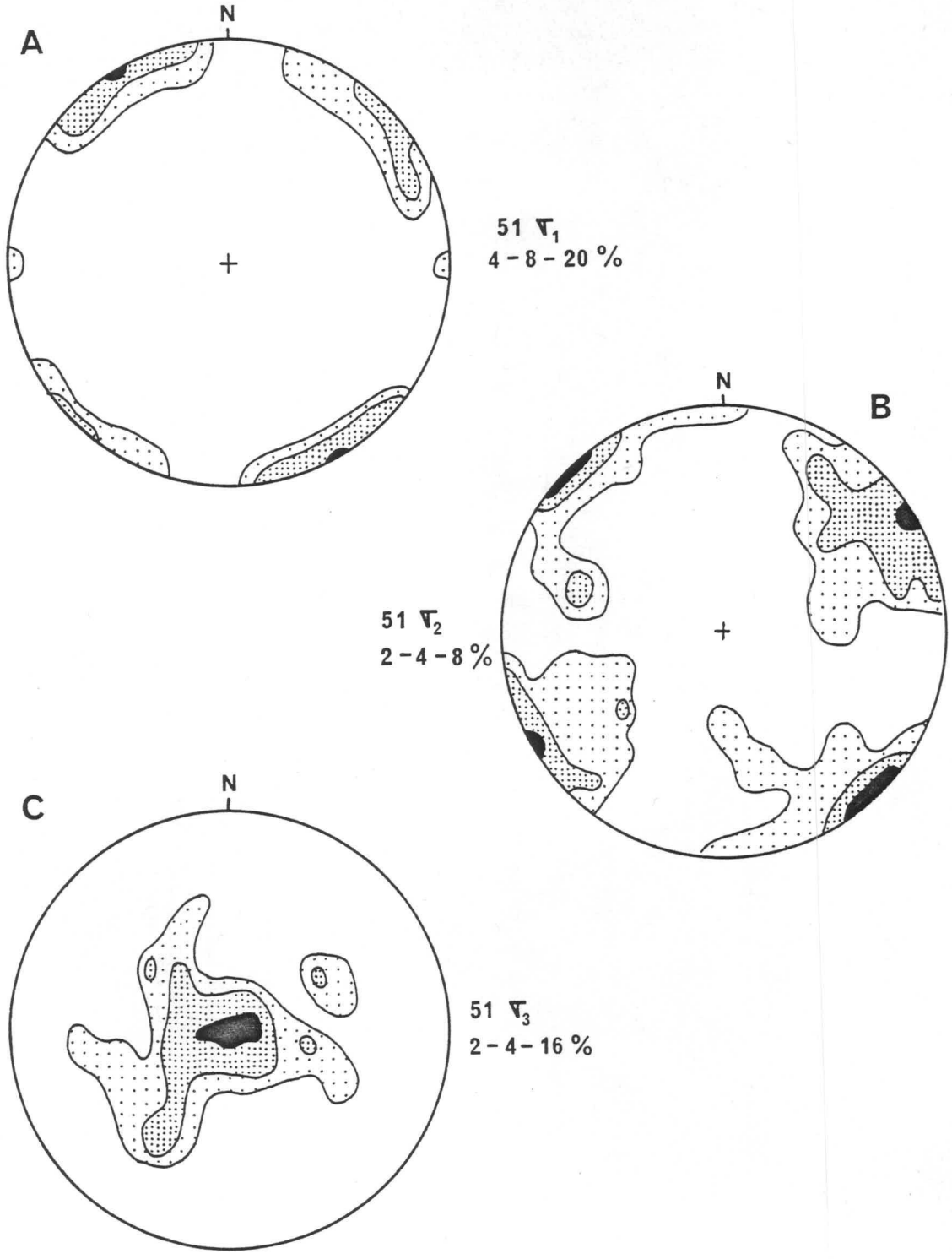

Figure 8.2
Contoured σ_1, σ_2 and σ_3 orientations for all areas covered by Witteberg Group rocks in the Ceres Syntaxis (all contours per 1% area).

Stellenbosch University http://scholar.sun.ac.za

9. MICROFABRIC

9.1 INTRODUCTION

The term "microfabric" encompasses the microstructure and crystallographic preferred orientation of a deformed rock aggregate. The microfabric of a tectonite is controlled by P-T conditions, the strain rate and, for silicates, by the OH-content as well.

Plastic deformation in quartz, involving classical slip processes, leads to the formation of undulose extinction, extinction bands, deformation lamellae, subgrains and, most important of all, to the development of preferred c-axes orientations. For some time now, geologists have noted that crystallographic preferred orientations develop in grains of deformed quartz-rich rocks, without any signs of recrystallization. Comparisons of laboratory experiments and computer models with naturally deformed quartzites, indicate that quartz microfabric is a powerful tool in structural investigations. Dynamic analyses of the preferred orientations of quartz c-axes, deformation lamellae and microfractures can reveal the type of strain, its intensity, orientation and even the strain history of a quartzite under favourable conditions (Carter and Friedman, 1965; Hara, 1971; Tullis et al., 1973; Blacic, 1975; Marjoribanks, 1976; Carreras et al., 1977; Bouchez, 1977; Lister et al., 1978). Dynamic analyses are best suited for slightly to moderately deformed rocks, because the stress history is relatively simple, and recrystallization has

Stellenbosch University http://scholar.sun.ac.za

not obliterated useful fabric elements.

Crystallographic preferred orientations may be successfully correlated with grain shape data (Marjoribanks, 1976; Law, 1986). However, in rocks where secondary quartz overgrowths are common, it is useless to try and estimate grain flattening (strain axial ratios), without the aid of cathodoluminescence. A correlation between crystallographic fabrics and quantatively determined strains is usually only meaningful in tectonites where strain markers, such as deformed reduction spots or calcareous ooids, have been preserved.

Recovery and recrystallization are two processes that occur during the tectonic deformation of quartz. Both processes are driven by forces that attempt to reduce the dislocation and crystal defect density in the strained grains. Recovery leads to the development of both subgrains and new grains (White, 1977). Recrystallization of the deformed rock is sometimes accompanied by marked changes in preferred orientation of quartz c-axes (Hobbs et al., 1976).

The low deformational intensity in the Ceres Syntaxis, as indicated by the absence of cleavage in the Bokkeveld shales, and the relatively low P-T conditions experienced by Witteberg quartzitic sandstones in general (De Swardt and Rowsell, 1974) are ideal for a microfabric analysis. Some 65 samples, taken from various locations and representing different strain intensities, were investigated for microstructural habit. Eight of these samples were later selected for the preferred orientation analyses.

Stellenbosch University http://scholar.sun.ac.za

9.2 MICROSTRUCTURE

Most Witteberg sandstones consist of more than 90 per cent monocrystalline quartz grains. In samples where original grain boundaries are preserved, the quartz grains appear moderately to well-rounded and well-sorted. The clay mineral content is rarely more than 5%, which makes them quartz-framework arenites (Dapples, 1979). Secondary quartz overgrowths are ubiquitous and several clean sandstones display interlocked grain mosaics. More than 70% of the sandstones have an average grain size of 350 µm.

Grain boundaries are mostly straight to concavo-convex (Figure 9.1). Serrated boundaries (Figure 9.2) are uncommon and have no preferred orientation towards maximum compressive stress. Some pressure solution at points of grain contact is indicated by quartz fibre growth in pressure shadows adjacent to large quartz grains.

Optical features associated with plastic deformation in the quartz grains are seen as undulatory extinction, extinction bands and deformation lamellae in many samples. Stretched rutile needles in grains containing lamellae (Figure 9.3) provide further evidence of the plastic deformation that occurred. Deformation lamellae terminate at detrital grain (plus overgrowth) boundaries and are usually approximately normal to extinction bands and quartz c-axes, i.e. sub-basal lamellae (Figure 9.4). Most samples contain only single sets of lamellae, but some intensely strain-hardened grains may

Stellenbosch University http://scholar.sun.ac.za

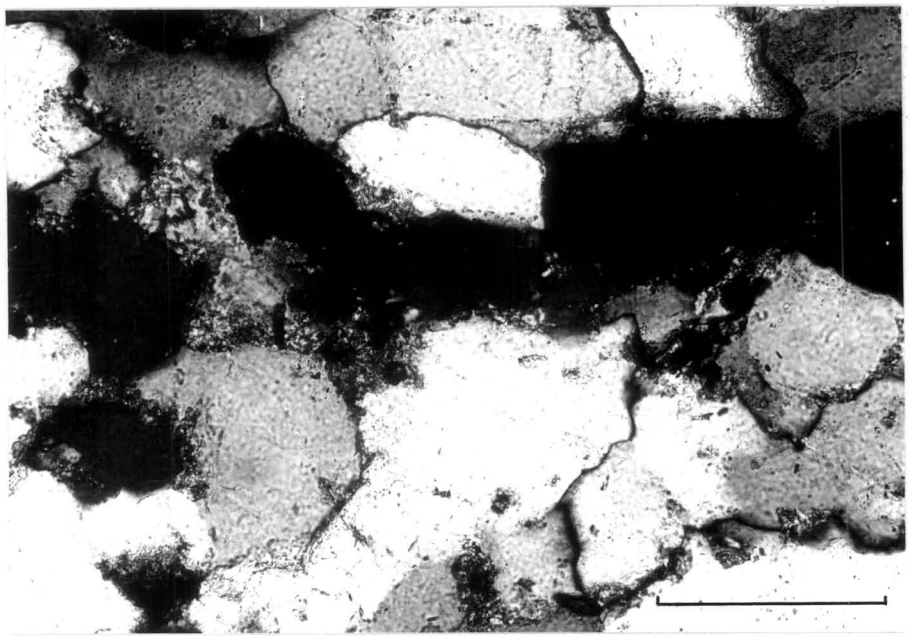

Figure 9.1
Straight and concavo-convex grain boundaries in Sample CFB 62 from the Baviaansberg megakink. Length of scale bar is 360µm. Crossed nicols.

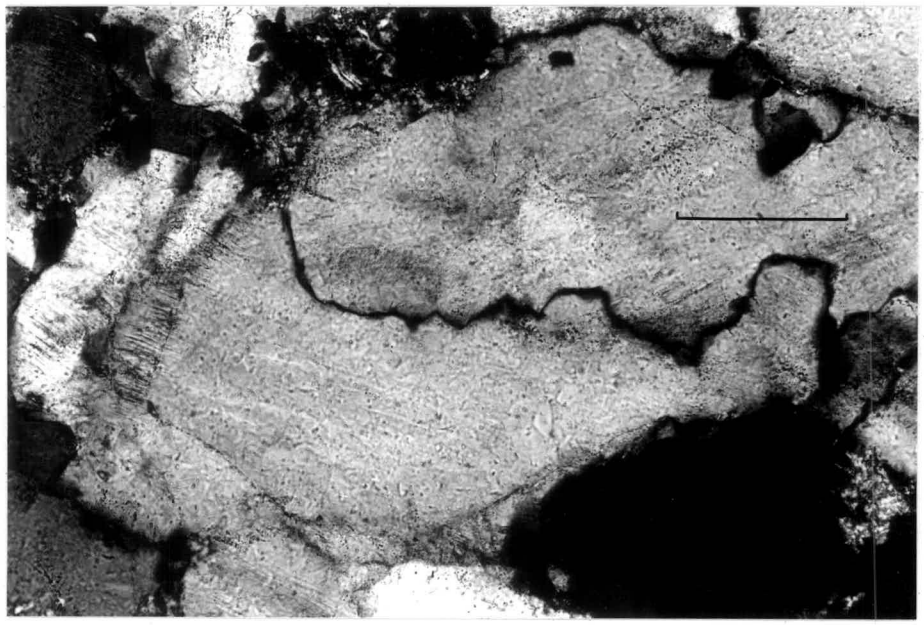

Figure 9.2
Serrated (stylolitic) grain boundary in sandstone of Sample CFB 64 from Seekoegat. Length of scale bar is 100µm. Crossed nicols.

Stellenbosch University http://scholar.sun.ac.za

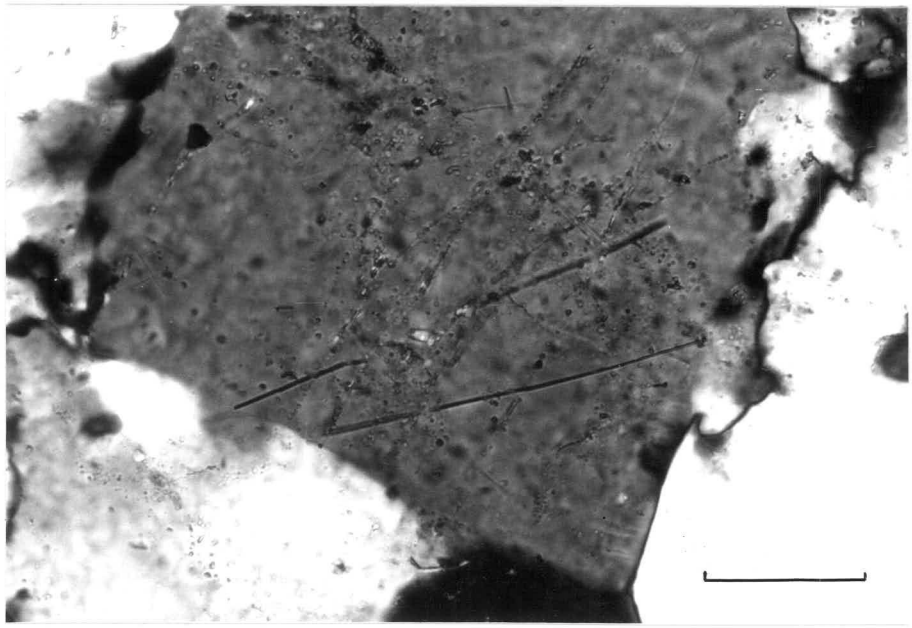

Figure 9.3
Intragranular plastic strain indicated by ruptured rutile needles. Length of scale bar is 30µm. Crossed nicols.

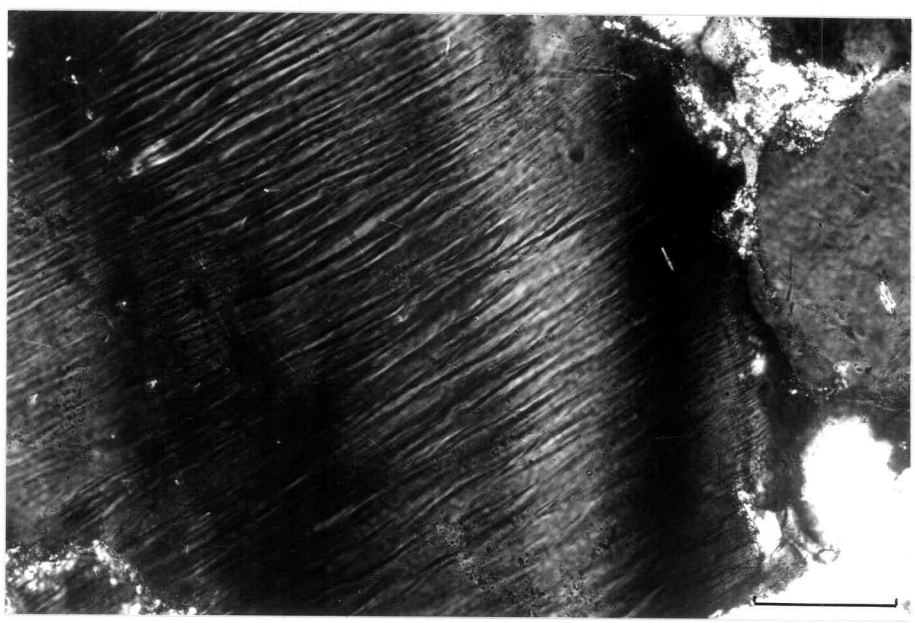

Figure 9.4
Deformation lamellae, subperpendicular to extinction bands, in a large plastically deformed quartz grain (Sample CFB 64). Length of scale bar is 90µm. Crossed nicols.

Stellenbosch University http://scholar.sun.ac.za

contain up to three sets. The general observation that lamellae continue from the detrital grain into the cement which has grown in optical continuity with the host grain, has two implications. Firstly, it indicates that cementation preceded the formation of lamellae, and secondly, that the lamellae are not relict structures inherited from the source rock. Lamellae usually occupy the whole grain, but in some instances only occupy the outer (overgrowth) rim of grains, where contact pressure during deformation was at a maximum. Some lamellae are decorated by lines of inclusions, while others are recognised only by the change in refractive index.

Healed microfractures which are now marked by planes of fluid and solid inclusions that transect a number of grains, are widely encountered in samples that underwent substantial deformation. In a sample from the Seekoegat fold zone, unhealed microfractures, which are invisible in hand specimen, are oriented parallel to the ab mesoscopic fabric plane of the small fold, and evidently represent an embryonic fracture cleavage.

The appearance of subgrains is a good microstructural indicator for recovery. As recovery proceeds, some subgrains grow at the expense of others by secondary grain growth, until eventually a new fabric, with grains differently oriented from the parent grain, results. Only then has complete dynamic (secondary) recrystallization taken place. The presence of subgrains in many Witteberg samples, normally at grain boundaries, but also inside grains, indicate that substantial recovery has occurred.

Stellenbosch University http://scholar.sun.ac.za

New, very small grains, that are exclusively present only at some grain boundaries, are rare. This indicates that nucleation, followed by recrystallization, did not contribute much to the observed microstructure of these rocks. The process of recovery may account for the low density of lamellae concentrations in some highly deformed samples, excluding those with a high sericite content. In the latter instance, intergrain pressure was never high enough to effectively transmit the stresses into, and through the quartz grains.

Primary recrystallization may be identified by the presence of 120 degree triple-grain junctions, leading to the so-called "foam texture". Though some grains in fact show these junctions, a seemingly paradoxical relationship between their abundance and deformational intensity was sometimes found. In a sample taken from horizontal Witteberg quartzitic sandstone at Elandsdrift (3219DA), less than 25% of the quartz grains contain lamellae, but the sample shows the most perfect stable grain boundary arrangement found over the entire study area. Perfect triple-grain junctions are, however, also commonplace in so-called "Ganister" or flexible quartz-framework arenites that have undergone pore compaction and no tectonic deformation (Dapples, 1979). The structure of the anomalous sample may be explained by assuming intergranular grain boundary migration under load stress. This led to the development of bilateral grain boundaries and the ultimate stable arrangement. Total recrystallization of quartzites in the Cape Supergroup, with the development of a new equilibrium structure, was so far only found in the Outeniqua Mountain Range of the southern Cape Fold

Stellenbosch University http://scholar.sun.ac.za

Belt Hälbich and Cornell, 1983), where temperatures just above 350°C were reached with the presence of prograde biotite in intercalated shales. These high temperatures were evidently never attained in the Ceres Syntaxis.

9.3 CRYSTALLOGRAPHIC PREFERRED ORIENTATION

The present investigation centred around quartz c-axes and lamellae orientations, as well as standard dynamic analysis (Carter and Friedman, 1965). The overall absence of flattened or elongate grains in most Witteberg samples excluded a comparison of grain shape with microfabric. Computer simulations by Lister et al.(1978), who investigated the effects of different combinations of active glide systems on quartz preferred orientations, were compared with c-axes fabric diagrams of the samples. The samples under consideration showed little effects of recrystallization, therefore the data sets relate only to strained old (detrital) grains and their quartz overgrowths. An attempt was made to find out more about four main aspects concerning the Witteberg structures, namely:

(1) What is the nature and origin of the penetrative B-lineations?

(2) How does c-axis orientation reflect the existence of two main stress vectors that operated in the cross-folded beds?

(3) What was the orientation of the main stress axes σ_1, σ_2 and σ_3 in folds from meso to megascale?

Stellenbosch University http://scholar.sun.ac.za

(4) Can the microfabric signature of these rocks provide further evidence for soft sediment folding?

Sample locations are given in Figure 9.5. The orientations of quartz c-axes, lamellae and microfractures were measured in each sample by standard universal stage techniques (Turner and Weiss, 1963; Phillips, 1971). Orientations were measured on one thin section prepared from each of two mutually perpendicular surfaces cut perpendicular to bedding. Their attitude is shown on Figure "A" of every sample. For lineations, one cut was made parallel, and the other perpendicular, to the plunge. The preferred orientations are depicted in lower hemisphere, equal-area projections. On these projections, X is normal to bedding, Y is the strike of bedding or fold axis attitude, Z is the direction of dip, or the direction perpendicular to the XY-plane on the scale of the sample. Mesoscopic fold fabric axes are denoted in the conventional way as a,b and c (Dennis,1972). In many cases, sections were cut in such a way that X= a, Y= b and Z= c . Because we are dealing with well-bedded rocks, X, Y and Z may also approximate the axes of extension, intermediate strain, and shortening, respectively, of Lister et al. (1978) on sample scale.

Data were rotated and contoured by the author, using computer programmes available at the Henno Martin Laboratory, P.R.U., University of Cape Town. For control, many of the data sets were also rotated and contoured manually. For the derivation of σ_1, σ_2 and σ_3 inter alia by "standard dynamic analysis", in

Stellenbosch University http://scholar.sun.ac.za

which c-axes of single grains are joined by great circle paths to their corresponding lamella poles, data points had to be numbered. These data sets were manually treated, because no suitable programmes were available.

9.4 RESULTS

9.4.1 SAMPLE 56

This sample from Skitterykloof (Figure 9.5) was chosen in order to investigate the microfabric expression of the penetrative B-lineation (Figure 9.6). It was taken from the closure of a tight, upright, NNW-plunging, Class 2 (similar), small fold. This fold belongs to the NE-SW trend, but has been rotated into a northerly attitude by compression subparallel to its axis, related to formation of the nearby NW-SE trending monocline (see Figure 7.21). The lineation in the sample plunges 354/25 and the local fold axial plane is vertical. Because of the sample location, X = a, Y = b and Z = c. The rock consists largely of monocrystalline, well-sorted, subrounded quartz grains with an average size of 270 µm and <5% sericite. Quartz overgrowths are common and grain boundaries are straight to slightly serrated. Undulose extinction is ubiquitous and lamellae are fairly common. Sections cut perpendicular to the lineation and parallel to the axial plane that contain the lineation, fail to show any grain elongation.

The c-axis fabric (Figure 9.6B) has poorly developed girdles crossing near the fold axis (B-lineation = Y), but no maximum

Stellenbosch University http://scholar.sun.ac.za

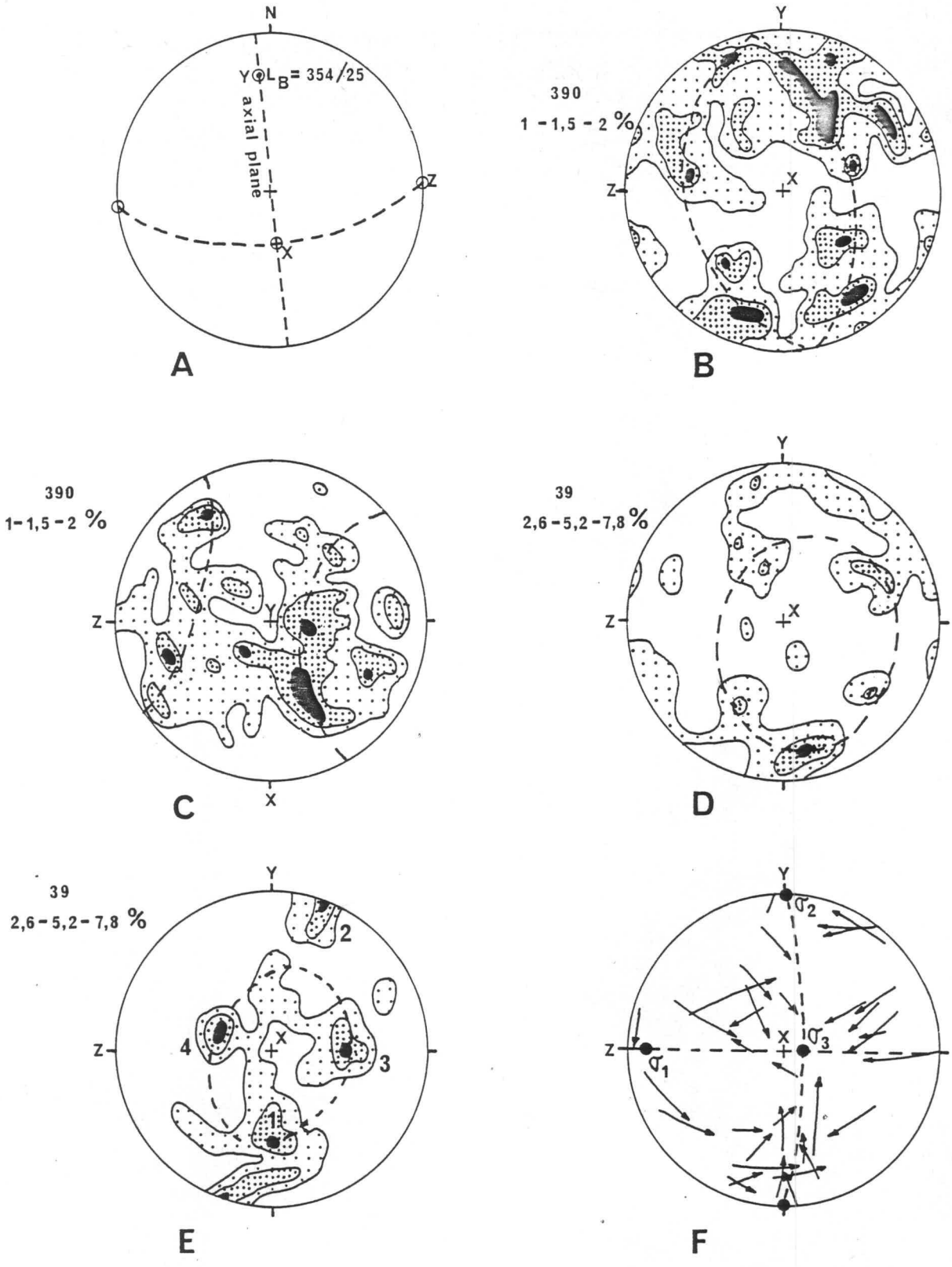

Figure 9.6
Sample CFB 56 from Skitterykloof. (A) Orientation of L_B and thin sections(broken lines); (B) 390 c-axes projected onto ZY plane; (C) 390 c-axes projected onto XZ plane; (D) 39 c-axes with lamellae projected onto YZ plane; (E) 39 lamellae poles; (F) dynamic analysis (arrow diagram). Contours per 1% area.

Stellenbosch University http://scholar.sun.ac.za

has developed there. The opening angle about Z is about 40 - 50 degrees, and Z is a pole-free area. The anisotropy of the c-axis fabric is intermediate in strength and approximates orthorhombic symmetry. For direct comparison with the data of Lister et al. (1978), the total number of c-axes were also projected onto the XZ microfabric plane (Figure 9.6C). In this projection, the c-axis fabric has a fairly well-defined small-circle (opening angle of 50 degrees, inclined at 20 degrees to Z) that is connected approximately through Y. This, combined with the tendency of some maxima to lie near Z, as well as X being a pole-free area, indicate a combination of axially symmetric shortening and plane strain. The opening angle around Z is rather large compared to that of the model, but this is to be expected in natural samples (Lister et al., 1978). The total c-axis fabric evidently does not fit those predicted by Lister et al. (1978) for quartzites that suffered axially symmetric extension, thus the lineation (parallel to B = Y) is not a stretching phenomenon. The latter is also corroborated by the absence of preferred orientation of grain long axes parallel to Y. The generally diffuse spread of all c-axes indicates a very heterogeneous deformation and possibly an input by the cross-folding, with compression directed NE-SW. Further evidence for the latter will be presented below.

The c-axis-fabric of grains that contain lamellae (Figure 9.6D) defines maxima near the Y-axis and others that lie along a small circle centred slightly away from X. The latter thus describes a cone with apical angle of 80 - 100 degrees and an axis that almost coincides with the bedding pole (X). The

Stellenbosch University http://scholar.sun.ac.za

general spread of c-axes is interpreted as being the result of two triaxial strains working together at a certain stage of fold development. It is possible that the strong maximum near Y (Figure 9.6D) indicates the dominance of NE-SW directed compression during the time of lamellae formation.

The lamellae fabric (Figure 9.6E) again resembles a small circle distribution oriented 45 degrees from the bedding pole (X) and connected to a maximum near the attitude of the B-lineation (Y). The latter maximum in fact indicates that quite a number of lamellae lie subperpendicular to the B-lineation. These lamellae probably formed as a result of NE-SW directed compression of the cross-folding trend. According to Scott et al.(1965), poles to quartz lamellae commonly define two point maxima nearly 90 degrees apart (small circle 40 - 50 degrees around X) which may be used to determine the intermediate (σ_2) stress axis. The intersection of the two "average" orientations of lamellae (fabric Y-axis) approximately parallels σ_2 and the bisectors of the angles between these two orientations, approximately pass through σ_1 and $\sigma 3$. For sample CBF 56, it is impossible to determine unique positions of σ_1 and σ_2, because maxima 1+2 and 3+4 (Figure 9.6E) lie along two mutually perpendicular great circle girdles (planes).

A majority of data in the arrow diagram for sample CFB 56 (Figure 9.6F) indicates that σ_3 was oriented near X, that is, perpendicular to the B-lineation and near the bedding pole. The total dynamic analysis, therefore, indicates that σ_3 may be

Stellenbosch University http://scholar.sun.ac.za

uniquely determined, while the positions of σ1 and σ_2 are interchangeable. Taking the sample location into account, these results seem reasonable.

The dynamic analysis also shows that most lamellae are sub-basal I types, because the arrows are shorter than 30 degrees. This means that low temperatures and moderate strain rates accompanied the deformation at low pressures (Carter and Friedman, 1965).

9.4.2 SAMPLE CFB 64

This sample was taken from the closure of a small, tight,WSW plunging similar fold at Seekoegat (Figures 7.26 and 9.5). Wavelength and amplitude of the fold are 40 and 80 centimetres respectively. Thin sections were cut perpendicular and parallel to the axial plane that contains a penetrative B-lineation plunging 257/50 (Figure 9.7A). Because the sample was taken from the fold hinge, X = a = pole to bedding, Y = b = B-lineation, and Z = c. Grain size in this dominantly quartzitic sandstone varies from 270 to 360 μm. Original grain boundaries are only visible from the distribution of rutile needles that are usually unstretched. Deformation lamellae developed in about 20% of the grains and extinction bands are common. In the section cut parallel to the b-lineation, grain elongation is again absent, as in Sample CFB 56.

For comparison with the computer models of Lister et al. (1978), total c-axes fabric was projected onto the XZ plane

Stellenbosch University http://scholar.sun.ac.za

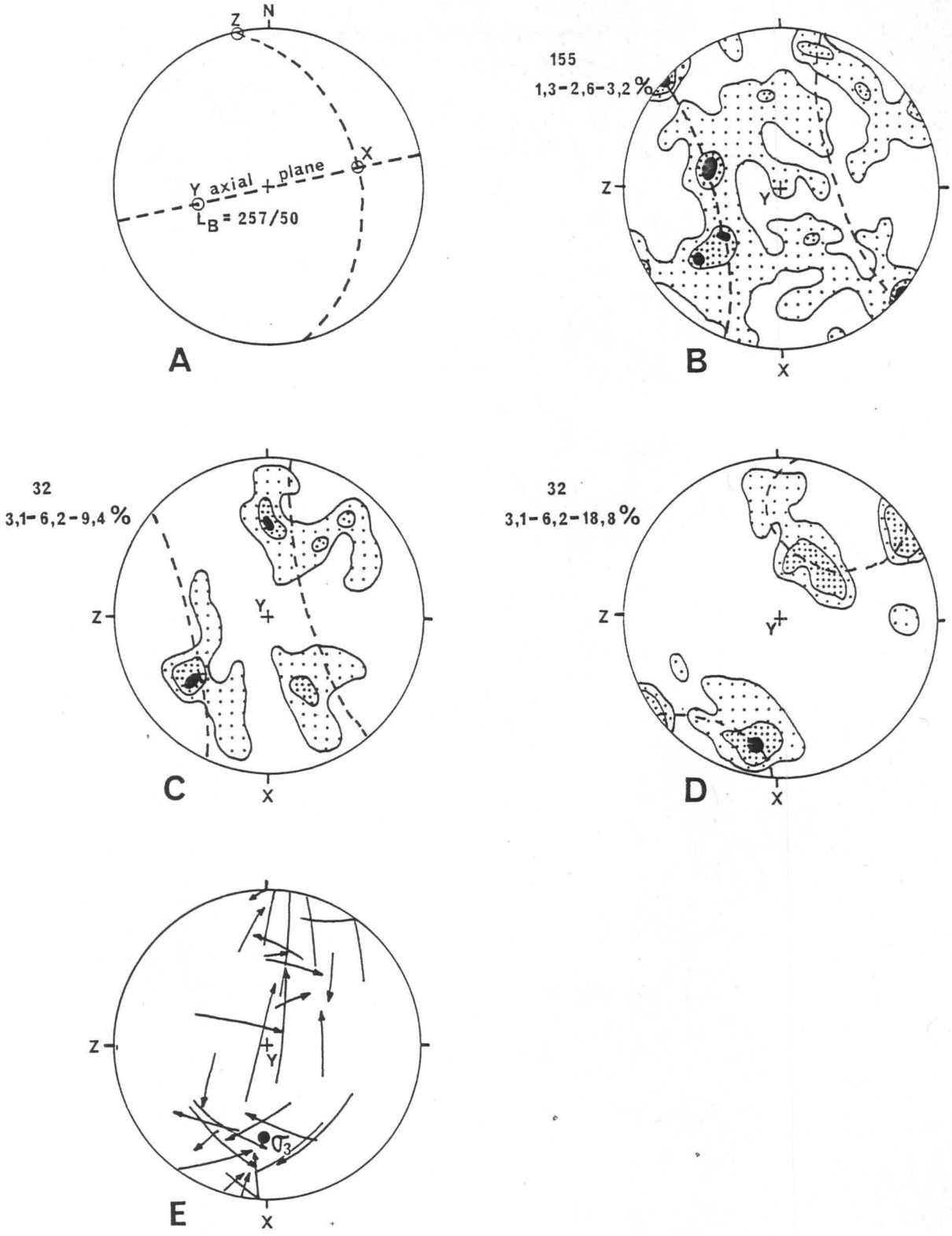

Figure 9.7
Sample CFB 64 from Seekoegat. (A) Orientation of L_B, S_O and thin sections; (B) 155 c-axes projected onto XZ plane; (C) 32 c-axes with lamellae projected onto XZ plane; (D) 32 lamellae poles projected onto XZ plane; (E) dynamic analysis. Contours per 1% area.

Stellenbosch University http://scholar.sun.ac.za

(Figure 9.7B). The diagram reveals two small circle girdles with opening angles 40 - 45 degrees from an axis near Z. Two subordinate girdles, about 45 degrees from X, also exist. This may be the result of the cross-folding trend as in sample CFB 56. X and Z are relatively pole-free areas. In sample CFB 64, again, the total c-axis fabric does not indicate axially symmetric extension, but axially symmetric shortening and plane strain in two mutually perpendicular directions (for models I and II quartzites of Lister et al., 1978). Again, the anisotropy of the fabrics is rather weak when compared to the high strains accommodated by the beds in the tight fold from which the sample was taken.

The fabrics displayed by Figure 9.7C for c-axes of grains containing lamellae may indicate a rotational stress field in which the formation of lamellae and most of the intragranular plastic deformation postdated the lineation. One would expect rather complicated fabrics, because the sample comes from highly deformed beds towards the central part of the NE-SW trending fold zone.

The fabric of lamellae poles (Figure 9.7D), namely a small circle around an axis inclined at nearly 20 degrees to the ZX plane, is consistent with intense shortening perpendicular to the b-lineation and the axial plane, followed by a rotational or shear strain. The dynamic (arrow) analysis (Figure 9.7E) indicates that σ_3 was located near the microscopic fabric x-axis. This again demonstrates that the b-lineation is not related to plastic stretching of the quartz grains. Arrow

Stellenbosch University http://scholar.sun.ac.za

lengths in Figure 9.7E also indicate low-T conditions, as in Sample CFB 56. The total microfabric analysis indicates little intragranular plastic deformation of the quartz grains, because few rutile needles are stretched, lamellae are uncommon, and the intensity of the crystallographic orientations is not very pronounced. This may imply that most deformation occurred while these middle- Swartruggens Formation sediments were still unconsolidated.

9.4.3 SAMPLE CFB 60

The sample was taken from the flatly north-dipping long limb of the southern Baviaansberg megakink (Figures 9.5 and 4.5). Attitudes of the bedding, kink axis, the axial plane, and the two orthogonal thin sections, are indicated in Figure 9.8A. For independent control, orientation of the main stresses responsible for the Baviaansberg conjugate megakinks, as determined by the method of Ramsay (1962), are shown on figure 9.8A. The attitudes of σ_1, σ_2 and σ_3 are 343/0, 255/4 and 075/86, respectively. Owing to the geometry of the fold as one half of a conjugate kink pair, X,Y and Z axes in this sample lie very close to the directions of maximum extension, intermediate strain and maximum shortening, respectively, of the conjugate setup. Grain size of the quartz varies between 90 and 180 µm. The 10% clay mineral content in the sample consists of detrital kaolinite books, as well as long, slender muscovite grains and sericite. Some of the latter was derived from the alteration of feldspar. Grain boundaries are concavo-convex to straight and lamellae are common, though usually only one set has developed.

Stellenbosch University http://scholar.sun.ac.za

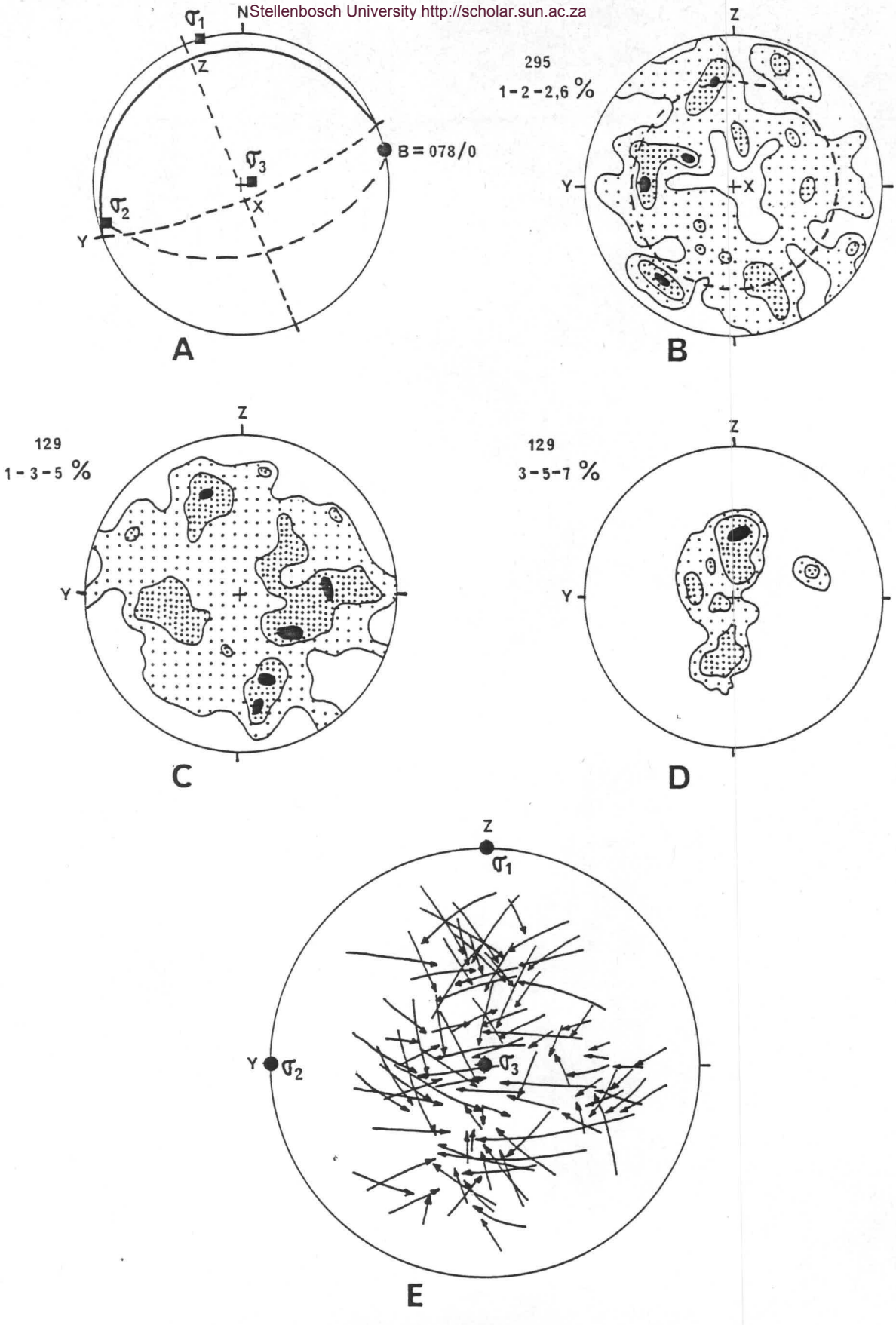

Figure 9.8
Sample CFB 60 from Baviaansberg. (A) Orientation of bedding (S_o), thin sections, and of σ_1, σ_2, and σ_3 as determined for the conjugate megakinks by the method of Ramsay (1962). (B) 295 c-axes projected onto bedding (YZ) plane; (C) 129 c-axes with lamellae projected onto bedding plane; (D) 129 lamellae poles projected onto bedding plane; (E) dynamic analysis. Contours per 1% area.

Stellenbosch University http://scholar.sun.ac.za

The total c-axis fabric (Figure 9.8B) has maxima spaced roughly 60 degrees apart along a small circle, 40 - 45 degrees from the bedding pole X. Grains that contain lamellae display a similar fabric (Figure 9.8C). Poles to lamellae (Figure 9.8D) lie on a small circle situated about 30 degrees from the bedding pole with two strong maxima in the XZ plane. The dynamic analysis (Figure 9.8E) shows that σ_3 was almost vertical near X and in the XZ-plane. This, together with the XZ orientation of the plane containing lamellae maxima, indicate that σ_2 was oriented parallel to Y. The dynamic analysis, as well as the distributions of c-axes in grains with lamellae and the lamellae poles, indicate that lamellae are mostly of the sub-basal I type. The total quartz microfabric of sample CFB 60 indicates a coaxial deformation at low intensities and at slow rates, under conditions of similarly low temperature and pressure. Good agreement between mesoscopically and microscopically determined main stress orientations were achieved. The symmetrical distribution of microfabric data on the bedding plane (YZ-plane) indicate that the main stress vectors stayed parallel to bedding throughout development of the structure.

9.4.4 SAMPLE CFB 62

The sample was taken from the short, kinked limb of the Baviaansberg megakink, where So dips 63 degrees north (Figure 9.9A). X, Y and Z as before, are pure sample fabric reference axes. It was thought that these axes would also correspond with those of Lister et al.(1978), because microfabric usually only

Stellenbosch University http://scholar.sun.ac.za

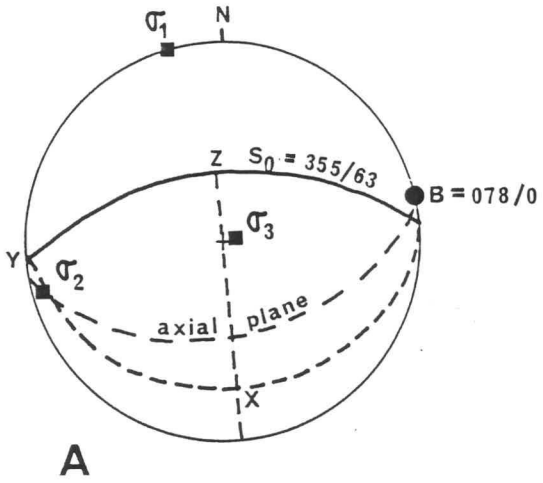

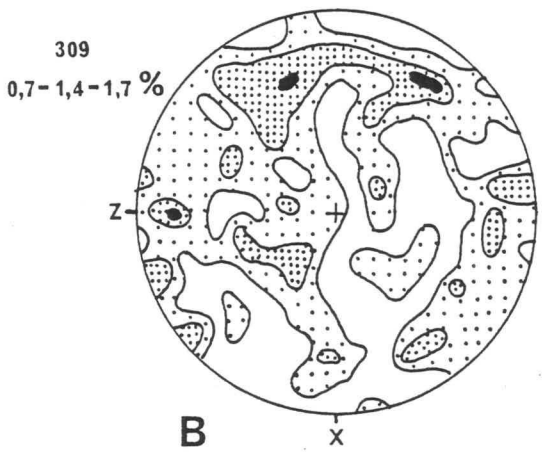

Figure 9.9
Sample CFB 62 from Baviaansberg. (A) Orientation of bedding (S_o), thin sections, and of σ_1, σ_2 and σ_3 as determined for the conjugate megakinks by the method of Ramsay (1962). (B) 309 c-axes projected onto XZ plane. Contours per 1% area.

Stellenbosch University http://scholar.sun.ac.za

rotates passively with fold limbs (Scott et al.,1965; Coetzee, 1979). This, however, will only happen if the rock is able to transmit stresses that can deform quartz plastically. The rock of Sample CFB 62 is a fine-grained, well-sorted quartz arenite with some 10% detrital muscovite and authigenic sericite. Fine-grained sericite occurs between grains and as feldspar grain replacements. Grain boundaries are straight to slightly concavo-convex. The ubiquitous presence of feldspar replacement by illite suggests that the rock was originally a subarkose with 30 - 40% original pore space. Most grains display effects of slight plastic deformation by the presence of undulose extinction, but lamellae are rare.

The results of the preferred orientation study were disappointing, probably due to the low intensity of intragranular plastic deformation. The total c-axis fabric (Figure 9.9B) does not compare well with plane strain, axial compression, axial elongation or simple shear fabrics (Tullis, 1977; Lister, 1977; Lister et al., 1978). A total of 309 c-axes were measured, but only 18 of these grains contained lamellae. As usual, the best clues to principal stress directions could be gained from the dynamic analysis (not depicted, because of the low number of lamellae). The latter showed that σ_3 was oriented perpendicular to the bedding pole, and σ_1 in the north-south plane. Reasons for the few lamellae in sample CFB 62 may be the timing of intragranular plastic deformation and the state of compaction of the beds during initial rotation of the kink limb. The widespread sericitization of detrital feldspar grains and the fact that aggressive solutions have attacked the cement, tend to support the argument.

Stellenbosch University http://scholar.sun.ac.za

9.4.5 SAMPLE CFB 68

In Subarea 11, relatively open NW structures are cut by linear, NE trending fold zones. Sample CFB 68 was taken to investigate the extent to which horizontal beds outside the fold zones became strained and also to determine the effect of synchronous cross-folding on the fabric, if this had been recorded at all. The sample was taken one kilometre south-east of the Stompiesfontein fold zone, in horizontal beds at the same stratigraphic level as those affected by the latter (Figure 9.5). Two thin sections, oriented in vertical planes that trend 337 and 067 degrees, were investigated (Figure 9.10A). The orientations of the cuts were dictated by the overall regional fold trends in the subarea. Sample fabric axes X, Y and Z therefore correspond with mesoscopic fold fabric axes a, b and c, respectively (with regard to the NE trending fold zones).

The rock is a tough, sugary, white quartzitic sandstone with average grain size of 360 µm. It consists of close to 100% monocrystalline quartz, in which the grains form an interlocking mosaic, while a substantial number of compound grains occur. Grain boundaries are straight to slightly curved, but serrated boundaries are rare. Very small (< 20 µm) strain-free new grains occur at grain boundaries, while many subgrains have formed within grains. Though real extinction bands are rare, most grains display undulose extinction and lamellae are common. Multiple sets of lamellae in some grains show that substantial strain hardening has occurred. Although

Stellenbosch University http://scholar.sun.ac.za

the grain aggregate is exceptionally well cemented, 120 degree triple-grain junctions are rare. There is no evidence of bulk recrystallization of the rock.

The preferred orientation study of the microfabric was surprisingly rewarding, when compared to other samples. Strong maxima and preferred orientations of total c-axes, c-axes of grains with lamellae, lamellae poles, as well as a clear dynamic analysis were obtained. The total c-axis fabric is shown (Figure 9.10B) as projected onto the ZX plane. A comparison of c-axes with the orientation of the great circle that contains the lamellae maxima (Figure 9.10D), suggests that the σ_1-σ_3-plane was also oriented approximately parallel to the ZX-plane. The total c-axis fabric has two maxima inclined at about 40 degrees to the mesoscopic Z, with Z a pole-free area and minor maxima near X. The main maxima fall on a small circle situated at 40 degrees around Z. Assuming deformation of a Model I or II quartzite, in which basal and rhomb dislocation glide occurred (at low T), the suggested fabric indicates a combination of general triaxial strain and plane strain (Marjoribanks, 1976; Lister et al., 1978; Law, 1987). Plane strain computer simulation fabrics (Lister et al., 1978) and experimental, as well as natural examples (Tullis, 1977; Marjoribanks, 1976) show crossed-girdle patterns. The total c-axis fabric of sample CFB 68 compares well with these patterns, but lamellae are mostly of the sub-basal I type. The latter indicates that deformation occurred at low P-T conditions and consequently a Model III or IV quartzite, for which the above plane strain crossed-girdle patterns were

Stellenbosch University http://scholar.sun.ac.za

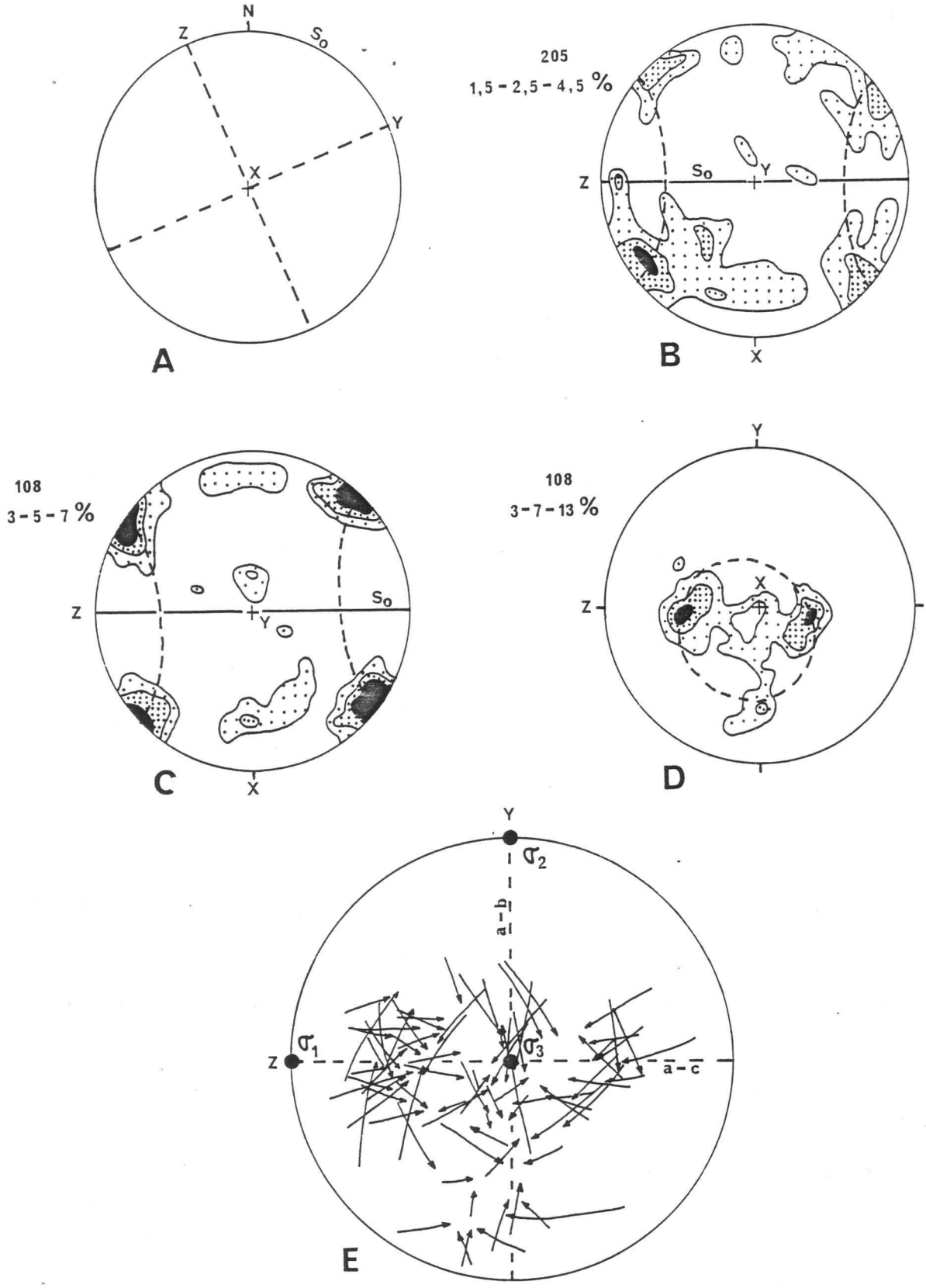

Figure 9.10
Sample CFB 68 from near Stompiesfontein. (A) Horizontal beds and thin section orientations; (B) 205 c-axes projected onto ZX plane; (C) 108 c-axes with lamellae projected onto ZX plane; (D) 108 lamellae poles projected onto the bedding plane; (E) dynamic analysis. Contours per 1% area.

Stellenbosch University http://scholar.sun.ac.za

derived (Lister et al., 1978), does not fit the tectonic environment. However, White (1975) suggested that a high water content will have the same effect on microfabric as higher temperatures. The weak maxima situated near X are probably related to post-tectonic uplift. They do not fit a small circle girdle through the maxima that lie at 30-40 degrees to Z.

The c-axis fabric of grains that contain lamellae (Figure 9.10C) certainly indicates that the lamellae-forming stresses were primarily oriented near Z and therefore approximately NNW-SSE. This was also indicated by the low degree of preferred orientations of c-axes seen in computer plots of unrotated data from the section that was cut parallel to the 067 degrees (XY) vertical plane. The lamellae fabric (Figure 9.10D) shows a small-circle distribution with axis near the bedding pole. The apical angle of the cone is about 38 degrees. Major maxima lie on a great circle, 80 degrees to bedding and oriented 23 degrees west of north. A weak maximum near Y suggests a contribution by lamellae that resulted from NE-SW compression (Z oriented at 067-247 degrees). However, the total c-axis fabric, c-axes with lamellae fabric, as well as the lamellae fabric, indicate that NNW-SSE compression was the main contributing factor to the microfabric. The dynamic analysis (Figure 9.10E) shows that σ_3 was near-vertical during development of the microfabric. The diagram also indicates that most lamellae are of the basal- to sub-basal I type (angle between c-axis and pole to lamella between 16 - 30 degrees); thus slip on (001) in a low P-T environment is indicated. The

Stellenbosch University http://scholar.sun.ac.za

size of the opening angle (≈ 40 degrees) of the small circle defined by lamellae poles suggests that deformation rates were less than 10^{-9}/s.

The microfabric of sample CFB 68 indicates that horizontally disposed Witteberg sandstones became penetratively and fairly homogeneously strained on a grain scale. In these beds, deformation occurred by intragranular plastic mechanisms and pressure solution, without buckling. These results confirm the conclusions that were reached with regard to the origin of the NE trending "fold zones". The overall domination of NE fold-related microfabrics over those of the NW trend in Sample CFB 68, is consistent with the localized higher NE meso- and macro-fold intensity reached in Subarea 11.

9.4.6 SAMPLE CFB 72

Samples CFB 72, CFB 73, and CFB 74 were taken from the northern limb, near the trough and from the southern limb of a small, upright syncline towards the middle of the Stompiesfontein NE trending fold zone (Figures 6.5 and 9.5). The main reasons for this rather detailed investigation, were to determine the relative timing of plastic intragranular deformation, as well as the microfabric expression of the Class 2 (similar) fold geometries. All three samples were taken from the same bed, therefore a general description of the microtexture, valid for all three samples, is presented.

The rock is a highly siliceous quartzitic sandstone, with

Stellenbosch University http://scholar.sun.ac.za

average grain size of 210 µm. Only a few detrital mica grains were observed. Grain boundaries are serrated, concavo-convex and straight. Substantial recovery is indicated by the presence of small (34 - 90 µm) subgrains at grain boundaries, as well as a few subgrains within larger detrital grains. Original grain boundaries are no longer visible, due to optically continuous quartz overgrowths and the formation of compound grains. Healed microfractures with inclusion trails, as well as relatively common lamellae and stretched rutile needles, indicate that the grains have undergone both brittle and plastic deformation.

Preferred orientation of the quartz microfabric will be discussed separately for each sample. Mesoscopic fold fabric axes are a, b and c. At first sight it might seem peculiar that b and c slightly differ in orientation for each sample, but this arises from the fact that the measured bedding strike, even of samples on the limbs of a horizontal, upright fold in nature, seldom coincides exactly with the true mesoscopic fold axis. For reasons stated earlier, more meaningful or more readily interpreted fabric distributions are expected to occur when c-axis data are projected onto the ac planes used in these analyses. X, Y, and Z are again fabric reference axes on sample scale. Lamellae data and the "dynamic analysis" are usually more easily interpreted when projected onto the YZ sample fabric plane, i.e. looking down onto bedding.

Sample CFB 72 was taken from the northern limb of the syncline, where So dips 122/62 (Figure 9.11A). The total c-axis fabric

Stellenbosch University http://scholar.sun.ac.za

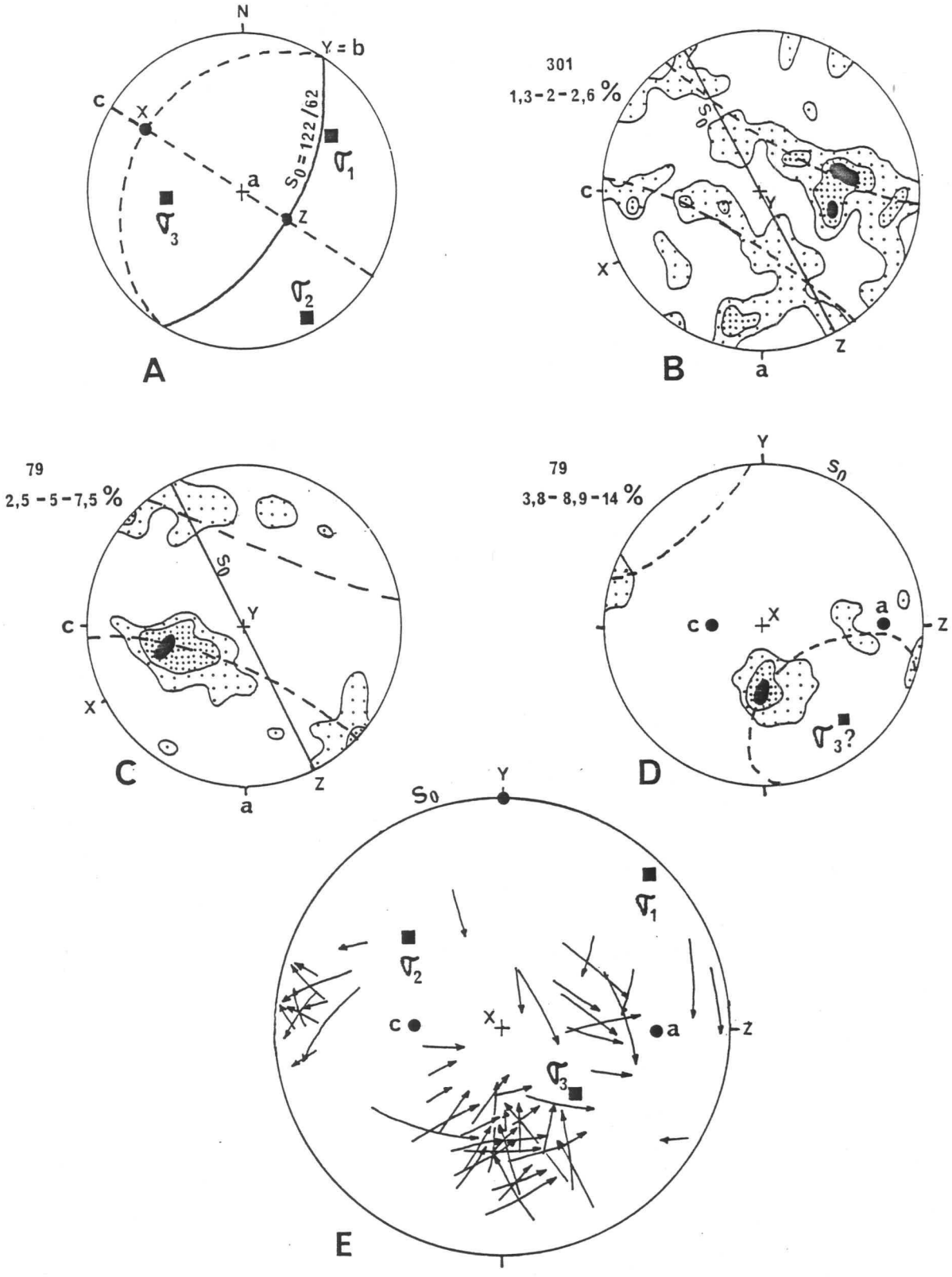

Figure 9.11
Sample CFB 72 from Stompiesfontein fold zone. (A) Orientation of bedding (So) and thin sections; (B) 301 c-axes projected onto the XZ plane; (C) 79 c-axes with lamellae projected onto the XZ plane; (D) 79 lamellae poles projected onto bedding plane; (E) dynamic analysis. Contours per 1% area.

Stellenbosch University http://scholar.sun.ac.za

(Figure 9.11B) describes two small circle girdles with common axis roughly midway between the mesoscopic a-and c-axes. The opening angle of the small circle of c-axes is 60 degrees. Such a fabric indicates uniaxial shortening and intense flattening strains (Marjoribanks, 1976; Lister et al., 1978). The c-axis fabric of grains that contain lamellae (Figure 9.11C), defines a maximum shortening (flattening) axis roughly halfway between X and a, and about 25 degrees inward from the primitive circle of the diagram. The opening angle around the axis of maximum shortening ("Z" of Lister et al.,1978) in Figure 9.11C is slightly less than that defined by the total c-axis fabric in Figure 9.11B. When rotated into the ZY-plane, it becomes clear that this axis of maximum shortening does not coincide exactly with the axis of maximum compression (σ_1), because it lies within only 60 degrees from the position of σ_3 indicated by the lamellae fabric. The lamellae fabric (Figure 9.11D) descibes a small circle of which the axis indicates the position of σ_3. The strong maximum of lamellae near X may suggest severe extension in the latter direction (Riley, 1947). Figure 9.11D also indicates a non-symmetric arrangement of principal stress axes to the mesoscopic fabric. The dynamic analysis (Figure 9.11E) shows that most lamellae are of the sub-basal I type and that the fabric of c-axes of grains that contain lamellae can indicate in which quadrant of the diagram σ_1 could be expected to lie. The direction in which the arrowheads point, gives the most reliable position of σ_3. The latter position shows that the lamellae fabric resulted from triaxial compression with a strong component of extension parallel to X. The σ_1-σ_3 plane trends nearly vertical in a

Stellenbosch University http://scholar.sun.ac.za

general NE direction, with σ_1 plunging north-east at a moderate angle and the σ_2 axis not coinciding with mesoscopic b (Figure 9.11A).

The total preferred orientation of the microfabric (c-axes and lamellae, together with the dynamic analysis) indicates general triaxial, rotational strain with respect to the mesoscopic fabric. Though the sample was taken from heterogeneously deformed beds in the Stompiesfontein fold zone, the generally strong preferred orientations relate fairly well to one another. It is suggested that the orientations of σ_1, σ_2 and σ_3 as derived from the fabric also reflect upon the age of the intragranular plastic deformation of the quartz grains. Microfabric preferred orientations that were induced early in the deformational history of the bed, commonly become only rotated, and not modified, by later movements (Scott et al., 1965; Coetzee, 1979; Hälbich and Swart, 1983). The orientation of σ1 close to the bedding and halfway between Z and Y (Figure 9.11A), does not provide conclusive evidence that the folds at Stompiesfontein initially formed in relatively soft beds. The generally plastic (Class 2) fold style in the fold zone, however, indicates deformation of soft sediments under these known conditions of low metamorphic grade. It is suggested that the orientations of σ_1, σ_2 and σ_3 derives from a combination of rotational stress axes and deformation of non-lithified beds.

9.4.7 SAMPLE CFB 73

This sample, taken centimetres away from the synclinal hinge

Stellenbosch University http://scholar.sun.ac.za

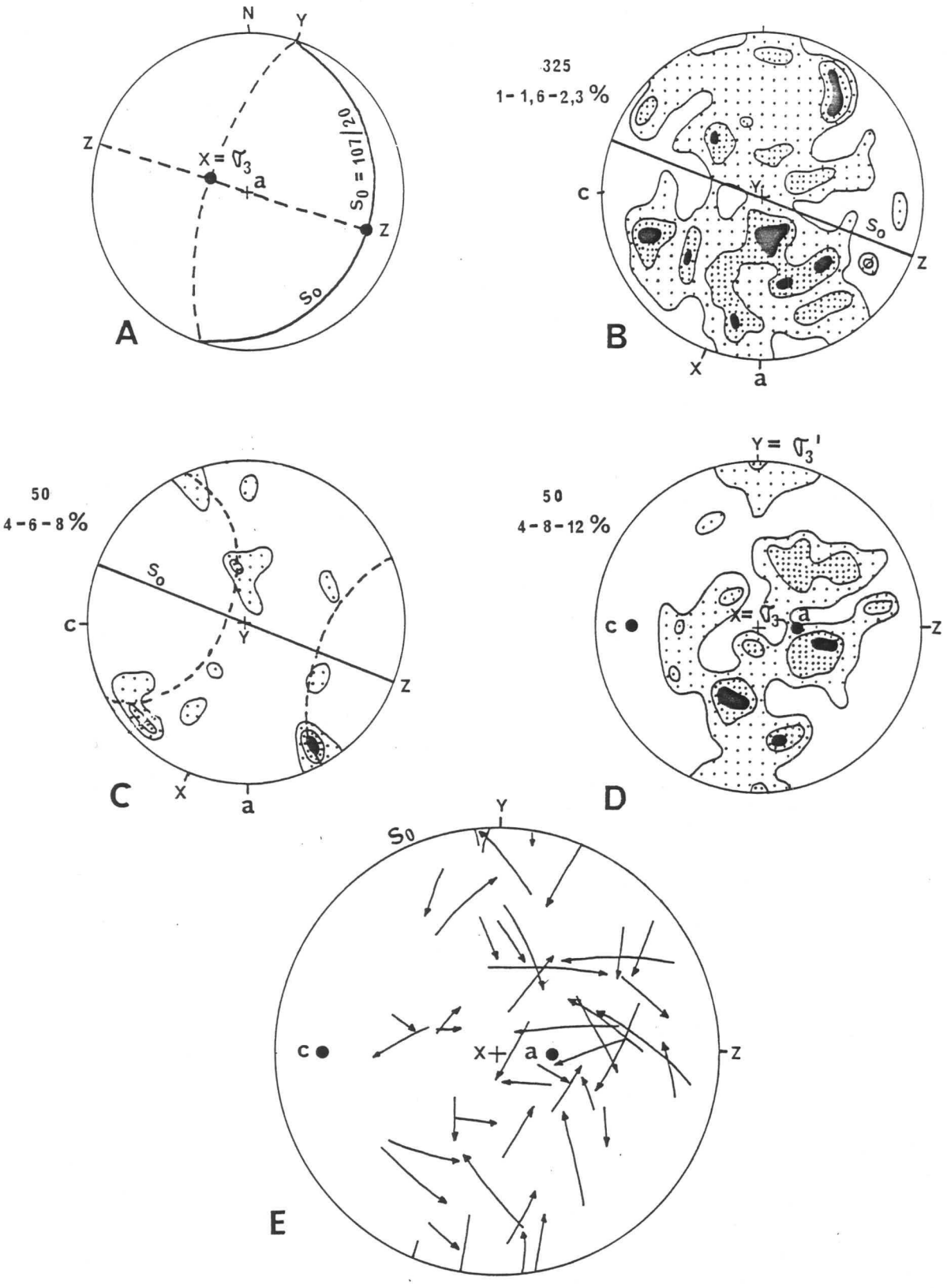

Figure 9.12
Sample CFB 73 from Stompiesfontein. (A) Orientation of bedding (So) and thin sections; (B) 325 c-axes projected onto XZ plane; (C) 50 c-axes with lamellae projected onto the XZ plane; (D) 56 lamellae poles projected onto bedding plane; (E) dynamic analysis. All contours per 1% area.

Stellenbosch University http://scholar.sun.ac.za

where the bed dips 107/20, (Figure 9.12A), contains only some 16% grains with lamellae. The total c-axis fabric (Figure 9.12B) shows a fairly random orientation, with only Z being pole-free. It shows no resemblance to expected fabrics for constrictive, plane strain or flattening strain, probably because of low intragranular plastic deformation. The low incidence of lamellae supports the latter deductions, because it is not likely that strain features were annealed out at these low temperatures. The c-axis fabric of grains that contain lamellae (Figure 9.12C) indicates maxima along a poorly defined small circle with opening angle of about 60 degrees around an axis inclined to mesoscopic c and subparallel to bedding. This fabric suggests axially symmetric shortening (Lister et al., 1978), rather than plane strain. The maxima of poles to lamellae (Figure 9.12D), though slightly diffuse, lie approximately along a small circle with opening angle of 45 degrees around X as well as at a point-maximum close to Y. The dynamic analysis (Figure 9.12E) suggests that the σ_3 axis is near the bedding pole (X) and the megascopic a-direction (as indicated in Figure 9.12D), but the positions of σ_1 and σ_2 cannot be uniquely defined (Figure 9.12A). The latter may be expected near the fold hinge. Lamellae are again mostly of the sub-basal I type, which indicates intragranular slip parallel to the basal and rhomb glide systems under low P-T conditions.

9.4.8 SAMPLE CFB 74

This sample was taken from the severely thinned part of the bed, that dips 307/65 on the south-eastern limb of the small syncline (Figure 9.13A). Clear new grains at grain boundaries

Stellenbosch University http://scholar.sun.ac.za

are particularly common and a multi-stage cementation history is indicated by two ages of iron oxide coatings at original grain boundaries. Attack of detrital grains by aggressive solutions can be identified, because rutile needles clearly indicate original grain boundaries. Most lamellae are decorated by lines of inclusions and some intense strain hardening is suggested by up to three different sets of lamellae inside a single grain.

The total c-axis plot (Figure 9.13B) displays a small circle distribution with axis almost parallel to X, i.e. perpendicular to bedding. The small circle is nearly symmetrically disposed about mesoscopic b. The fabric indicates severe flattening almost perpendicular to the bedding plane, because the small circle axis lies at only 45 degrees to the mesoscopic a and c. Thus, bedding has rotated 20 degrees beyond the orientation of this shortening axis. The c-axis fabric of grains that contain lamellae (Figure 9.13C) compares, with some exceptions, fairly well with the total c-axis fabric. The poles to lamellae (Figure 9.13D) lie at a diffuse point-maximum between mesoscopic a and Z. The dynamic analysis (Figure 9.13E) supports the fact that σ_1 operated nearly perpendicular to the bedding plane and σ_3 nearly parallel to it. Both σ_1 and σ_3 are very nearly contained in the ac mesoscopic fold fabric plane (i.e. sample ZX-plane). Figure 9.13E, as well as a comparison between Figures 9.13C and D, show that most lamellae are again of the sub-basal I type, though some 20% prismatic types occur. The development of a single lamellae maximum near the extension axis points to high strain intensity (Riley, 1947).

Stellenbosch University http://scholar.sun.ac.za

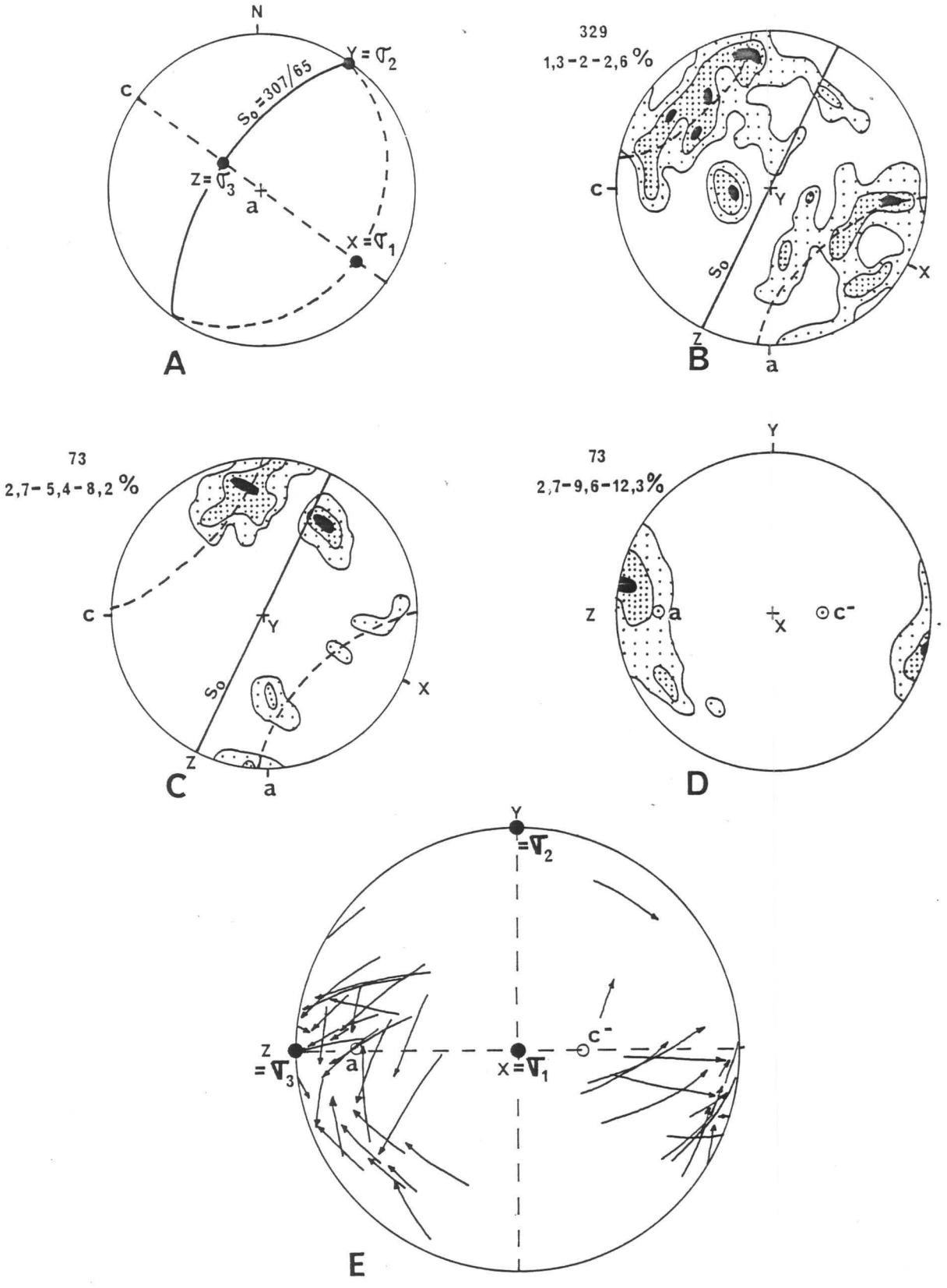

Figure 9.13
Sample CFB 74 from the Stompiesfontein fold zone.
(A) Orientation of bedding and thin sections; (B) 329 c-axes projected onto XZ plane; (C) 73 c-axes with lamellae projected onto XZ plane; (D) 73 lamellae poles projected onto bedding plane; (E) dynamic analysis. Contours per 1% area.

Stellenbosch University http://scholar.sun.ac.za

The microfabric preferred orientations of sample CFB 74 indicate severe flattening strains subperpendicular to the bedding plane and substantial stretching subparallel to the bedding dip direction. This supports the similar (Class 2: Ramsay, 1967) fold geometry observed on this limb, as well as the presence of tension gashes with high aspect ratios subperpendicular to the bedding and tautozonal about mesoscopic b (Figure 6.5). The fact that only the late-stage flattening (and stretching) strains are recorded in the microfabric, suggests that the intragranular plastic deformation recorded here, only occurred in the fold limb after an advanced stage of rotation by buckle deformation. Work done by Scott et al. (1965) and Coetzee (1979) indicates that, where internal homogeneous shortening occurs prior to buckle deformation of a bed, or where the angles of tilt of buckled beds are still low, σ_1 is oriented parallel to bedding. This would only occur if the sediment was already somewhat lithified, otherwise no plastic deformation, with its characteristic microfabric preferred orientations, would have been produced. Under low P-T conditions, the microfabric will be "frozen in" and will only rotate passively with the bedding. The lamellae types that occur in Sample CFB 74 suggest that syntectonic temperatures were relatively low (well below 300°C), even during the late-stage flattening of the folds.

The results of Samples CFB 72 to 74 have shown that it may be possible to determine the timing of intragranular plastic deformation in these rocks from detailed microfabric analysis. Comparisons between microfabric and bedding orientation of CFB

Stellenbosch University http://scholar.sun.ac.za

74 revealed that much buckle shortening may have occurred while the beds were still unlithified. The microfabric of Sample CFB 74 also matches the observed Class 2 (Ramsay,1967) fold geometry very well, because the dynamic analyses were able to reflect stretching close to bedding. Dynamic analyses of the data obtained from some of these samples show remarkable consistency. The position of σ_3 with relation to mesoscopic a, b and c, is exactly the same for Samples CFB73 and 74, differing only slightly for CFB 72. The good agreement between CFB 74 and 73 probably results from the low angle of bedding dip for CFB 73. Due the influence of bedding anisotropy, it is conceivable why the orientation of σ_3 in CFB 72 should slightly differ from that of the other two samples. The orientation of σ_3 in all of these samples fits in excellently with the orientation of quartz-filled tension gashes with high aspect (i.e. length : width) ratios. The tension gashes probably started opening up at the time when intragranular plastic deformation became important, due to advanced lithification of the quartzite.

9.5 CONCLUSIONS FROM THE MICROFABRIC ANALYSIS

1. Low buckling strain intensities in the Ceres Syntaxis did not hamper microstructural investigations, but sample location played a major role in recording the degree of preferred orientation in the fabric.
2. Quartz grains from horizontal beds, like those adjacent to the Baviaansberg megakink (sample CFB 60) and south of the Stompiesfontein fold zone (sample CFB 68) have higher

Stellenbosch University http://scholar.sun.ac.za

deformation lamellae densities than some severely shortened beds from Skitterykloof and Zeekoegat (samples CFB 56 and CFB 64, respectively). This may indicate that optimal lamellae development occurs under low P-T conditions, where beds remain relatively unrotated under prolonged bulk stress.

3. Only relatively pure quartz arenites should be sampled. Silty parts of the succession should be avoided, because they tend to act as a strain "sponge", both by concentrating shear deformation along them, and possibly also by inhibiting expulsion of water from the arenites.

4. Samples with a mesoscopic penetrative lineation parallel to the local fold axis, do not display as much intragranular deformation as those without the lineation. A higher initial clay mineral content in these well-lineated samples may partly explain this. Apparently, connate water laden with clay particles, moved preferably along bedding surfaces, but also along minute laminae planes, in the unconsolidated sediment. Movement of this water took place preferably in the direction of the fold axis. Plastic intragranular slip deformation later recorded the same stress distribution that prevailed before most water was expelled from the beds. Preferred orientations and dynamic analyses show that the lineation is not a stretching lineation formed by plastic intragranular deformation. This is supported by the absence of elongate grain dimensions parallel to the lineation. The low temperature/pressure tectonic regime conditions as indicated by the total microfabric, confirm

Stellenbosch University http://scholar.sun.ac.za

that the lineation was produced in plastic and semi-plastic sediments.

5. Multiple stages of overgrowth, corrosion of detrital quartz grains, as well as the presence of some large illitized feldspar grains, indicate that Witteberg sediments retained their water long after deposition. The fact that only late-stage flattening strains were recorded in some highly shortened beds within the Stompiesfontein fold zone, suggests that the rocks were not well-indurated during initial stages of buckling.

6. The standard dynamic analyses indicate that most lamellae are of the Sub-basal I type. This suggests low temperature and pressure, as well as low strain rates.

7. The microfabric of sample CFB 68 appears to have been greatly influenced by the stress axes that existed during formation of the intense NE trending fold zones, and to a lesser extent by those responsible for the NW trending folds.

Stellenbosch University http://scholar.sun.ac.za

10. DATING THE DEFORMATION

10.1 INTRODUCTION

The 40Ar/39Ar stepwise degassing technique is now widely used to date tectonic and metamorphic events. In low-grade areas, the presence of cleavage micas in the rocks, will greatly enhance the reliability of the ages obtained from the method. The most significant interpretations of 40Ar/39Ar age spectra, are those in which a single age plateau can be related to a single recrystallization event. Lacking this, it is also possible to interpret the tectonic history of rocks with multiple mica parageneses with a reasonable degree of confidence, especially if many samples were taken from widely separated localities. Both ways of data interpretation were employed by Hälbich et al. (1983) in the Cape Fold Belt, where paroxysmic ages of about 278 Ma., 258 Ma., 247 Ma., 230 Ma. and 215 Ma. were derived.

In the Ceres Syntaxis, it was hoped that the 40Ar/39Ar stepwise degassing technique would give different ages for the two main NW and NE fold trends. The only rock type that displays a cleavage in structures with these respective trends, is black laminated shale from the Cedarberg Formation. Samples (1) and (2) were taken from the NW trending Hansiesberg and NE trending Hex River mega-anticlines respectively. Cubes, some 4 centimetres on edge, were cut from fresh samples obtained west of the farm Elandsfontein (19°19,4'E, 33°10,2'S) and at Groothoekkloof (19°39,7'E, 33°25,3'S). The two samples were

Stellenbosch University http://scholar.sun.ac.za

analysed at the Cambridge (UK) dating laboratory by the total rock argon-40/argon-39 age spectrum method as described in Fitch et al. (1969) and Hälbich et al. (1983).

10.2 SAMPLE DESCRIPTION AND AGE SPECTRA

Examination of thin sections suggests that many relict detrital minerals exist in both samples. Particularly important in this context are unaltered fine-grained mica flakes lying on the bedding planes. In both samples, the cleavage is of the regular or irregular, discrete type, usually discontinuous, but always with dark to opaque colouring along it. No recrystallized micas occur along cleavage planes. The microstructural habit of the cleavage indicates very low strain intensity, comparable only to Sample no. FM 8039 of Hälbich et al. (1983). The latter sample came from a mudstone unit in the Abrahamskraal Formation (Lower Beaufort Group) and displayed only one local solution cleavage event without new mica growth.

The most useful diagrams in argon-40/argon-39 dating, are those that relate age to the cumulative percentage of argon-39 released at the various heating steps. These age spectra for samples (1) and (2) are given in Figures 10.1 and 10.2 respectively. The age spectrum for sample (1) climbs through an inflection around 325 Ma. to reach a plateau just under 450 Ma. The importance of these two age components is again emphasized on the argon 40/36 versus 39/36 correlation diagram (Fitch and Miller, 1987). Further argon losses, related to later minor events, are evident. The age spectrum of sample

Stellenbosch University http://scholar.sun.ac.za

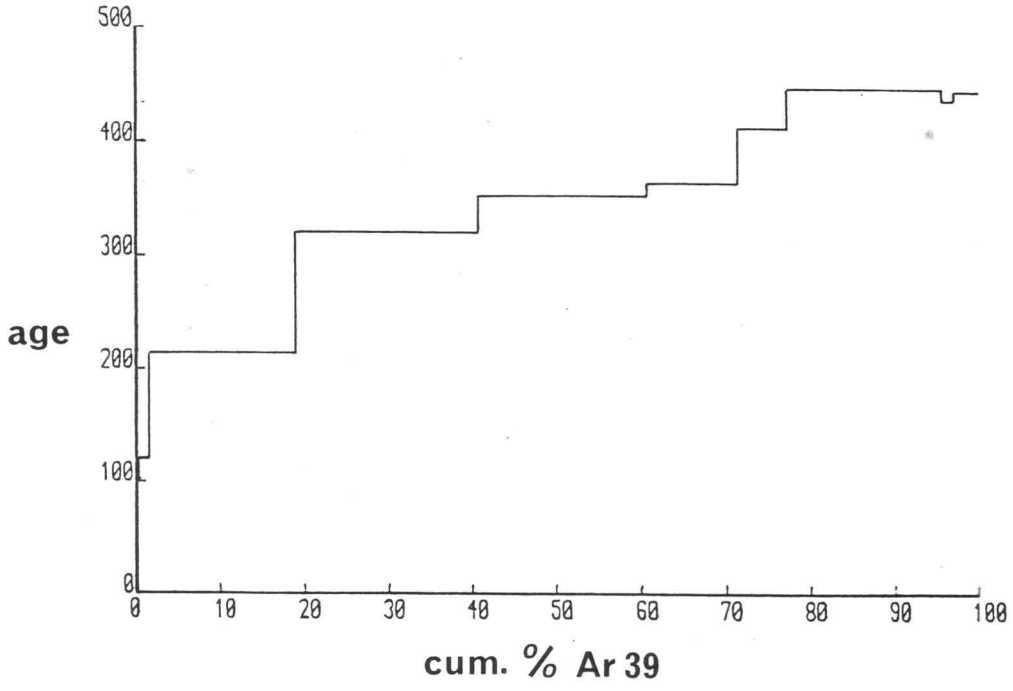

Figure 10.1
Sample (1) from the Hansiesberg anticline. For explanation, see text.

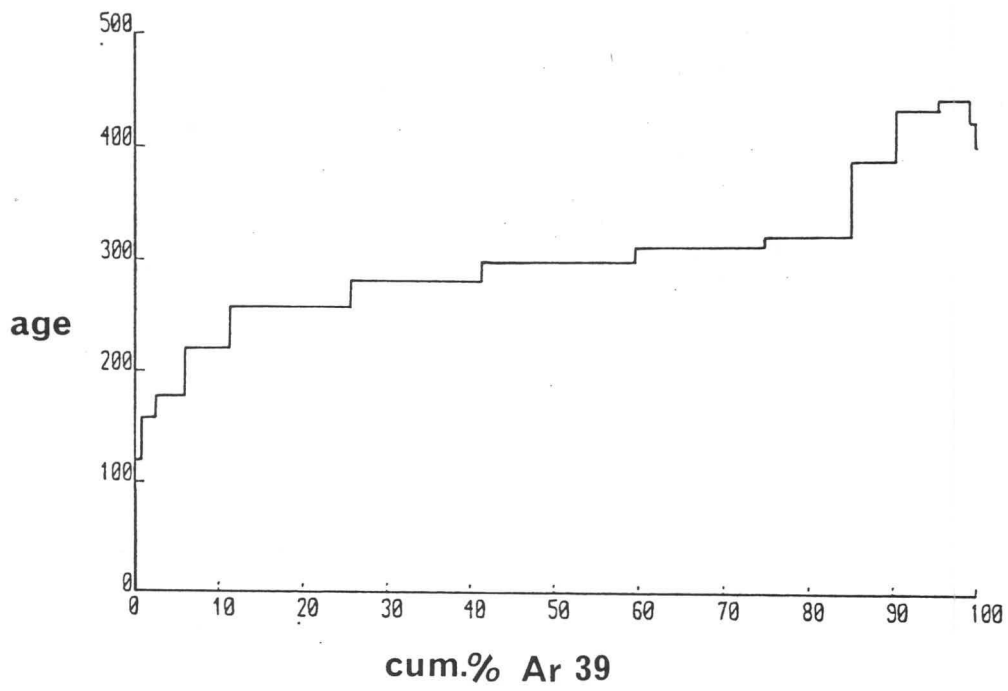

Figure 10.2
Sample (2) from the Hex River anticline.

Stellenbosch University http://scholar.sun.ac.za

(2) is generally similar in form to that of sample (1), i.e. it climbs through a sharp inflection close to 325 Ma. to a peak age of 445±6 Ma. In the latter case, further minor argon losses have also occurred.

Combined evidence from the two samples demonstrates their close relationship. It is evident that both samples suffer from an absence of clearly defined plateaux. Most probably, the sub-plateaux seen around 446±6 Ma. can be accepted as a time at which major changes in the composition of originally detrital micas occurred. The widely accepted upper Ordovician age of the Cedarberg shale, compares well with this plateau. Later events can be seen to have eroded the oldest plateaux in both samples. Sample (2) has suffered greater argon losses than Sample (1). This is consistent with the finer average grain size and the slightly more intense cleavage developed in this rock. It is suggested that the prominent argon releases in both samples around 322 Ma. represent mixed ages. The 322 Ma. age is older than any known paroxysmic age for the Cape Fold Belt. The different plateaux-forming steps around 322 Ma. in Sample (1) from the NW trend, do not mean that this trend is actually older than the NE trend. It rather reflects the lower cleavage intensity in this sample and less complete radiogenic resetting since the 446 ±6 Ma. event. Argon losses subsequent to 322 Ma. are more sharply defined in sample (2) and suggest that the major tectonic events occurred between 230 - 300 Ma. Significantly, the ages obtained by Hälbich et al. (1983) fall exactly in this range.

Stellenbosch University http://scholar.sun.ac.za

It is perhaps appropriate to compare the results of Samples (1) and (2) of the present study with those obtained from some of the earlier (Hälbich et al., 1983) study. Except for the earlier-mentioned sample FM 8039, the only other comparable sample of the previous study is FM 8176. This sample came from black, pyritic shale of the Cedarberg Formation in the NNE-trending Villiersdorp Syncline. The cleavage-forming event, however, was accompanied by the growth of moderately-sized micas. The cleavage style of Samples (1) and (2) from the Ceres Syntaxis, is more akin to that of FM 8039, because no new micas appear to have formed. Sample FM8039, however, came from Beaufort mudstone and not from Cedarberg shale. A direct comparison of the texture and ages obtained from the present study to those of Hälbich et al. (1983), is therefore not advisable. However, the results of FM 8039 were, like those of Sample (1) from the Hansiesberg anticline, indicative of overlapping age components. Sample (2) from the Hex River anticline, though new micas are absent, produced very similar results to FM 8176 of Hälbich et al. (1983), where major events were indicated around 276, 255, and 238 Ma.

Final resolution of the interpretative problems that arise from the analysis of the two samples may have to await an isochron dating of the cleavage-forming event in a better cleaved rock, with new mica growths parallel to this structure.

Stellenbosch University http://scholar.sun.ac.za

11. SYNTHESIS

Fold styles of the NW and NE fold trends are the same for any one given lithological unit. However, different lithologies led to the development of either sinusoidal or kink-like fold geometries along both trends. The well- and thin-bedded character of Witteberg Group multilayers, with their low competency contrasts and relatively high layer-parallel shear resistance, favoured the development of angular kink and box fold geometries. True sinusoidal and flattened sinusoidal folds of metre-scale developed locally in Witteberg sediments where, due to silty interbeds, the multilayer had higher competency contrasts. Larger structures on the other hand, always have angular forms, because buckling was controlled by the competent units that had a high resistance to bedding-parallel shear. The megakink or monoclinal folds are true compressional features formed by flexural slip, without major décollement along thrust planes. The second-order kinks on the limbs of Table Mountain Group megastructures of both the NW and NE trends are related to secondary shear stresses that acted on the rotating limbs of these structures during horizontal compression. A "vertical" or gravity tectonics model for that part of the western fold belt exposed in the Ceres Syntaxis, does not fit the above observations.

The positioning of the South-western Cape Syntaxis was largely influenced by older Pan-African structural architecture (De Villiers, 1956). This statement does not imply that fold trends in the Cape-Karoo cover succession are everywhere the

Stellenbosch University http://scholar.sun.ac.za

same as those in the pre-Cape basement. However, the swing in basement tectonic grain from NW-SE to E-W, faithfully duplicated by a similar change in trend of the Cape Fold Belt, points to strong basement control over fold trends in the cover. The trend of young fold belts forming in sediments that were deposited between, or on, earlier consolidated platform regions is often determined by the structural contours of the latter, and is often fixed by the boundaries of the sedimentary basin (Jaroszewski, 1984). The development of the Cape and Karoo depositories in relation to the edge of the Kalahari Craton, the effect of axes of down- and upwarp during deposition of the Table Mountain, Bokkeveld and Witteberg Groups (Rust, 1973), paved the way for the observed fold trends, given the right compressional regime.

The Cedarberg fold trend in the South-western Cape Syntaxis is N-S, whereas north thereof, it varies from NNW to NW. Similarly, the E-W trending southern Cape folds are deflected continuously towards a NE-SW orientation in the syntaxis. South of the Worcester Fault, many faults trend NE-SW, but the latter trend is completely absent in the Ceres Syntaxis. Instead, the few faults that occur strike NW-SE. It is therefore clear that the NW-SE trending Cedarberg and E-W trending southern Cape folds meet in an arcuate fashion with a major NE-SW trending controlling factor in the area of the syntaxis. The Stettyn Rise (Figure 11.1) was an active element throughout the history of the Cape basin (Rust, 1973). Differential compaction of sediments above this (NE-SW) trending flexure could have provided the anisotropy needed for

Stellenbosch University http://scholar.sun.ac.za

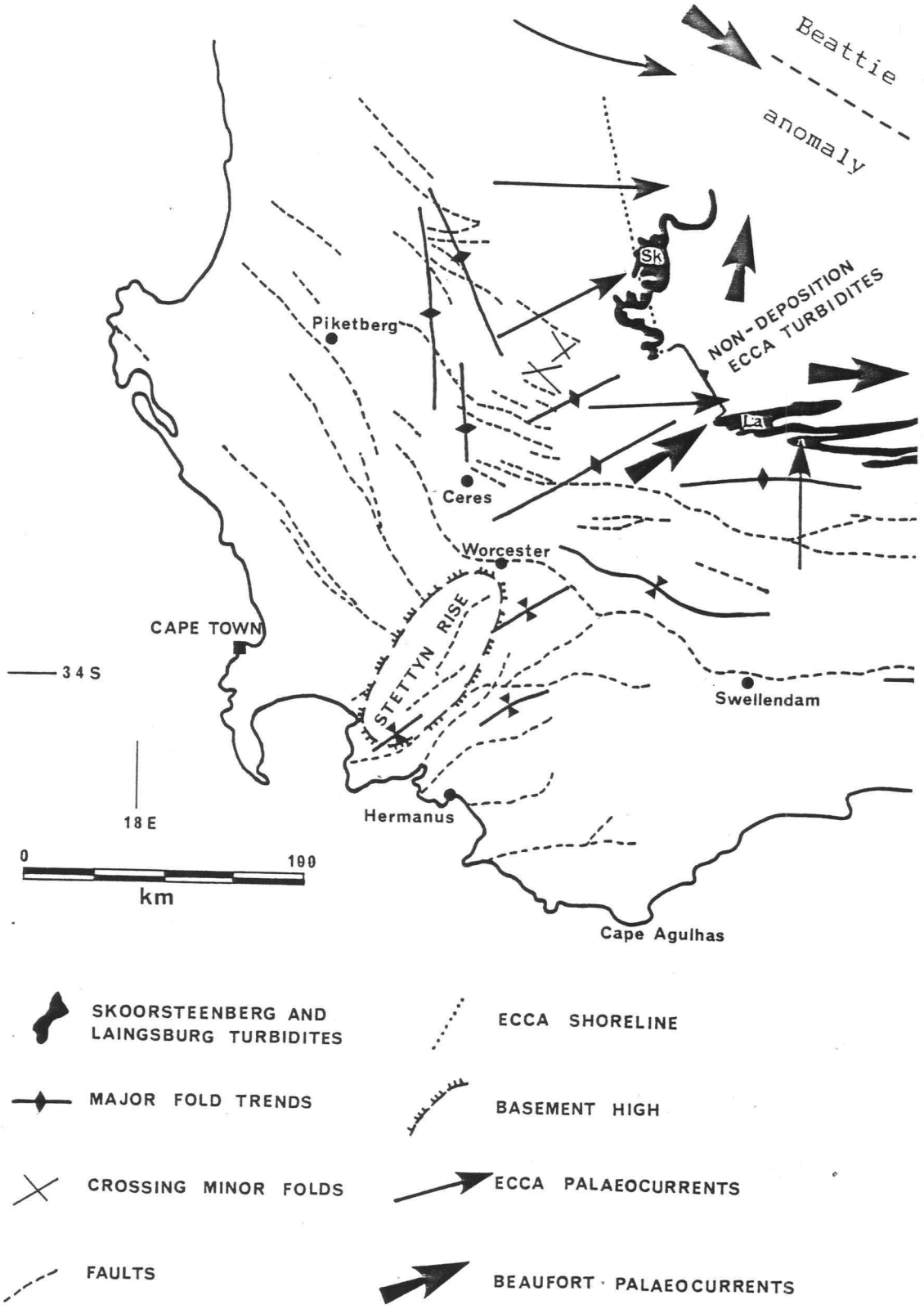

Figure 11.1
Interaction between structural development of the SW Cape Syntaxis and deposition in the western Karoo Basin. Data were taken from own observations (1986), Rust(1967), Wickens(1984) and D.I.Cole, pers. comm.(1989).

Stellenbosch University http://scholar.sun.ac.za

deflection of the external tectonic forces. The adjustment of fold trends to the contours of adjoining rigid elements is visible inside many fold belts (De Villiers, 1944; Söhnge, 1983; Jaroszewski, 1984; Biswas, 1987).

Fold trends in the Ceres Syntaxis are controlled by the western Hansiesberg-Witzenberg megastructures and the southern Hex River mega-anticline. The control of the western, N-S megastructures gradually diminishes towards the north and east, because Cedarberg folds become NNW, NW and WNW oriented (see Map 1). In the southern Ceres Syntaxis, where the NE-SW trend prevails, Bokkeveld Group fold orientations are strictly controlled by the Hex River mega-anticline. Fold trends in the Witteberg Group, though mostly oriented NE, may vary between ENE and NE. Fold axis orientation is much more variable in the Witteberg Group than in the Bokkeveld or Table Mountain Groups, though the former occurs stratigraphically within half a wavelength of Table Mountain Group megastructures, which is the dominant member of the structural lithic unit (Dennis, 1972). As a result of very special physical properties of the deforming Witteberg multilayer, it was able to accurately reflect local stress conditions by changing the trend of its exceptionally linear fold axes.

The deformational intensities of the Cedarberg and Hex River fold trends are not equal. In the western Ceres Syntaxis, N-S folds in the Bokkeveld and Witteberg Groups only developed close to the Hansiesberg-Witzenberg megastructures. The central and southern parts of the area are dominated by the

Stellenbosch University http://scholar.sun.ac.za

NE-SW trend to such an extent, that NW folds are almost totally absent south of the Winkelhaak Fault (Map 1). West of Platklip, the NW trend converges upon NE folds of the southern and central Ceres Syntaxis. North of the Winkelhaak Fault, the NW and NE trends are of roughly the same intensity. The Cedarberg fold trend dies out rapidly east of the Swartruggens Mountain Range in the Tanqua Karoo. The NE trend dies out near the 32°30' latitude well north of the southernmost development of western fold belt structures near Ceres, and also extends much farther into the Karoo Sequence than the Cedarberg folds. It is therefore evident that, for the NE trend to have developed that far north, its intensity must have been considerably higher than that of the Cedarberg trend.

Considerable control by the Winkelhaak fault over fold trends in the central Ceres syntaxis was outlined above. Around N'wardouw, a similar control of NW trending small faults over local fold directions, demonstrates that these faults, although their displacements are relatively small, represent important planes along which stresses could be transmitted. It is also important to note that the NE fold trend dies out roughly where the probable extension of the Beattie static magnetic anomaly (Beattie, 1909, Figure 11.1) traverses the western fold belt.

There is no distinct age difference between the NW, NE and E-W fold trends. True cross-folding is displayed only by the Witteberg Group, in which it occurs as intersecting, linear and conjugate zones of high buckle shortening. At these intersections, there is a slight tendency for the NW trending

Stellenbosch University http://scholar.sun.ac.za

structure of the conjugate pair to have been initiated earlier than the NE structures. The latter relations, however, only hold for the northern Ceres Syntaxis, because further south, the NW and NE trends only converge upon each other and do not intersect. Due to the flexural slip mechanism of most folds, cross-folding was registered as structures following the bedding plane attitude of existing folds. Largely divergent fold trends that developed in different parts of the multilayer, were accommodated by oblique bedding plane slip. Structures such as "accommodation folds" and the general observation that intensely deformed zonal folds of both trends rarely cross, but mostly impinge on one another, tend to support their origin by contemporaneous compression in two directions.

The absence of cleavage and the measurement of megakink limb lengths, indicate that total tectonic shortening in the Ceres Syntaxis did not exceed 20% on a regional scale. Measurement of bed lengths along the structural profiles of the southern Ceres Syntaxis indicates buckle shortening of 10% to 15%.

Similar, as well as isoclinal fold geometries associated with the described B-lineation in highly shortened beds and under non-metamorphic conditions, point to a high water content and a high primary porosity during at least the initial development of buckles in the Witteberg Group. The conclusion of De Swardt and Rowsell (1974) that the Cape Supergroup sediments were rigid and well lithified under at least 7000 metres of overburden, with little or no pore fluid present at the time of

Stellenbosch University http://scholar.sun.ac.za

folding, is strongly questioned for outcrops of Witteberg rocks in the Ceres Syntaxis.

Well-sorted arenites possess porosities of between 40% and 50% at the sedimentational surface (Dapples, 1979). The inability of these sands to lose their water will be greatly enhanced by shaly interbeds and overlying thick shaly successions that act as sealing agents. Syntectonic injection of sandy material into the basal Kweekvlei shales at Skitterykloof (p.73), indicates a high water content in the underlying Witpoort Formation during at least the initial stages of deformation. The burial depth of the Witteberg sediments during the first two paroxysms of the Cape Orogeny (Hälbich et al., 1983, p.158), was approximately 900 metres and 2000 metres respectively for the 276 and 258 Ma events. Relationships between porosity and burial depth (Sclater and Christie, 1980) for North Sea sediments, suggest that the upper Witteberg Group sediments would still have had porosities of the order of 28 and 20% respectively, during the above two paroxysms.

Hälbich and Swart (1983) showed that the Dwyka tillite lithified during and after the first paroxysm. The present study indicates that certain units of the Witteberg Group, also, were essentially unlithified during at least initial deformation. The observed structures and suggested degree of lithification of the Witteberg rocks agree with recent findings that kink folds are not a brittle phenomenon, and that they can also form under conditions of low overburden pressure (Rixon et al., 1983). Microstructural evidence obtained during

Stellenbosch University http://scholar.sun.ac.za

the present study for some severely shortened Witteberg beds, indicates dominantly low P-T conditions and initial deformation by grain sliding mechanisms, to be followed later by plastic intragranular deformation.

As the Karoo Sequence was deposited during the Cape Orogeny, therefore one expects to find evidence for the impact of the western and southern fold belts on these sediments. Available evidence (Hälbich et al., 1983) indicates that the first paroxysm in the Cape Fold Belt occurred during the Early Permian, around 278 Ma. The Dwyka Formation tillites were deposited during Late Carboniferous and Early Permian times. During the Late Carboniferous ice flowed from both the south and north into an east-west trending tectonic basin (Visser and Loock, 1982). Ice flow directions in the area now occupied by the Tanqua Karoo, that is, along the western, NS-trending fold belt, were towards the west. A downfaulted block of Dwyka tillite north-east of Gydo Pass indicates that only the Waaipoort Formation of the Witteberg Group was possibly removed by erosion. As erosion may have taken place by fluvial as well as by glacial processes (Visser and Loock, 1982), the above evidence suggests that the western Cedarberg folding did not have much, if any, surface expression at that time. Striated surfaces cut in Middle Witteberg beds in the Tanqua Karoo (J.N.Theron, pers. comm.) do not prove that these sediments were lithified, because permafrost would have had the same effect.

Stellenbosch University http://scholar.sun.ac.za

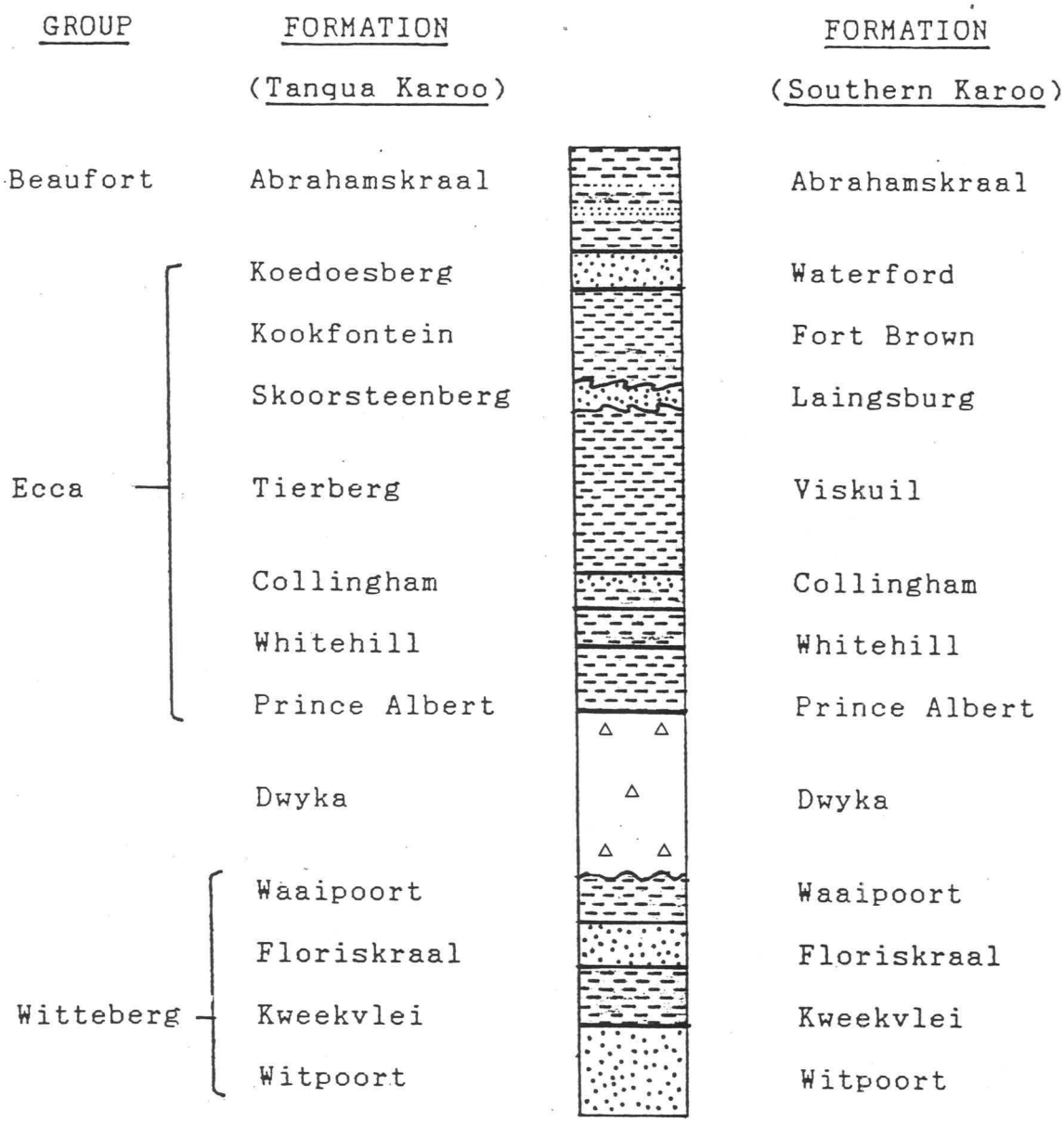

Figure 11.2
General stratigraphy of the western Karoo, based on data from Wickens, 1984.

Stellenbosch University http://scholar.sun.ac.za

The occurrence of volcanic ash beds within the lower 100 metres of Dwyka tillite (J. Viljoen, pers. comm.) in the southern and south-western Cape, together with the fact that these tillites were derived from the south, points to uplift being a secondary effect of subduction at the proto-Pacific (Smellie, 1981) plate margin. The tuffs are generally of acid types, which confirm their relationship to plate tectonics and calc-alkaline volcanism in an orogenic belt (Lock and Johnson, 1974; J. Viljoen, pers. comm.). It is suggested that, although the folding in both the western and southern fold belts did not have much surface expression during deposition of the Dwyka Formation, the orogeny that led to a climax in the Permian had already started to operate to the south of the present continental margins.

The Whitehill Formation (Figure 11.2) also provides evidence that the Cape Orogen in this area was still very subdued during Early Permian times. It was deposited uninterruptedly in a shallow sea that stretched over the areas that were later to become the western and southern Cape Fold Belts (Visser, 1987). Whitehill outcrops in the South-western Cape Syntaxis, south of Worcester, show much the same thicknesses as those to the north and east (J. Viljoen, pers. comm.). Volcanic ash beds are interbedded with Permian Prince Albert shales and are also numerous in the Collingham Formation that directly overlies the Whitehill Formation.

The orientation of the palaeo-coastline during deposition of Ecca Group sediments in the western and south-western Karoo,

Stellenbosch University http://scholar.sun.ac.za

follows the curvature of the Ceres syntaxis faithfully (Figure 11.1). The sedimentary source-areas were situated towards the west and the south-west (Wickens, 1984). The Laingsburg turbidites wedge out in an area that is situated along the north-eastward continuation of the NE trending Hex River mega-anticline. The point at which the Skoorsteenberg turbidites disappear, is also situated along the north-eastward extension of the Baviaanshoek mega-anticlinorium. Therefore, the area where turbidites were not deposited coincides exactly with that part of the Ceres Syntaxis where the NE fold trend dominates over the NW trend(Figure 11.1). At the southern termination of the Skoorsteenberg turbidites, shallow water conditions as well as tectonic activity are indicated by ripple-marked shale and slump structures. (H. de V. Wickens, pers. comm.). The above evidence strongly suggests that, by this time, the proto Hex River anticline and the adjoining Baviaansberg anticlinorium had some surface expression which influenced the deposition of the turbidites. Deposition of the Lower Ecca, including the Laingsburg turbidites, has been correlated with the first (278 Ma) paroxysm (Hälbich et al., 1983). The more-or-less similar stratigraphic position of the two turbidite formations, as well as the ages suggested by the 40Ar/39Ar dating of Cedarberg shales (p.113), confirm this. It furthermore indicates that the western fold belt could not be older than the NE folds, which are related to the southern fold belt.

During deposition of the Beaufort Group in the south-western Karoo, fluvial transport directions were dominantly from the SW towards the north and east (Figure 11.1). Folding and

Stellenbosch University http://scholar.sun.ac.za

uplift during the 258 Ma event (Hälbich et al., 1983) were responsible for this sediment dispersal pattern (D. Cole, pers. comm.). The early development of the north-east Hex River megastructure resulted in its early erosion, leading to the entry of river systems from the south-western syntaxis area. A lesser, south-eastward directed palaeoflow introduced Beaufort sediments from an area to the north-west, where the Cedarberg folds in the western ranges disappear and Cape Supergroup rocks become essentially flat-lying.

The above situation shows that the intensity of the Cedarberg fold trend is a maximum in the southern part of the western fold belt. A genetic relationship between the western and southern fold belts is thus indicated. Structural evidence provided in this study also illustrates that the conjugate NW and NE fold trends in the Witteberg Group are synchronous.

The NW and NE fold trends in the cover rocks of the Ceres syntaxis formed contemporaneously on a heterogeneous basement. The external stress configuration was resolved into components which acted simultaneously towards the north-west and north-east. This was probably influenced by the tectonic grain of the basement, as was block- and possible minor wrench-faulting.

Stellenbosch University http://scholar.sun.ac.za

ACKNOWLEDGEMENTS

The author gratefully acknowledges support from the following people and institutions:

The Geological Survey of South Africa for allowing the use of information from project RG85/7.

Dr. J.N. Theron of the Geological Survey in Bellville, for suggesting the project.

Prof. I.W. Hälbich, my study leader, for his continued interest and support.

Helena and Willie Bester, Renate and Jürgen Reck, as well as many other farmers in the Ceres area for their hospitality and moral support during many months of field work.

Dr. P.G. Gresse at the Geological Survey, for many interesting discussions, as well as improvement of the manuscript.

Annamie van der Westhuizen for typing and retyping of the manuscript.

My faithful field assistants, Tommy Brooks and Karel Muller, without whom this work would not have been possible.

Stellenbosch University http://scholar.sun.ac.za

REFERENCES

Basson, W.A. (1984). Stratotype description of the Swartruggens Formation. Intern. Rep. geol. Surv. S. Afr., (unpubl.), 3 pp.

Beach, A. (1977). Vein arrays, hydraulic fractures and pressure solution structures in a deformed flysch sequence, S.W. England. Tectonophysics, **40**, 201-225.

Beattie, J.C. (1909). Report of a magnetic survey of South Africa. R. Soc. Lond. Publs., Cambridge Univ. Press.

Bell, C.M. (1981). Soft-sediment deformation of sandstone related to the Dwyka glaciation in South Africa. Sedimentology, **28**, 321-329.

Bell, T.H. (1981). Foliation development - the contribution, geometry and significance of progressive bulk, inhomogeneous shortening. Tectonophysics, **75**, 273-296.

Bhattacharji, S. (1959). Theoretical and experimental investigations on crossfolding. J. Geol., **66**, 625-667.

Biswas, S.K. (1987). Regional tectonic framework, structure and evolution of the western marginal basins of India. Tectonophysics, **135**, 307-327.

Blacic, J.D. (1975). Plastic-deformation mechanisms in quartz: The effect of water. Tectonophysics, **27**, p. 271-294.

Blignault, H.J. (1970). Contemporaneous glacial folding in the Table Mountain Group, Western Cape. M.Sc. thesis (unpubl.), Univ. Stellenbosch.

Bouchez, J. (1977). Plastic deformation of quartzites at low temperature in an area of natural strain gradient. Tectonophysics, **39**, 25-50.

Stellenbosch University http://scholar.sun.ac.za

Carreras, J., Estrada, A., and White, S. (1977). The effects of folding on the c-axis fabrics of a quartz mylonite. Tectonophysics, **39**, 3-24.

Carter, N.L., and Friedman, M. (1965). Dynamic analysis of deformed quartz and calcite from the Dry Creek Ridge Anticline, Montana. Am. J. Sci., **263**, 747-785.

Coetzee, D.S. (1979). Styl en intensiteit van vervorming in die Kaap- en Karoo-opeenvolging vanaf Meiringspoort tot by Beaufort-Wes langs 22½° oosterlengte. M.Sc. thesis (unpubl.), Univ. Stellenbosch, 86 pp.

Collier, M. (1978). Ultimate locking angles for conjugate and monoclinal kink bands. Tectonophysics, **48**, T1-T6.

Dapples, E.C. (1979). Diagenesis of sandstones, 31-97. In: Larsen, G. and Chilingar, G.V., Eds., Diagenesis in sediments and sedimentary rocks : Developments in sedimentology 25A. Elsevier, New York, 579 pp.

Dennis, J.G. (1972). Structural geology. The Ronald Press Company, New York, 532 pp.

De Swardt, A.M.J., Fletcher, O., and Toschek, P. (1974). Note on orogenic style in the Cape Fold Belt. Trans. geol. Soc. S. Afr., **77**, 53-57.

De Swardt, A.M.J., and Rowsell, D.M. (1974). Note on the relationship between diagenesis and deformation in the Cape Fold Belt. Trans. geol. Soc. S. Afr., **77**, 239-245.

De Villiers, J. (1944). A review of the Cape Orogeny. Ann. Univ. Stellenbosch, **22, Sect. A**, 183-208.

-----, (1956). Die drie sintaksisse in die Suidwestelike Kaapprovinsie. Tegnikon, **9**, 75-85.

Stellenbosch University http://scholar.sun.ac.za

Dewey, J.F. (1965). Nature and origin of kink-bands. Tectonophysics, **1**, 459-494.

Faill, R.T. (1973). Kink-band folding, Valley and Ridge Province, Pennsylvania. Bull. geol. Soc. Am., **84**, 1289-1314.

Fitch, F.J. and Miller, J.A. (1987). Geochronological Report No. FMK/3016. FM Consultants Limited, Kent, 26 pp.

-----, Miller, J.A. and Mitchell, J.G. (1969). A new approach to radio-isotopic dating in orogenic belts, 157-195 In: Kent, P.E., Satterthwaite, G.E. and Spencer, A.M. Eds., Time and place in orogeny. Geol. Soc. London.

Gay, N.C. and Weiss, L.E. (1974). The relationship between principal stress directions and the geometry of kinks in foliated rocks. Tectonophysics, **21**, 287-300.

Ghosh, S.K. (1967). Experiments of buckling of multilayers which permit interlayer gliding. Tectonophysics, **6**, 207-249.

-----, (1974). Strain distribution in superposed buckling folds and the problem of reorientation of early lineations. Tectonophysics, **21**, 249-272.

----- and Ramberg, H. (1968). Buckling experiments on intersecting fold patterns. Tectonophysics, **5**, 89-105.

Gresse, P.G. (1976). The structure and metamorphism of the pre-Cape rocks in the coastal strip south of George. M.Sc. thesis (unpubl.), Univ. Stellenbosch, 120 pp.

Hälbich, I.W. (1983a). Intra-formational folding in the Cape Fold Belt, 125-130 In: Söhnge, A.P.G. and Hälbich, I.W., Eds., Geodynamics of the Cape Fold Belt, Spec. Publ. geol. Soc. S. Afr., **12**, 184 pp.

Stellenbosch University http://scholar.sun.ac.za

-----, (1983b). Geodynamics of the Cape Fold Belt in the Republic of South Africa, a summary, 21-29. In: Rast, N., and Delaney, F.M., Eds., Profiles of Orogenic Belts, Am. Geophys. Un. Geodynamics Series, **10**, 310 pp.

-----, and Cornell, D.H. (1983). Metamorphic history of the Cape Fold Belt, 131-148. In: Söhnge, A.P.G. and Hälbich, I.W., Eds., Geodynamics of the Cape Fold Belt. Spec. Publ. geol. Soc. S. Afr., **12**, 184 pp.

-----, and Swart, J. (1983). Structural zoning and dynamic history of the cover rocks of the Cape Fold Belt, 75-100. In: Söhnge, A.P.G. and Hälbich, I.W., Eds., Geodynamics of the Cape Fold Belt. Spec. Publ. geol. Soc. S. Afr., **12**, 184 pp.

-----, Fitch, F.J., and Miller, J.A. (1983). Dating the Cape orogeny, 149-164. In: Söhnge, A.P.G. and Hälbich, I.W., Eds., Geodynamics of the Cape Fold Belt. Spec. Publ. geol. Soc. S. Afr., **12**, 184 pp.

Hara, I. (1971). An ultimate steady-state pattern of c-axis fabric of quartz in metamorphic tectonites. Geol. Rdsch., **60**, 1142-1174.

Hartnady, C.J.H. (1969). Structural analysis of some pre-Cape formations in the Western Province. Bull. Chamb. Mines. Precambr. Res. Unit, **6**, 70 pp.

Hobbs, B.E., Means, W.D., and Williams, P.F. (1976). An outline of structural geology. Wiley, New York, 571 pp.

Honea, E., and Johnson, A. M. (1976). A theory of concentric, kink and sinusoidal folding and of monoclinal flexuring of compressible, elastic multilayers. IV. Development of

Stellenbosch University http://scholar.sun.ac.za

sinusoidal and kink folds in multilayers confined by rigid boundaries. Tectonophysics, 30, 197-239.

Jaroszewski, W. (1984). Fault and fold tectonics (W.L. Kirk, transl. ed.), John Wiley and Sons, England, 565 pp.

Julivert, M., and Marcos, A. (1973). Superimposed folding under flexural conditions in the Cantabrian Zone, Hercynian Cordillera, N.W. Spain. Am. J. Sci., 273, 353-375.

Krynauw, J.R. (1977). The George granite pluton and its relationship to the Kaaimans Formation. M.Sc. thesis, (unpubl.), Univ. Stellenbosch, 209 pp.

Laubscher, H.P. (1976). Geometrical adjustments during rotation of a Jura fold limb. Tectonophysics, 36, 347-365.

Law, R.D. (1986). Relationships between strain and quartz crystallographic fabrics in the Roche Maurice Quartzites of Plougastel, Western Brittany. J. Struct. Geol., 8, 493-515.

-----, (1987). Crystallographic fabrics and deformation histories. J. geol. Soc. London, 144, 675-678.

Le Roux, J.P. (1977). The stratigraphy, sedimentology and structure of the Cango Group north of Oudtshoorn, C.P.. M.Sc. thesis (unpubl.), Univ. Stellenbosch, 159 pp.

Lister, G.S. (1977). Discussion: Crossed-girdle c-axis fabrics in quartzites plastically deformed by plane strain and progressive simple shear. Tectonophysics, 39, 51-54.

-----, Paterson, M.S., and Hobbs, B.E. (1978). The simulation of fabric development in plastic deformation and its application to quartzite : The model. Tectonophysics, 45, 107-158.

Stellenbosch University http://scholar.sun.ac.za

Lock, B.E. (1980). Flat-plate subduction and the Cape Fold Belt of South Africa. Geology, **8**, 35-39.

-----, and Johnson, M.R. (1974). A crystal tuff from the Ecca Group near Lake Mentz, Eastern Cape Province. Trans. geol. Soc. S. Afr., **77**, 373-374.

Loock, J.C. (1967). The stratigraphy of the Witteberg-Dwyka contact beds. M.Sc. thesis (unpubl.), Univ. Stellenbosch, 139 pp.

Maltman, A. (1984). On the term "soft sediment deformation". J. Struct. Geol., **6**, 589-592.

Marjoribanks, R.W. (1976). The relation between microfabric and strain in a progressively deformed quartzite sequence from Central Australia. Tectonophysics, **32**, 269-293.

Newton, A.R. (1973). A gravity-folding model of the Cape Fold Belt. Trans. geol. Soc. S. Afr., **76**, 145-152.

-----, 1975. Structural applications of remote sensing in the Cape Province, and a new model for the evolution of the Cape Fold Belt. Ph.D. thesis (unpubl.), Univ. Cape Town, 86 pp.

-----, (1980). Intra-plate nature of the Cape Fold Belt. S. Afr. J. Sci., **76**, 272-273.

Odonne, F., and Vialon, P. (1987). Hinge migration as a mechanism of superimposed folding. J. Struct. Geol., **9**, 835-844.

Phillips, W.R. (1971). Mineral Optics - principles and techniques. W.H. Freeman, San Francisco, 249 pp.

Ramberg, H. (1964). Selective buckling of composite layers with contrasted rheological properties, a theory for

Stellenbosch University http://scholar.sun.ac.za

simultaneous formation of several orders of folds. Tectonophysics, 1 (4), 307-341.

Ramberg, I.B., and Johnson, A.M. (1976). A theory of concentric, kink and sinusoidal folding and of monoclinical flexuring of compressible, elastic multilayers. Tectonophysics, 32, 295-320.

Ramsay, J.G. (1962). The geometry of conjugate fold systems. Geol. Mag., 99, 516-526.

-----, (1967). Folding and fracturing of rocks. McGraw-Hill, New York, 568 pp.

----- and Huber, M.I. (1987). The techniques of modern structural geology. Volume 2: Folds and fractures. Academic Press Inc., London, 700 pp.

Rast, N., and Platt, J.I. (1957). Cross-folds. Geol. Mag., 94, 159-167.

Reches, Z., and Johnson, A.M. (1976). A theory of concentric kink and sinusoidal folding and of monoclinal flexuring of compressible, elastic multilayers. VI. Asymmetric folding and monoclinal kinking. Tectonophysics, 35, 295-334.

Rhodes, R.C. (1974). Discussion of: A gravity-folding model of the Cape Fold Belt by A.R. Newton. Trans. geol. Soc. S. Afr., 77, 207-209.

Riley, N.A. (1947). Structural petrology of the Baraboo quartzite. J. Geol., 55, 453-475.

Rixon, L.K, Bucknell, W.R., and Rickard, M.J. (1983). Mega kink folds and related structures in the Upper Devonian Merrimbula Group, south coast of New South Wales. J. geol. Soc. Aust., 30, 277-293.

Stellenbosch University http://scholar.sun.ac.za

Rust, I.C. (1967). On the sedimentation of the Table Mountain Group in the western Cape Province. D.Sc. thesis (unpubl.), Univ.Stellenbosch.

-----, 1973. Tectonic and sedimentary framework of Gondwana basins in Southern Africa, 537-564. In: Campbell, S.K.S.W., Ed., Proc. Papers 3rd Gondwana Symp., Canberra, Australia.

Ryan, P.J. (1967). Stratigraphy of the Ecca Series and lowermost Beaufort Beds (Permian) in the Great Karroo basin of South Africa, 945-965. Int. Un. geol. Sci. Symp. on Gondwana Stratigraphy, Buenos Aires.

Sclater, J.G., and Christie, P.A.F. (1980). Continental stretching: An explanation of the post-mid-Cretaceous subsidence of the Central North Sea Basin. J. Geophys. Res., **85**, 3711-3739.

Scott, W.H., Hansen, E., and Twiss, R.J. (1965). Stress analysis of quartz deformation lamellae in a minor fold. Am. J. Sci., **263**, 729-746.

Skjernaa, L. (1975). Experiments on superimposed buckle folding. Tectonophysics, **27**, 255-270.

Smellie, J.L. (1981). A complete arc-trench system recognised in Gondwana sequences of the Antarctic Peninsula region. Geol. Mag., **118**, 139-159.

Söhnge, A.P.G. (1983). The Cape Fold Belt - perspective, 1-6. In: Söhnge, A.P.G. and Hälbich, I.W., Eds., Geodynamics of the Cape Fold Belt, Spec. Publ geol. Soc. S. Afr., **12**.

----- and Hälbich, I.W. (1983). Geodynamics of the Cape Fold Belt. Spec. Publ. geol. Soc. S. Afr., **12**.

Stellenbosch University http://scholar.sun.ac.za

South African Committee for Stratigraphy (SACS) (1980). Stratigraphy of South Africa. Part 1 (Comp. L.E. Kent). Lithostratigraphy of the Republic of South Africa, South West Africa/Namibia, and the Republics of Bophuthatswana, Transkei and Venda. Handbk. geol. Surv. S. Afr., 8, 690 pp.

Stubley, M.P. (1989). Fault and kink-band relationships at Mystery Bay, Australia. Tectonophysics, **158**, 75-92.

Tankard, A.J., Jackson, M.P.A., Eriksson, K.A., Hobday, D.K., Hunter, D.R., and Minter, W.E.L. (1982). Crustal evolution of Southern Africa - 3,8 billion years of earth history. Springer-Verlag, New York, 523 pp.

Theron, A.C. (1967). The sedimentology of the Koup Subgroup near Laingsburg. M.Sc. thesis (unpubl.), Univ. Stellenbosch.

Theron, J.N. (1972). The stratigraphy and sedimentation of the Bokkeveld Group. D.Sc. thesis (unpubl.), Univ. Stellenbosch.

Toogood, D.J. (1976). The structural geology of the Malmesbury Group between De Wet and Vink, Cape Province. Ann. geol. Surv. S. Afr., **11**, 29-46.

Tullis, J. (1977). Preferred orientation of quartz produced by slip during plane strain. Tectonophysics, **39**, 87-102.

-----, Christie, J.M., and Griggs, D.T. (1973). Microstructure and preferred orientations of experimentally deformed quartzites. Bull. geol. Soc. Am., **84**, 297-314.

Turner, F.J. and Weiss, L.E. (1963). Structural analysis of metamorphic tectonites. McGraw-Hill, New York, 545 pp.

Stellenbosch University http://scholar.sun.ac.za

Visser, J.N.J. (1979). Changes in sediment transport in the Cape-Karoo Basin (Silurian-Triassic) in South Africa. S. Afr. J. Sci., **75**, 72-75.

-----, (1982). Implications of a diachronous contact between the Dwyka Formation and Ecca Group in the Karoo basin. S. Afr. J. Sci., **78**, 249-251.

-----, (1986). Lateral lithofacies relationships in the glacigene Dwyka Formation in the western and central parts of the Karoo Basin. Trans. geol. Soc. S. Afr., **89**, 373-383.

-----, (1987). The palaeogeography of part of southwestern Gondwana during the Permo-Carboniferous glaciation. Palaeogeogr. Palaeoclimatol. Palaeoecol., **61**, 205-219.

----- and LOOCK, J.C. (1982). An investigation of the basal Dwyka tillite in the southern part of the Karoo Basin, South Africa. Trans. geol. Soc. S. Afr., **85**, 179-187.

Watkinson, A.J. (1981). Patterns of fold interference: influence of early fold shapes. J. Struct. Geol., **3**, 19-23.

White, S. (1975). The effects of polyphase deformation on the intra-crystalline defect structures of quartz, II: Origin of the defect structures. Neues. Jb. Miner. Geol. Paläont. Abh., **123**, 327-352.

-----, (1977). Geological significance of recovery and recrystallization processes in quartz. Tectonophysics, **39**, 143-170.

Whitten, E.H.T. (1969). Structural geology of folded rocks. Rand McNally and Co., Chicago, 678 pp.

Stellenbosch University http://scholar.sun.ac.za

Wickens, H. de V. (1984). Die stratigrafie en sedimentologie van die Groep Ecca wes van Sutherland. M.Sc. thesis (unpubl.), Univ. Port Elizabeth, 86 pp.

THE GEOLOGY OF THE CERES SYNTAXIS

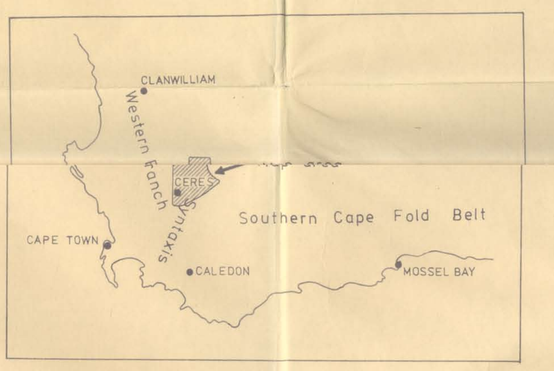

32°45' 19°15'

19°30'

19°45' 32°45'

33°00'

33°15'

33°23'

19° 15'

19°30'

19°45' 33°23'

KEY

- Main roads
- Secondary roads
- Rivers
- Geological contacts
- Inferred geological contacts
- Faults (downthrow indicated)
- Anticlines
- Synclines
- Kinks
- Minor anticlines
- Minor synclines
- Minor kinks
- Fold zones
- 50 Attitude of bedding

LEGEND

- Alluvium , surface deposits
- Pp Prince Albert Formation — ECCA GROUP
- Pd Dwyka Formation
- Cw Waaipoort Formation — Lake Mentz Subgroup
- Cf Floriskraal Formation — Lake Mentz Subgroup
- Ck Kweekvlei Formation — Lake Mentz Subgroup
- Dwp Wittepoort Formation — Weltevrede Subgroup — WITTEBERG GROUP
- Ds Swartruggens Formation — Weltevrede Subgroup
- Dbb Blinkberg Formation — Weltevrede Subgroup
- Dwd Wagendrift Formation — Weltevrede Subgroup
- Dkp Karoopoort Formation — Bidouw Subgroup
- Dob Osberg Formation — Bidouw Subgroup
- Dkk Klipbokkop Formation — Bidouw Subgroup
- Du Wuppertal Formation — Bidouw Subgroup
- Dwb Waboomberg Formation — Bidouw Subgroup
- Dbp Boplaas Formation — Ceres Subgroup — BOKKEVELD GROUP
- Dt Tra-tra Formation — Ceres Subgroup
- Hex River Formation — Ceres Subgroup
- Dv Voorstehoek Formation — Ceres Subgroup
- Dh Gamka Formation — Ceres Subgroup
- Dg Gydo Formation — Ceres Subgroup
- Sn — Nardouw Subgroup / Winterhoek Subgroup — TABLE MOUNTAIN GROUP
- Oc
- Op Peninsula Formation

1 : 100 000

1 0 2 4 6 8 10 Kilometer

1 : 50 000 MAP INDEX

3219 CD	3219 DC	
3319 AB	3319 BA	3319 BB
3319 AD	3319 BC	3319 BD

Lithological boundaries from Geological Survey maps and this study

Structure by C. de Beer (1986)

Map compiled and drawn by C. de Beer (1987)